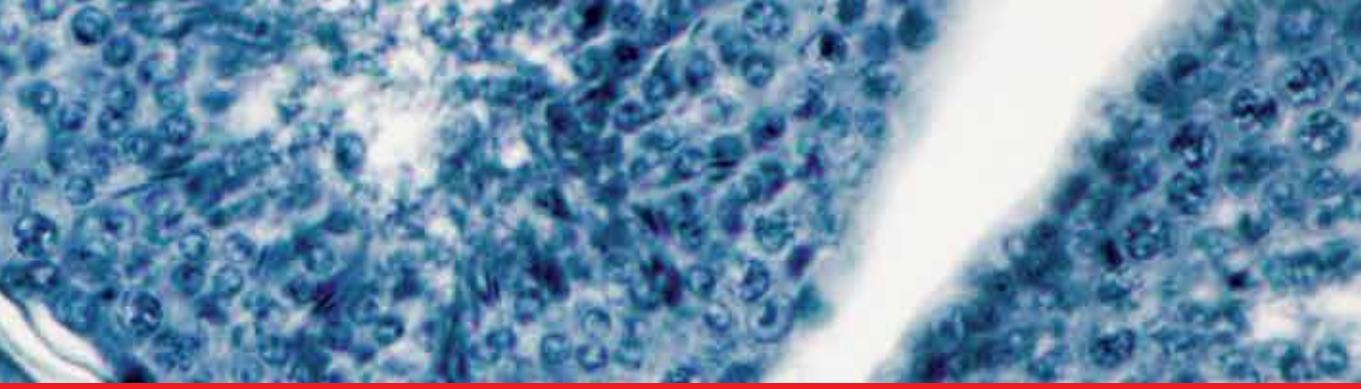

IntechOpen

Histology

Edited by Thomas Heinbockel and Vonnie D.C. Shields

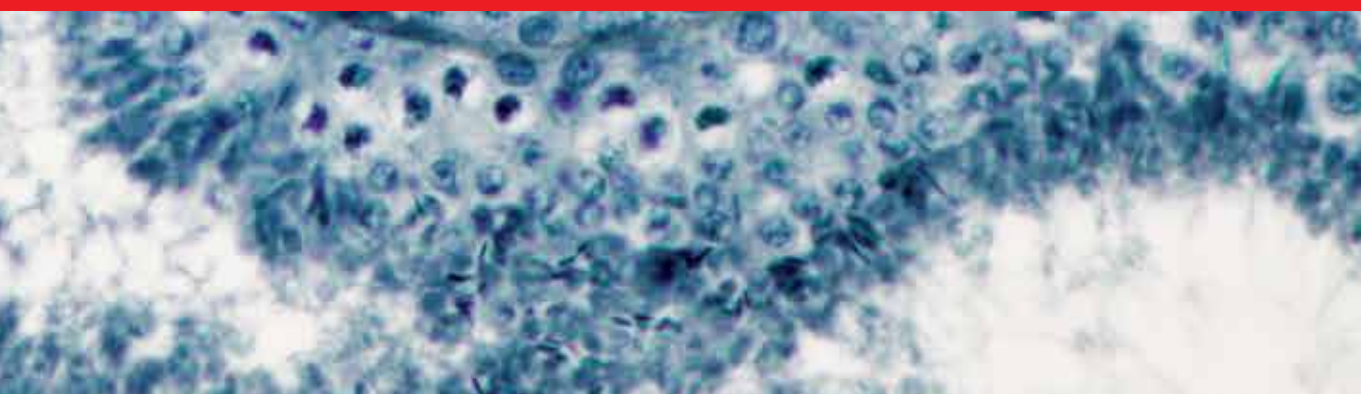

HISTOLOGY

Edited by **Thomas Heinbockel**
and **Vonnie D.C. Shields**

Histology
http://dx.doi.org/10.5772/intechopen.75080
Edited by Thomas Heinbockel and Vonnie D.C. Shields

Contributors

Luis Barrios, Sonia Gupta, Nitin Ahuja, Vaso Kecojevic, Felicia Galos, Gabriela Năstase, Cătălin Boboc, Cristina Coldea, Mălina Anghel, Anca Orzan, Mihaela Bălgrădean, Tatsuaki Tsuruyama, Toshiyuki Kawakami, Keiko Kaneko, Tatsuo Takaya, Saeka Matsuda, Rina Muraoka, Norimasa Okafuji, Mihoko Tomida, Masahito Shoumura, Naoto Osuga, Keisuke Nakano, Hidetsugu Tsujigiwa, Hitoshi Nagatsuka, Agustin G Zapata, Juan J Muñoz, Thomas Heinbockel

Notice

First published in London, United Kingdom, 2019 by IntechOpen
eBook (PDF) Published by IntechOpen, 2019
IntechOpen is the global imprint of INTECHOPEN LIMITED, registered in England and Wales, registration number: 11086078, The Shard, 25th floor, 32 London Bridge Street
London, SE19SG – United Kingdom
Printed in Croatia

British Library Cataloguing-in-Publication Data
A catalogue record for this book is available from the British Library

Additional hard and PDF copies can be obtained from orders@intechopen.com

Histology
Edited by Thomas Heinbockel and Vonnie D.C. Shields

p. cm.

Print ISBN 978-1-78984-970-7

Online ISBN 978-1-78984-971-4

eBook (PDF) ISBN 978-1-83881-813-5

Meet the editors

Thomas Heinbockel, PhD, is a professor in the Department of Anatomy, Howard University College of Medicine, Washington, DC. Dr. Heinbockel's laboratory engages in multidisciplinary research to elucidate organizational principles of neural systems in the brain, specifically the limbic and olfactory system. His research has been directed at understanding brain mechanisms of information processing and their relation to neurological and neuropsychiatric disorders. His laboratory also works on translational projects, specifically the development of novel anti-epileptic drugs and pharmacotherapeutic treatment options of drug addiction. His laboratory analyzes drug actions at the epi- and genetic level using next-generation sequencing technology. At Howard University, Dr. Heinbockel teaches histology to graduate and professional students. He studied biology at the Philipps-University, Marburg, Germany. His studies of the brain started during his MS thesis work at the Max-Planck-Institute for Behavioral Physiology, Starnberg/Seewiesen, Germany. Subsequently, he completed a PhD in Neuroscience at the University of Arizona, Tucson, Arizona, USA. After graduating, he was a research associate at the Institute of Physiology, Otto-von-Guericke-University School of Medicine, Magdeburg, Germany. Prior to his arrival at Howard University, Dr. Heinbockel held joint research faculty appointments in the Department of Anatomy and Neurobiology and the Department of Physiology at the University of Maryland School of Medicine, Baltimore, Maryland, USA. He still maintains an adjunct appointment in these departments.

Vonnie Shields, PhD, is currently Full Professor in the Biological Sciences Department and Acting Dean in the Fisher College of Science and Mathematics at Towson University, Towson, MD, USA. Dr. Shields' laboratory engages in multidisciplinary research directed towards exploring the importance of gustatory, olfactory, and visual cues in the selection of food sources. She carries out behavioral and electrophysiological studies on larval and adult insects. In addition, her laboratory examines the structural organization of insect sense organs using transmission electron and scanning electron microscopy. The overall goal of this research is to acquire a better understanding of the sensory mechanisms by which insects find host plants and detect plant-associated volatiles. The aim is to discover possible novel biocontrol agents against insect pests. At Towson University, Dr. Shields teaches a histology course for both undergraduate and graduate students and has developed a graduate-level Modern Microscopy and Microtechniques course, where she teaches, in addition to the lecture component,

a hands-on laboratory component to allow students to learn histological techniques. Prior to beginning accepting a faculty position at Towson University, Dr. Shields studied biology at the University of Regina, Regina, Saskatchewan, Canada. Her interest in insect chemosensory research began after her undergraduate studies, when she started her PhD studies at the same institution. For her PhD she carried out research at the University of Regina and the University of Alberta, Edmonton, Alberta, Canada. After graduating, she was a research associate and conducted postdoctoral studies at the Arizona Research Laboratories Division of Neurobiology, University of Arizona, Tucson, Arizona, USA.

Contents

Preface

Histology is the science of tissues and as such histology studies cells and tissues of organs using a variety of techniques. Histology goes back more than 200 years when the French surgeon Bichat used the term "tissues," followed by the introduction of the term "histology" by Karl Meyer in the early nineteenth century. Among the early histologists were Camillo Golgi and Santiago Ramon y Cajal who presented the wonders of cellular building blocks to the world and started to elaborate the structure of cell and tissue specimens, specifically nerve cells. From their time to today's most sophisticated analysis of cell structure and function, microscopes and imaging techniques have undergone an exciting evolution that allows us to understand microscopic details and cellular function at the molecular level. Histological techniques are used in different disciplines: research, teaching, and clinical applications. This book explores the research currently being carried out at the molecular, subcellular, and cellular levels, both in normal and pathological processes, from genetic mechanisms to intra- and intercellular signaling. This book includes cutting-edge research reviews and descriptions of technological advances to modify bodily cells and tissues. Targeted at students and researchers in biological, medical, and related disciplines, this book will provide an overview of the work being done in this field, and will highlight any gaps and areas that would benefit from further exploration.

The book contains eight chapters in four sections and presents reviews in different areas of histology written by experts in their respective fields. Basic histology, cell biology, histopathology, and histological techniques are featured prominently as a recurring theme throughout several chapters. This book will be a most valuable resource for histologists, cell biologists, pathologists, and other scientists alike. In addition, it will contribute to the training of current and future biomedical scientists who find histology and its associated disciplines as fascinating as many generations before them.

Chapter 1 introduces the topic of this book by discussing histological processing and preparation of tissues. Thereby, the chapter familiarizes the reader with histological microtechniques, including tissue acquisition, fixation, dehydration, clearing, infiltration, embedding, microtomy, section acquisition, and staining.

In Chapter 2, authors discuss the histological, cellular, and molecular mechanisms that govern early epithelium development in the thymus. The authors emphasize the resemblance of the thymus with the process of branching morphogenesis and tubulogenesis that occurs in other epithelial organs such as those derived from the gut such as the mammary gland, salivary glands, lungs, kidneys, and pancreas. These organs repeatedly fold to reach an enlarged area, which is necessary to perform their major functions, namely, gas exchange, excretion,

nutrient transport, and others. It is epithelial–mesenchyme interactions that determine the tissue patterning through specific combinations of common molecular signaling pathways.

Chapter 3 reviews the umbilical cord as one of the most important anatomical structures in the development of animals due to its participation in the exchange of nutrients and protection of structural vessels. The author describes research on histological characteristics of the constituents of the umbilical cord to improve our understanding of the main histological differences found among mammals. The chapter is of benefit not only to veterinary medicine but also to all pathologists and surgeons studying reproduction.

Chapter 4 addresses the secretion of one of our bodily fluids, saliva, by the salivary glands in the oral cavity. The authors review the tubuloacinar structure of salivary glands and the acini as their functional units. The authors explore the duct system of salivary glands and compare the three major salivary glands, namely, the parotid, submandibular, and sublingual gland. In addition, the authors describe various minor salivary glands. A discussion of the functional role of saliva for oral and general health is included in the chapter.

In Chapter 5, authors address a major health problem, namely, that a bacterium, *Helicobacter pylori*, leads to the most common chronic bacterial infections in the world. About half of the world's population is infected with the bacterium. The bacteria move into the digestive tract where they can cause ulcers in the lining of the stomach or upper part of the small intestine or even cause stomach cancer. In the clinic, correct diagnosis and effective treatment of *H. pylori* gastric infection are essential in controlling this infection. The authors review available diagnostic methods, the eradication therapy of *H. pylori* infection, antibiotic resistance, and antimicrobial susceptibility tests. The authors describe a prospective study to analyze patients with *H. pylori* gastric infection with positive histology and positive culture versus positive histology and negative culture.

In Chapter 6, authors explore remodeling of the periodontal ligament (PDL). The authors describe remodeling of the PDL with bone marrow-derived cells (BMCs) through BMC migration into the PDL using a green fluorescent protein (GFP) bone marrow-transplanted model mouse. The authors review how BMCs have the ability to migrate and differentiate into tissues and organs in the body. The authors include immunohistochemical data for the GFP-positive cells in the PDL.

In Chapter 7, author combines histology, morphology, and pathology to explore an abnormality of the lateral meniscus of the knee, the discoid meniscus. The author focuses on the microstructure of the discoid meniscus with respect to content and arrangement of collagen fibers. The cartilage portion of the meniscus is different in shape, thickness, and collagen proportion. Even though this abnormality was first described over 130 years ago, the origin is still unknown. Given that the discoid meniscus is typically asymptomatic, little is known about its epidemiology. This chapter helps to understand its histological and cell biological basis.

In Chapter 8, authors review histological research techniques, specifically mass spectrometry. It is used for the identification of biomarkers using pathologic samples such as blood and urine analyses. It has limited use for tissue analysis. The authors describe several recent technological developments such as matrix-assisted laser desorption/ionization, which has been applied to mass spectrometry analysis for the identification of diagnostic markers and pharmacological monitoring for drug delivery systems. In this chapter, the authors introduce mass spectrometry imaging using formaldehyde-fixed paraffin-embedded tissues. As

the authors point out, these new strategies and analytical methods are useful for the study of drug pharmacokinetics, metabolism, discovery of biomarkers, and treatment-specific effects on the proteome.

We are grateful to IntechOpen for initiating this book project and for asking us to serve as its editors. Many thanks go to Dajana Pemac at IntechOpen for moving the book project ahead in a timely fashion. Thanks are due to all contributors of this book for taking the time to write a chapter proposal, compose their chapter, and make my requested revisions to it. Hopefully, all contributors will continue their histological research with many intellectual challenges and exciting new directions. We would like to thank our son, Torben Heinbockel, for his patience and understanding over the past several months when we were working on this book project. Finally, V.S. would like to thank posthumously both her mother, a biochemist, and her father, a pathologist, Janus and Martin Shields, respectively, for introducing her to the world of biology and science in general. Her father was instrumental, especially, for introducing her to the field of histology and ultrastructure. T.H. is grateful to his parents, Erich and Renate Heinbockel, for their continuous support and interest in his work over many years.

Thomas Heinbockel, PhD
Professor
Department of Anatomy
Howard University College of Medicine
Washington, DC, USA

Vonnie D.C. Shields, PhD
Acting Dean and Professor of Biology
Jess & Mildred Fisher College of Science and Mathematics
Towson University
Towson, MD, USA

Introduction

Chapter 1

Introductory Chapter: Histological Microtechniques

Vonnie D.C. Shields and Thomas Heinbockel

Additional information is available at the end of the chapter

http://dx.doi.org/10.5772/intechopen.82017

1. Introduction

1.1. Background and overall preparation of tissues for microscopic examination

Histology is the branch of anatomy that focuses on the study of tissues of animals and plants. The term tissue refers typically to a collection of cells. In humans, organs comprise two or more tissue types, including epithelial, connective tissue, nervous, and muscular. The word "histology" stems from the Greek word "histos," meaning web or tissue, and "logia," meaning branch of learning. In brief, histological processing involves obtaining fresh tissue, preserving it (i.e., fixing it) in order to allow it to remain in as life-like a state as possible, cutting it into very thin sections (3–8 microns), mounting it on glass microscopic slides, and then staining the sections so that they can be observed under a microscope to identify different histological components within the tissue.

2. Techniques

2.1. Preparing the tissue

For tissue removal, it is necessary to gather first the informed consent of the patient, as tissue taken from a live individual for diagnosis or treatment requires his/her consent. In other words, the patient must know at the time he/she consents, the purpose of tissue removal (e.g., diagnosis, research purposes, etc.) [1]. Similarly, harvesting tissue from an animal requires approval of the procedure by the institutional review board (Institutional Animal Care and Use Committee, IACUC) [2, 3]. An important first step in the histological process is tissue acquisition. This step can be achieved by means of traditional tissue dissection or endoscopic ultrasound (EUS)-guided fine needle aspiration [4]. If the former dissection

method is chosen, it is important to ensure that sharp dissecting tools are used to minimize crushing the tissue while cutting for removal. The tissue should be kept moist (e.g., 0.85% saline, isotonic) while dissecting and trimming. The tissue should be trimmed 1–2 cm in width/length (but should not be more than 5 mm thick). There should be at least one to two cut sides for easy penetration of the fixative. It is important, at this stage, to determine the desired orientation of the tissue and that all tissue components are represented during this trimming stage, if possible [5].

2.2. Fixation

It is important to maintain cells in as life-like a state as possible and to prevent post-mortem changes as a result of putrefaction (destruction of tissue by bacteria or fungi) and autolysis (destruction of tissue by its own enzymes). In the latter case, as cells die, they release enzymes from their lysosomes and other intracellular organelles, which start to hydrolyze (i.e., break down or decompose by reacting with water) components of the tissue, such as proteins and nucleic acids with the help of proteases and nucleases, respectively. Cases of autolysis are most severe in tissues rich in enzymes (e.g., liver, brain, kidney, etc.) and are less rapid in tissues such as elastic fibers and collagen. Therefore, it is critical that fixation be carried out as soon as possible after removal of the tissues to prevent autolysis and putrefaction, as well as to prevent the tissue from undergoing osmotic shock, distortion, and shrinkage. Unfortunately, fixatives may, unintentionally, introduce artifacts which can interfere with interpretation of cellular ultrastructure [6–10].

As fixation is typically the first step to prepare the tissue for microscopic, or other, analysis, the choice of fixative and fixation protocol is very important. The fixative acts to denature proteins by (i) coagulation (of secondary and tertiary protein structures to form insoluble gels), (ii) forming additive compounds (cross-linking end-groups of amino acids), or (iii) a combination of coagulative and additive processes. In addition, fixatives (iv) promote the attachment of dyes to particular cell components by opening up protein side groups to which dyes may attach, (v) remove bound water to increase tissue refractive index to improve optical differentiation, and (vi) alter the refractive index of tissues to improve contrast for viewing without staining. Prolonged fixation may result in the chemical masking of specific protein targets and prevention of antibody binding during immunohistochemistry protocols. In such cases, alternative fixation methods may be incorporated depending on the biological material. Therefore, there is no universal fixative which will serve all requirements. Each fixative has specific properties and disadvantages. There is no single fixative, or combination of fixatives, that has/have the ability to preserve and allow the demonstration of every tissue component. Some fixatives have only special and limited applications, while mixtures of two or more reagents may be necessary to employ the special properties of each. So, it is important to identify specifically which histological structures one is trying to demonstrate, as well as the effects of short-term and long-term storage of the tissues [6–10].

When tissue is fixed, it is important to keep the sample size small, if possible (i.e., 2–3 mm^3), as increased thickness will retard fixative penetration. The volume of the fixative should be

20–25 times the volume of the tissue. The peritoneum or capsule around the tissue should be removed or pierced. The blood and mucus should be rinsed off with saline. The tissues should be cut with a new, sharp razor blade/scalpel, rather than scissors, as the latter could result in squeezing of the tissue, causing damage. Some tissues/organs (e.g., lung, eye, etc.) will require special handling to ensure that the fixative reaches all internal components. Care should be given to ensure that the specimen has one or more cut sides to guarantee good penetration of the fixative. Sometimes, an agitating instrument can be employed to ensure that the fixative reaches all surfaces. At no time should the tissue be allowed to dry out. Each fixative will have its own fixation time and post fixation treatment for best preservation of cellular detail. Typical fixatives, depending on the type of tissue and microscopy technique intended, may include, formalin, Zenker's fixative, Bouin's fixative, Helly's fixative, Carnoy's fixative, glutaraldehyde, osmium tetroxide, chromic acid, potassium dichromate, acetic acid, alcohols (ethanol, methanol), mercuric chloride, and acetone [5–10].

2.3. Microwave irradiation

Microwave fixation has been found to be useful in increasing the molecular kinetics giving rise to accelerated chemical reactions (i.e., faster fixation time, accelerated cross-linking of proteins). [11]. While conventional formalin-fixed, paraffin-embedded tissue offers superior cellular morphology and long-term storage, microwave-assisted tissue fixation with phosphate-buffered saline [12] of normal saline [13] offers the removal of the use of noxious and potentially toxic formalin fixation and a decrease in the turnaround time. In addition, staining of the microwave-fixed tissues was found to be sharper and brighter in most of the tissues than those obtained after conventional fixation [12, 14]. Interestingly, cold microwave irradiation procedures can offer rapid fixation and staining of tissues for electron microscopy and ultrastructural analysis [15].

2.4. Classification of fixatives

Fixatives can be classified on the basis of three main criteria: (i) action on proteins; (ii) types of fixative solution; and (iii) use [6–10, 16, 17].

i. Action on proteins
Fixatives can have two main actions on proteins. They can be coagulant or non-coagulant fixatives. Coagulant fixatives affect proteins in such a way that a coagulum (clot) forms (e.g., white of an egg when cooked). In contrast, non-coagulant fixatives result in a smoother "gel" formation. Cytoplasm is converted typically into an insoluble gel. In addition, while organelles are preserved, there is typically poor tissue penetration and artifacts are more likely to occur.

ii. Types of fixative solution
There are two main types of fixatives: primary and compound. Primary fixatives consist of a single fixative in solution (e.g., may be in absolute form, such as absolute ethanol or 10% formalin). Compound fixatives consist of two or more fixatives in solution, such as Zenker's, Helly's, and Bouin's fixatives.

iii. Their use and mechanism of action
The intention of microanatomical fixatives is to preserve components of organs, tissues, or cells in spatial relation to each other. These fixatives are largely coagulant in nature (cell organelles are destroyed, typically), and used for light microscopy (e.g., neutral buffered formalin or NBF, Zenker's, Bouin's, and 10% formal saline). Cytological fixatives, on the other hand, preserve cellular structures or inclusions (e.g., mitochondria), often at the expense of even penetration and allow the tissues to be cut relatively easily. They are non-coagulant in nature and are used typically for electron microscopy. They can be further subdivided into nuclear (e.g., Carnoy's) and cytoplasmic (e.g., Helly's and 10% formal saline).

2.5. Types of fixatives

1. Aldehydes include formaldehyde (formalin, when in its liquid form), paraformaldehyde, and glutaraldehyde. Tissues are fixed through cross-linking agents that react with proteins and nucleic acids in the cell (particularly lysine residues). Formaldehyde is a good choice for immunohistochemical studies, while formalin (10% neutral buffered formalin or NBF) is standard. The buffer prevents acidity in the tissues. Formaldehyde offers low levels of shrinkage and good preservation of cellular detail. This fixative is used routinely for surgical pathology and autopsy tissues requiring hematoxylin and eosin (H and E) staining [6–10, 16, 17]. Since formalin is toxic, carcinogenic, and a poor preserver of nucleic acids, there have been attempts to find a more suitable substitute; however, this has proved difficult [18].

2. Glutaraldehyde causes deformation of the alpha-helix structure in proteins, so it should not be used for immunohistochemistry staining. While it fixes very quickly, which makes it an excellent choice for electron microscopic studies, it provides poor penetration. It gives very good overall cytoplasmic and nuclear detail and is prepared as a buffered solution (e.g., 2% buffered glutaraldehyde). This fixative works best when it is cold and buffered and not more than 3 months old [6–10, 16, 17].

3. Oxidizing agents include permanganate fixatives, such as potassium permanganate, dichromate fixatives (potassium dichromate), osmium tetroxide, and chromic acid. While these fixatives cross-link proteins, they cause extensive denaturation [6–10, 16, 17].

4. Alcohols, including methanol and ethanol, and protein denaturants (acetic acid) are not used routinely as they cause brittleness and hardness to tissues. They are useful for cytologic smears, as they act quickly and provide good nuclear detail. Alcohols are used primarily for cytologic smears. They are fast acting, cheap, and preserve cells through a process of dehydration and precipitation of proteins. Methanol has been shown to be effective during immunostaining [6–10, 16, 17, 19].

5. Mercurials fix tissues by an unknown mechanism. They contain mercuric chloride which is a known component in fixatives such as B-5 and Zenker's. These fixatives offer poor penetration and tissue hardness, but are fast and provide excellent nuclear detail, such as for visualization of hematopoietic and reticuloendothelial tissues (i.e., lymph nodes,

spleen, thymus, and bone marrow). These fixatives must be disposed of carefully. Mercury deposits must be removed (dezenkerized) prior to staining, otherwise black deposits will occur in tissue sections [6–10, 16, 17].

6. Picrates include fixatives with picric acid, such as Bouin's solution. These fixatives have unknown modes of action. The most common is Bouin's alcoholic fixative. This fixative provides good nuclear detail and does not cause much hardness. It is recommended for fixation of testis, gastrointestinal tract, and endocrine tissues. This fixative has an explosion hazard in dry form, so it must be kept submerged in alcohol at all times [6–10, 16, 17].
7. Other factors affecting fixation

   i. Buffering: Fixation is best performed at close to neutral pH (pH 6–8; formalin is buffered with phosphate at pH 7). Common buffers include: phosphate, bicarbonate, cacodylate, and veronal [6–10, 16, 17].

   ii. Penetration: Each fixative has its own penetration rate in tissues. While formalin and alcohol penetration are superior, glutaraldehyde is the worst. Mercurial fixatives are in between. The thinner the sections are cut, the better the penetration [6–10, 16, 17].

   iii. Volume: The volume of the fixative should be in at least a ratio of 10:1. Fixation can be enhanced if the fixative solution is changed at regular intervals and the specimen is agitated [6–10, 16, 17].

   iv. Temperature: If the temperature at which fixation is carried out is increased, it will yield an increased speed of fixation. Of course, too much heating of the fixative can result in cooking or creating tissue artifacts [6–10, 16, 17].

   v. Concentration: The concentration of the fixative should be as low as possible, because too high a concentration may adversely affect the tissue and provide artifacts (formalin is best at 10%, while glutaraldehyde is best at 0.25–4%) [6–10, 16, 17].

   vi. Time interval: The faster the fresh tissue can be acquired and fixed, the better, as to minimize cellular organelle degradation and nuclear shrinkage, resulting in artifacts. The tissue should always be kept moist with saline [6–10, 16, 17].

2.6. Decalcifying agents

Some animal tissues contain deposits of calcium salts which may interfere with sectioning, resulting in torn sections and damaged blades. Calcium compounds must be chemically removed (usually with an acid) before typical histological techniques can be used for the study of softer components. Tissues requiring decalcification include bone, teeth, and calcified cartilage [17, 20–22]. Pathological states include arteriosclerosis, tuberculosis, and several tumor types. Such tissues should be fixed prior to decalcification and washed for 12 hours in running water between fixation and decalcification. While decalcification agents remove typically calcium salts and do not interfere with staining reactions, they can cause minimal distortion to cells and connective tissue. The decalcifying agent should have a volume of

30–50 times that of the tissue and occasional agitation may be required to expedite this process. Heating should not be employed. The process is complete typically when bubbling has ceased. Over decalcification can cause a severe reduction (of what) in subsequent sectioning of the tissue. Some typical decalcifying agents include, nitric acid, Gooding and Stewart's fluid, Rapid Bone Decalcifier (RDO), and chelating agents. More recently, new methods have been discovered to allow hard tissues to be decalcified faster [23].

2.7. Dehydration

After fixation, and to begin the dehydration step (i.e., removal of water), tissues are placed in progressively increasing concentrations of a dehydrating agent (e.g., 70, 85, 95, and 100%) which is typically ethanol. Methanol, isopropanol, and acetone are alternative options, depending on the tissue being processed. It is important to include two absolute alcohol (i.e., 100%) steps to ensure that all remaining water has been removed. The dehydration step is critical, as water is immiscible with most embedding media (i.e., paraffin wax). Therefore, the tissue must be exchanged between polar (e.g., water) and non-polar (e.g., organic reagents, such as xylene) agents. If the tissue is incompletely dehydrated, it is not possible to "clear" the tissue. When it is exposed to a subsequent clearing agent (e.g., xylene) the tissue remains opaque and appears milky. This will necessitate re-dehydration of the tissue. Dehydration will also remove some of the lipoidal material in the tissue. If the lipids are supposed to be visible, it will be necessary to use an appropriate fixative that will preserve the lipids prior to the dehydration step (e.g., osmium tetroxide) [7–10, 16, 17, 21, 22].

2.8. Clearing

The term "clearing" is related to the appearance of the tissue after it has been treated with a dehydrating agent. Many agents have a similar refractive index to that of the tissue, rendering the tissue "clear" or translucent. In this step, the dehydrating agent must be removed from the tissue and replaced with a solvent of wax. A clearing agent should be used when the dehydrating agent (e.g., ethanol) is not miscible with the impregnating medium/embedding agent (i.e., paraffin wax). It is a wax solvent and must be miscible with both the dehydrating and embedding agents. The selection of a suitable clearing agent should be based on the speed and ease of removal from the embedding media (i.e., the lower the boiling point the more rapid the removal), interaction with the tissue, flammability, toxicity, and cost. The clearing step can be more effective with the use of a vacuum system and should be carried out in a fume hood. Typical clearing agents include xylene, chloroform, toluene, benzene, dioxane, carbon tetrachloride, cedarwood oil, isoamyl acetate, methyl benzoate, methyl salicylate, and clove oil. Due to the potential hazards of some of these chemicals, others have been proposed, such as some vegetable oils, terpenes, and alkanes. Some histological protocols have the potential option of processing the tissue without the use of a clearing agent (e.g., xylene) as a safe alternative to exposure to the hazardous effects of these chemicals. One such protocol includes the use of isopropanol as a safer alternative [7–10, 16, 17, 21, 22, 24–30].

2.9. Infiltration/impregnation

The role of the infiltration agent is to remove the clearing agent from the tissue and to completely permeate the tissue with paraffin wax. This will allow the tissue to harden and produce a wax block from which thin histological sections can be cut. Ideally, the consistency of any solidified embedding medium should be the same as the specimen it encloses. Unfortunately, this rarely happens due to the wide variation in consistency of tissue and the large variety in embedding media. Paraffin wax is commonly used and heated to a temperature that is 2–3°C above its melting point. Any higher temperature will result in tissue hardening. The paraffin wax should be 20–25 times the volume of the tissue. Generally, the tissues are transferred directly from the clearing agent to pure paraffin, but sometimes with fragile specimens, it is necessary to use graded mixtures of clearing agent and paraffin. The duration and number of changes of paraffin necessary for impregnation vary with the size and consistency of the tissue. As exposure of the tissue to paraffin increases, it is more likely that shrinkage and hardening will occur. Complete infiltration is only possible after complete dehydration and complete clearing. The selection of paraffin depends on the nature of the tissue to be embedded and thickness of section required. A high melting point of the wax (e.g., 55–60°C) increases the hardness and decreases the thickness to which the tissue may be sectioned (e.g., 45–50°C is considered soft). Paraffin wax can be purchased in the form of tablets, pellets, or granules. Numerous substances can be added to the molten paraffin to modify its consistency and melting point. Typically, the process of infiltration occurs with the use of a tissue processing machine, although this can be carried out using a heated container maintained 2–3°C above the melting point of wax. If residual clearing agents remain in tissue or improper processing of the tissue has occurred, this will lead to difficulties with sectioning. Evaporation of the clearing agent, infiltration with paraffin wax, and removal of any air bubbles trapped in the specimen will be more completely alleviated if clearing and infiltration procedures are carried out at reduced pressure (under vacuum) [7–10, 16, 17, 21, 22, 24–28].

2.10. Embedding

After the infiltration process has been completed, it is necessary to obtain a solid block containing the tissue. To accomplish this, it is necessary to first coat a stainless steel histological base mold of suitable size to fit the tissue with glycerol or "mold release" to prevent adherence of the wax block containing the tissue to the metal mold upon solidification. Pre-warming of the metal block is advised to prevent premature solidification of the wax block. In addition, using warmed forceps to help press the tissue against the base of the metal mold, in addition to reducing the chance of premature solidification, helps with this process. Prior to beginning the infiltration process, an embedding cassette should be placed on top of the mold and labeled with the name of the tissue, fixative, and date. If an embedding unit (machine) is being used, the combined unit should be dispensed two-thirds full with molten paraffin. The specimen should be oriented in the metal mold to ensure that the tissue will be cut in the correct plane of section. Alternatively, the mold can be filled slightly and the tissue can then be placed in the mold and positioned in the desired orientation at the base of the mold.

The combined unit should then be set out on the cooling tray of the embedding unit (machine) and not disturbed until the wax has cooled and solidified completely. After sufficient time, the cassette and mold should be separated and the paraffin block should be placed in the microtome in preparation for sectioning. If the tissue has been thoroughly fixed, dehydrated, cleared, and infiltrated, tissues embedded in paraffin wax provide good cutting qualities. On average, paraffin blocks remain durable and retain their good cutting qualities and staining characteristics indefinitely [7–10, 16, 17, 21, 22, 24–28].

2.10.1 Embedding media

The most common infiltrating agent and embedding medium is paraffin wax. Ester wax offers a lower melting point than paraffin wax and tends to be harder when solid, allowing this medium to be suitable for cutting thinner (i.e., 2–3 μm) sections with minimal tissue shrinkage.

When water-soluble waxes (i.e., polyethylene glycol waxes) are used, tissues are transferred directly from aqueous fixatives to wax for infiltration without dehydration or clearing. This results in less tissue shrinkage, but sectioning is more difficult than with paraffin wax. Tissue blocks must be kept in a dry atmosphere. If cellulose nitrate (i.e., celloidin/low-viscosity nitrocellulose) is chosen as an embedding medium, tissues must be dehydrated and embedded with solutions of cellulose nitrate dissolved in an alcohol/ether mixture. The solvent is allowed to evaporate to produce a tissue block of required consistency. No heat is applied using this method. This medium is used typically for large pieces of, for example, bone and brain tissues. Synthetic resins are used for preparing sections most typically for electron microscopy and light microscopy (0.5–2 μm sections), such as for undecalcified bone. Freeze-drying protocols can be applied when special staining techniques are used [7–10, 16, 17, 21, 22, 24–28].

3.Microtomy

Microtomes are used to cut the tissue into thin sections for microscopic viewing. The type of specimen will determine the type of microtome to be used. Rotary microtomes are the most common microtomy instrument. The feed mechanism is achieved by turning a wheel at one side of the machine. While the knife is fixed and is secured in a knife holder, the object moves against the cutting surface of the knife, according to the thickness of section required. The knife holder allows the knife to be set at an oblique angle to the specimen. One complete rotation of the operating wheel is equivalent to one complete cycle. The downward motion of the knife reflects the cutting stroke, while the upward stroke reflects the return stroke and activation of the advance mechanism. The feed mechanism is activated by turning a wheel located on the side or top of the microtome. The tissue block is passed across the knife at every stroke to produce a section. Microtomes have a feed mechanism to advance the specimen (or knife) to a predetermined thickness for sectioning (i.e., typically 5–10 μm) and can produce serial sections [7–10, 16, 17, 21, 22, 24–28].

3.1. Cryostat

A cryostat or freezing microtome is used for obtaining thin sections of unfixed tissues. It can be used, additionally, for observing fatty tissues. The microtome is maintained at −15 to −20°C in a refrigerated chamber. The cabinet is designed to operate at −5 to −30°C. The tissue block can be mounted in a high-viscosity water-soluble gel, such as 1% glucose, gelatin, or cellulose on the platform and must be frozen immediately. An anti-roll plate is used to keep sections flat on the knife blade for direct mounting onto the slide. Sections are cut one at a time. When a section is cut, the anti-roll plate is lifted and a section is picked up from the surface of the knife and placed onto a slide using a camel hair brush. Sections are fixed in 5% acetic acid in absolute alcohol and then subsequently stained (e.g., with hematoxylin and eosin). Frozen sectioning is typically used for rapid preparation and diagnosis by a pathologist [7–10, 21, 22].

3.2. Microtome knives

There are many different types of microtome knives (e.g., stainless steel, carbide, diamond, glass, or disposable blades). Wedge-shaped stainless steel knives are used for most paraffin-embedded specimens. They must be kept clean and well-oiled or lubricated. The knife's edge should be cleaned with a clearing agent with a soft, moistened cloth in a fume hood. As an alternative to wedge-shaped stainless steel knives, disposable blades provide an excellent cutting edge for paraffin sectioning and are available in different sizes and thicknesses. Glass, sapphire, and diamond knives are used for specimens embedded in hard resin plastic (e.g., epoxy, glycolmethacrylate). Diamond and sapphire knives tend to function better than glass knives, but are much more expensive. If a wedge-shaped stainless steel knife is used, it must be free of nicks and sharpened with a carborundum stone (manual sharpening) or by an automatic knife sharpener (with a glass wheel and with an abrasive). A process called stropping produces a finely polished, smooth, and even knife edge. The knife is secured at the desired angle place by adjusting holder screws [7–10, 16, 17, 21, 22, 24–28].

3.3. Section thickness and rough cutting

A thickness of 6 μm is standard for histological tissue sections. For highly cellular tissues (e.g., lymph nodes), 4 μm is used most often. For thicker sections, 10 μm is used. For neurological tissues and myelinated nerves, 6–20 and15–20 μm is used, respectively. The tissue block will be examined to establish how it needs to be oriented in the block holder. Excess paraffin should be trimmed away from each side of the tissue block to create a trapezoid shape. The longer edge should be parallel with the knife edge. The tissue block should be roughly cut by advancing the block manually and sectioning until the entire surface of the tissue is exposed [7–10, 16, 17, 21, 22, 24–28].

3.4. Section adhesives, sectioning tissues, and sealing of blocks

Section adhesives, such as gelatin, casein glue, starch, and albumin, can be used to aid in adhering sections to the slide prior to further processing, such as staining. Gelatin can be

added to the water bath. The use of adhesives in the water bath promotes bacterial and fungal growth. Daily cleaning of the water bath with sodium hypochlorite solution (e.g., Clorox soap) is necessary to prevent contamination. Alternatively, a thin coat of albumin can be applied directly to the slide by dipping it into the solution or using your fifth finger (i.e., most ulnar and smallest finger). This latter process is referred to as "subbing." A newer idea is to use "plus" (+) slides. Treatment of the slide with a reactive silicon or polylysine compound chemically changes the glass, such that it bears abundant amino groups, which ionize to provide a positively charged surface. Sections which contain a preponderance of anionic groups, such as carboxyls and sulfate-esters adhere strongly to this modified glass. When creating a ribbon (what is a ribbon), i.e., a series of adjacent tissue sections, the hand wheel should be turned at a slow and even speed. Rotating the wheel too rapidly will cause sections of unequal thickness. The floatation bath should be heated to a few degrees below the melting point of the paraffin wax. Tap, deionized, or distilled water can be used. The ribbon should be gradually lowered onto the flotation bath to eliminate wrinkles and entrapped air. Air bubbles may be removed with a camel's hair brush or by submerging a slide under the ribbon. If the sections are wrinkling, a 70% alcohol solution can be added to the water bath prior to section collection. If necessary, sections may be separated, depending on their sizes, and each can be placed on a clean, pre-marked glass slide. Individual sections or tissue ribbons may be picked up by submerging a clean glass slide into the water bath at a ~45° angle, directly beneath the location of the section or ribbon. The slide should be lifted out of the water slowly to ensure that the sections lay on the slide. The slides should be drained vertically on a paper towel for several minutes before placing them onto a warming table (37–40°C). The slides should remain on the warming table, overnight, for 20–30 minutes at approximately 58°C or a few degrees below the melting point of the paraffin wax. Failure to drain the slides will create air bubbles under the tissue and decrease the section's adhesion to the slide. Air bubbles produce section unevenness and staining artifacts, making the final preparation difficult to examine with the microscope. Once the desired sections have been cut, the block can be removed from the block holder and sealed with molten paraffin wax to ensure that the tissue will not dry out and become brittle (blocks can last for weeks, months, or years) [7–10, 16, 17, 21, 22, 24–28].

3.5. Problems encountered with sectioning tissue blocks

Histologists are confronted often with difficult tissue blocks that will not section easily. This may be the result of, for example, brittle or shrunken tissue, improperly infiltrated tissues, or sections with, for example, holes or scratches in them. If the tissue block appears to be brittle, a 10% diluted ammonium hydroxide solution may be applied (via soaking) to soften the tissue to prevent cracking and to more easily facilitate sectioning. If sections have holes in them, this can be indicative of incompletely infiltrated tissue. This may be alleviated by placing the tissue block back in the heated wax bath to melt it and then proceed to re-embed the block. If artifactual scratches or tears occur across the tissue sections, this may be indicative of flaws or dirt on the cutting edge of the knife and may be alleviated by repositioning or replacing the blade. Alternatively, other problems can occur if the tissue block appears to be too soft or too hard. If too soft, a remedy may be to place the block tissue side down on several sheets of Kimwipes or paper towel in the freezer (−15°C) or a refrigerator (0–4°C) (chilling times may vary), prior to sectioning. This technique will help to harden the wax so that it better matches the hardness

of the infiltrated tissue and will result in more successful tissue sectioning. If too hard, a piece of wet cotton/Kimwipe may be placed in lukewarm water and then placed over the surface of the block (times may vary). This will allow the tissue to expand/swell and soften as it absorbs water. It should be noted, however, that with either too soft or too hard tissue blocks, these solutions are temporary and may allow only a few successful sections to be cut [31, 32].

4. Staining

Staining of tissue slides is carried out by reversing the embedding process in order to remove the paraffin wax from the tissue to allow water-soluble dyes to penetrate the sections. This process is referred to as "deparaffinization." The tissue slides must be exposed to a clearing agent and subsequently taken through a descending alcohol series to water (also referred to as "bringing your slides to water"). Choosing the appropriate dye for a particular tissue slide is related to its ability to color otherwise transparent tissue sections and various cellular components of the tissue. The term "routine staining" includes the hematoxylin and eosin (i.e., H and E) stain. This stain is used routinely as it provides the pathologist or researcher with a detailed view of the tissue, clearly staining, for example, the cytoplasm, nucleus, and organelles. The term "special stains" refers to a large number of staining techniques, other than H and E, that allow the visualization of particular tissue structures, elements, or microorganisms that cannot be identified with H and E staining [6–10, 17, 21, 22, 24–28, 31–35]. Examples include, Masson's trichrome (e.g., skin; identification of collagenous connective tissue), GMS silver stain (e.g., lung; identification of *Pneumocystis* or *Aspergillus* spp.), Periodic acid-Schiff (e.g., kidney; identification of high proportion of carbohydrates, such as glycogen, glycoproteins, and proteoglycans), Perl's Prussian blue iron (e.g., liver; identification of ferric (Fe^{3+}) iron in tissue preparations or blood and bone marrow smears), Ziehl-Neelsen (acid-fast bacillus) (e.g., lung; identification of acid fast bacilli), Alcian blue (e.g., intestine; identification of acid mucopolysaccharide and acidic mucins), Alcian blue and PAS (intestine; combination of staining properties of both Alcian blue and Periodic acid-Schiff for identification of similar tissue components), Gomori trichrome (blue or green) (e.g., submucosa, identification of muscle fibers, collagen, and nuclei) [36].

Acknowledgements

This work was supported in part by grants from the National Institutes of Health (GM058264) and the National Science Foundation (1626326) to VDCS and from the National Science Foundation (1355034) and the Latham Trust Fund to TH.

Conflict of interest

The authors declare that there are no conflict of interests regarding the publication of this chapter.

Author details

Vonnie D.C. Shields[1]* and Thomas Heinbockel[2]*

*Address all correspondence to: vshields@towson.edu and theinbockel@howard.edu

1 Jess & Mildred Fisher College of Science and Mathematics, Towson University, MD, USA

2 Department of Anatomy, Howard University College of Medicine, Washington, DC, USA

References

[1] Kegley JA. Challenges to informed consent. EMBO Reports. 2004;**5**(9):832-836. DOI: 10.1038/sj.embor.7400246

[2] Office of Laboratory Animal Welfare National Institutes of Health. Institutional Animal Care and Use Committee Guidebook. Bethesda, MD: Office of Laboratory Animal Welfare National Institutes of Health; 2002. Available from: https://grants.nih.gov/grants/olaw/guidebook.pdf

[3] National Research Council of the National Academies. Guide for the Care and Use of Laboratory Animals. 8th ed. Washington, DC: The National Academic Press; 2011. Available from: https://grants.nih.gov/grants/olaw/guide-for-the-care-and-use-of-laboratory-animals.pdf

[4] Mukai S, Itoi T, Katanuma A, Irisawa A. An animal experimental study to assess the core tissue acquisition ability of endoscopic ultrasound-guided histology needles. Endoscopic Ultrasound. 2018;**7**(4):263-269. DOI: 10.4103/eus.eus_16_17

[5] Mescher AL. Junqueira's Basic Histology: Text and Atlas. 14th ed. New York: McGraw Hill Medical; 2016. 560 p

[6] Baker JR. Principles of Biological Microtechnique: A Study of Fixation and Dyeing. London, England: Methuen & Co. Ltd; 1958

[7] Sanderson JB. Biological Microtechnique. Royal Microscopical Society Microscopy Handbooks. Vol. 28. Preston, UK: Bios Scientific Publishers Limited, A.M.A. Graphics Ltd.; 1994. 224 p

[8] Preece A. Manual for Histologic Technicians. 3rd ed. Boston, MA: Little, Brown and Company; 1972. 428 p

[9] Armed Forces Institute of Pathology Laboratory Methods in Histotechnology. In: Prophet EB, Mills B, Arrington JB, Sobin LH, editors. American Registry of Pathology. Washington, DC; 1992. 275 p

[10] Clayden EC. Practical Section Cutting and Staining. 2nd ed. London, England: J. & A. Churchill Ltd.; 1951

[11] Mayers CP. Histological fixation by microwave heating. Journal of Clinical Pathology. 1970;**23**(3):273-275

[12] Tripathi M, Bansal R, Gupta M, Bharat V. Comparison of routine fixation of tissues with rapid tissue fixation. Journal of Clinical and Diagnostic Research. 2013;**7**(12):2768-2773

[13] Leong ASY, Duncis CG. A method of rapid fixation of large biopsy specimens using microwave irradiation. Pathology. 1986;**18**:222-225

[14] Panja P, Sriram G, Saraswathi TR, Sivapathasundharam B. Comparison of three different methods of tissue processing. Journal of Oral and Maxillofacial Pathology. 2007;**11**:15-17

[15] Wagenaar F, Kok GL, Davies JMB, Pol JMA. Rapid cold fixation of tissue samples by microwave irradiation for use in electron microscopy. The Histochemical Journal. 1998;**25**:719-725

[16] Klatt EC. Histotechniques in The Internet Pathology Laboratory for Medical Education. The University of Utah Eccles Health Sciences Library. Salt Lake City, UT: 1994-2018. Available from: https://library.med.utah.edu/WebPath/webpath.html#MENU

[17] Kiernan JA. Histological & Histochemical Methods: Theory & Practice. 2nd ed. Oxford, England: Pergamon Press; 1992

[18] Buesa RJ. Histology without formalin? Annals of Diagnostic Pathology. 2008;**12**(6):387-396. 433 p

[19] Levitt D, King MJ. Methanol fixation permits flow cytometric analysis of immunofluorescent stained intracellular antigens. Journal of Immunological Methods. 1987;**96**(2): 233-237

[20] Sanjai K, Kumarswamy J, Patil A, Papaiah L, Jayaram S, Krishnan L. Evaluation and comparison of decalcification agents on the human teeth. Journal of Oral and Maxillofacial Pathology. 2012;**16**(2):222-227. DOI: 10.4103/0973-029X.99070

[21] Gray P. Handbook of Basic Microtechnique. 3rd ed. New York: McGraw-Hill Book Company Inc; 1964. 302 p

[22] Humason GL. Animal Tissue Techniques. 4th ed. San Francisco, CA: W.H. Freeman and Company; 1979. 661 p

[23] Kapila SN, Natarajan S, Boaz K, Pandya JA, Raviteja S. Driving the mineral out faster: Simple modifications of the decalcification technique. Journal of Clinical and Diagnostic Research. 2015;**9**(9):ZC 93-ZC 97. DOI: 10.7860/JCDR/2015/14641.6569

[24] Willey RL. Micro techniques: A Laboratory Guide. New York: The Macmillan Company; 1971. 99 p

[25] Davenport HA. Histological and Histochemical Techniques. Philadelphia: W.B. Saunders Company; 1969. 401 p

[26] Sheehan DC, Hrapchak BB. Theory and Practice of Histotechnology. 2nd ed. St. Louis, MO: CV Mosby Company; 1987. 481 p

[27] Drury RAB, Wallington EA, Cameron SR. Carleton's Histological Technique. 4th ed. New York: Oxford University Press; 1976. 432 p

[28] Bancroft JD, Stevens A. Theory and Practice of Histological Techniques. 2nd ed. New York: Churchill Livingstone; 1982. 662 p

[29] Buesa RJ, Peshkov MV. Histology without xylene. Annals of Diagnostic Pathology. 2009; **13**(4):246-256. DOI: 10.1016/j.anndiagpath.2008.12.005

[30] Richardson DS, Lichtman JW. Clarifying tissue clearing. Cell. 2015;**162**:246-257

[31] Berlyn GP, Miksche JP. Botanical Microtechnique and Cytochemistry. Ames, IA: The Iowa State University Press; 1976. 326 p

[32] Rolls GO. 101 Steps to Better Histology. Leica Biosystems. Available from: https://www.leicabiosystems.com/fileadmin/biosystems/PDF/95.9890_Rev_C_Difficult_Blocks_and_Reprocessing.pdf

[33] Horobin RW, Bancroft JD. Troubleshooting Histology Stains. New York: Churchill Livingstone; 1998. 266 p

[34] Cook HC. Manual of Histological Demonstration Techniques. London, England: Butterworths & Co. Ltd.; 1974. 314 p

[35] Troyer H. Principles and Techniques of Histochemistry. Boston MA: Little, Brown and Company (Inc.); 1980. 431 p

[36] James A. An Introduction to Routine and Special Staining. Leica Biosystems. Buffalo Grove, IL. Available from: https://www.leicabiosystems.com/pathologyleaders/an-introduction-to-routine-and-special-staining/

Section 2

Basic Histology

Chapter 2

Epithelial Development Based on a Branching Morphogenesis Program: The Special Condition of Thymic Epithelium

Juan José Muñoz and Agustín G. Zapata

Additional information is available at the end of the chapter

http://dx.doi.org/10.5772/intechopen.81193

Abstract

Numerous epithelia undergo tubulogenesis and branching morphogenesis during their development (i.e., lung, salivary gland, pancreas) in order to establish sufficient available surface for their proper functioning. The thymus is a primary lymphoid organ constituted by pharyngeal-derived epithelium necessary to produce immunocompetent lymphocytes whose mechanisms of development are not fully known. In the current chapter, we review histological, cellular, and molecular mechanisms governing early thymic epithelium development emphasizing its resemblance with the process of branching morphogenesis and tubulogenesis occurring in other epithelial organs in which epithelial-mesenchyme interactions determine the tissue patterning through specific combinations of common molecular signaling pathways.

Keywords: branching morphogenesis, epithelium, tubulogenesis, thymus, thymic epithelium

1. Introduction

Many epithelia, particularly those derived from the gut, organize tubular structures (i.e., mammary gland, salivary glands, lungs, kidneys, pancreas) that repeatedly fold to reach an enlarged area necessary to perform their major functions (i.e., gas exchange, excretion, nutrient transport, etc.). Whereas a branching morphogenesis pattern of development is well established in the case of the respiratory system or in the exocrine glands, it appears to be less evident for other endoderm-derived organs, such as the endocrine glands or the lymphoid organs.

In the present chapter, we will examine prior studies supporting the claim that the development of other branching organs as lung, salivary gland, pancreas, or kidney, despite their morphological and functional differences, follows common patterning programs under the control of epithelium-underlying mesenchyme interactions governed by a few families of molecules (FGF/FGFR, Wnt, BMP/TGFβ, Shh), and that the thymus, an epithelial primary lymphoid organ derived from the ventral endoderm of the third pharyngeal pouch, despite following the same pattern, constitutes a special case. Remarkably, its functions are not related to those of other epithelia of similar origin but rather to the establishment of a 3D epithelial network necessary for the functional maturation of thymocytes. Before acquiring their specific features, distinct epithelial organs, therefore, follow a common complex pattern of development which includes different processes. After a first step of specification from the original embryonic layer, they undergo a process of **tubulogenesis** consisting of outgrowth and extension of the epithelial primordium forming a tubular structure. A complex program of **branching morphogenesis helps to** increase the functional area of the organ. Finally, **terminal epithelial differentiation** prepares the primordium to become a functional organ.

2. The early development of endodermal epithelial organs

2.1. Specification and primordium development

The process of development followed by these epithelial tissues is well exemplified by the early development of salivary glands. The primordium of submandibular glands raises from an evaginated thickening of ectoderm-derived oral epithelium into the neural crest-derived mesenchyme at the base of tongue [1]. The evaginated epithelium proliferates forming an epithelial "stalk" and a terminal bud. The stalk will evolve into excretory duct cells, and the buds will establish the named "pseudoglandular" area by repeated elongation and branching morphogenesis, which will finally differentiate into functional acini (**Figure 1**) [2].

In mice, mammary placodes are visible at E11-E12 and become buds at E13 when surrounded by several layers of mesenchyme. Signals from the mesenchyme of cardia and septum transversum determine the hepatic fate in the foregut endoderm, [3] inducing expression of the transcription factor Hhex, but not Pdx1, whereas the Hhex-Pdx1+ foregut endoderm will differentiate into the extrahepatic bile ducts and the ventral pancreas [4]. Apart from this ventral area, the embryonic pancreas in vertebrates forms from a dorsal protrusion of the primitive gut epithelium, which express Mnx1 [5]. These two pancreatic buds grow, branch, and fuse to form a multilayered epithelium (E9.0 to E11.5), which forms the definitive pancreas. This stratified epithelium consists of two domains: an outer layer of semipolarized "cap" cells, which express only basal markers, and an inner "body" of nonpolarized cells [6, 7] (**Figure 1**).

At E9.0-E9.5, Nkx2–1, a transcription factor specific of the lung, is determined on the ventral side of the anterior foregut by Wnt ligands expressed in the surrounding ventral mesoderm that activates the canonical Wnt pathway in the epithelium. One day later, Nkx2–1+ cells extend ventrally forming a primitive trachea and two lung buds, whereas Sox 2 expression restricted on the distal foregut endoderm will determine the esophagus. Next, the trachea and the esophagus become fully separated [8] (**Figure 1**). Thus, absence of Wnt signaling

http://dx.doi.org/10.5772/intechopen.81193

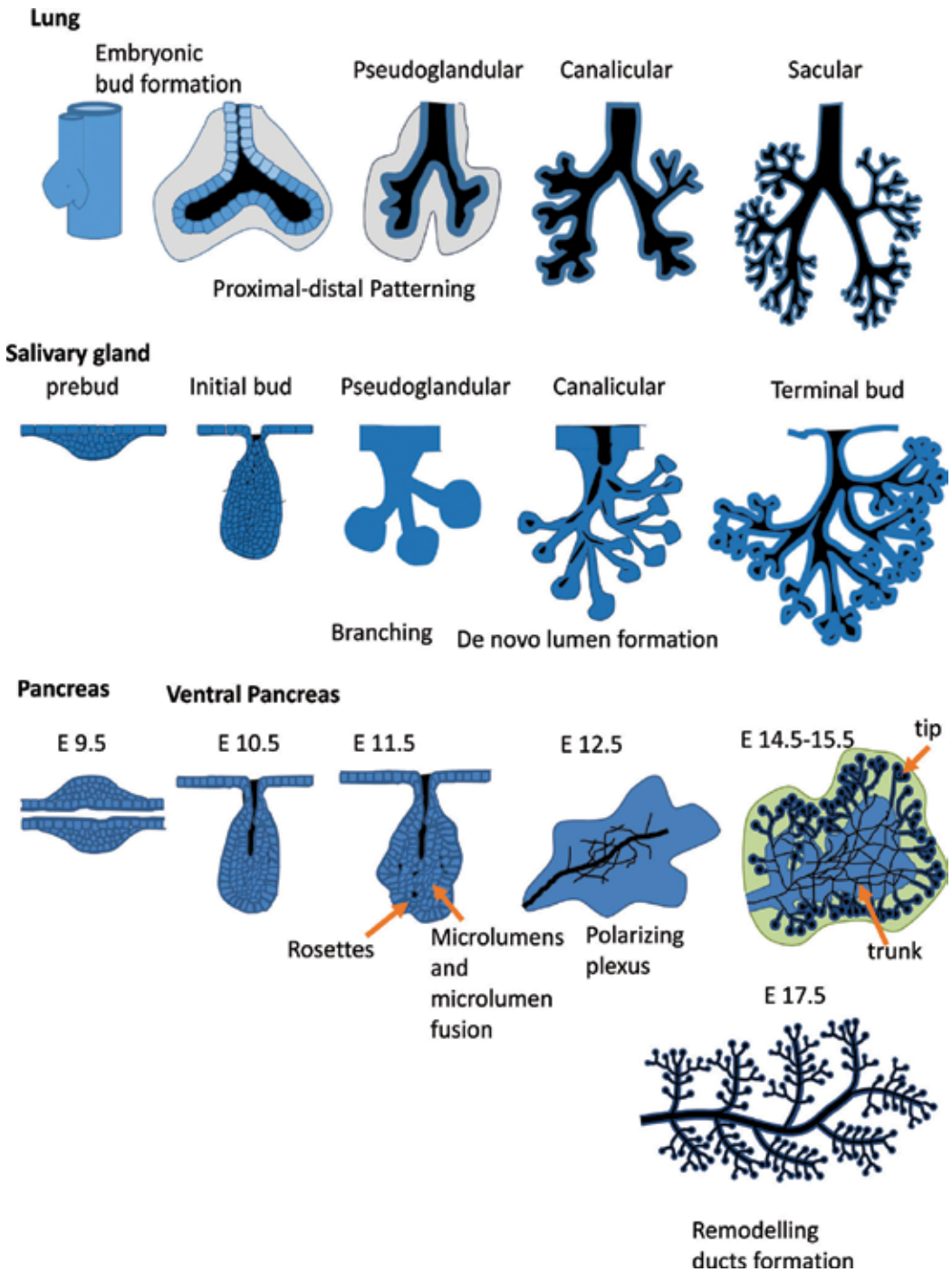

Figure 1. Different models of branching morphogenesis occurring during development of lung (branching of tubes), salivary gland (branching of an unpolarized primordium and later de novo lumen formation), and pancreas (polarization and remodeling of an unpolarized mass resulting in more synchronous branching, lumen formation, and differentiation). Modified from [5, 6, 140].

courses with lack of Nkx2–1 expression, absence of tracheal morphogenesis, and lung agenesis [9]. BMP expression in the ventral mesoderm is necessary to establish a proper location of the lung along the proximal distal axis of the foregut [8]. Also, FGF molecules expressed in the ventral mesoderm reinforce early lung specification of the foregut endoderm [8]. Murine embryos deficient in either FGF10 or FGFR2b exhibit a stopped salivary gland development at the initial bud stage [10], and conditioned deletion of FGF8 in the ectoderm results in arrest of salivary gland development [11]. The process could be more complex because specific overexpression of FGF7 in the salivary gland epithelium produces small glands that exhibit delayed differentiation [12], and elimination of FGF signaling antagonists, Sprouty 1 and 2, impairs salivary epithelium development [13]. Indeed, multiple branching organs undergo agenesis after deletion of either FGF10 or its receptor FGFR2b [10].

2.2. Tubulogenesis

Both mono- and pluristratified epithelia have the capacity to fold and form tubes [14]. Distinct mechanisms of cellular binding have been reported, including the orientation of cells via cell-to-cell and cell-ECM interactions, the establishment of apical-basal polarity, changes in the cellular shape and migration capacities, and formation and expansion of the luminal spaces, which eventually fuse establishing a unique cavity [14, 15].

Although some tubules show lumens surrounded by a single cell, they normally consist of multicellular lumens sealed by cell junctions. In addition, tubules may branch (see later) and/or differentiate into end buds or cap-like structures, as acini (pancreas, mammary, and salivary glands) or alveoli (lung) [16] (**Figure 1**). Further variability in the process of tubulogenesis is provided by the distinct mechanisms used for the formation of lumens. Budding, wrapping, entrapment, cavitation, and hollowing have been described in organs, which undergo tubulogenesis during their development. Budding or wrapping occur in polarized epithelia, as is the case of the lung, whereas the formation of tubules by entrapment, cavitation, or hollowing is performed by nonpolarized cells [16]. In the entrapment, migrating cells trap an extracellular space and form a lumen [17]. By contrast, the formation of lumens by cavitation, reported in mammary and salivary glands, implies programmed cell death to create a cell-free space [18], whereas in the hollowing, the luminal space is organized de novo via exocytosis of intracellular vesicles [19]. The salivary glands, the liver, or the pancreas undergo polarization from unpolarized primordia (**Figure 1**). In the pancreas, E10.5–11.5 individual cells within the inner body of pancreatic buds acquire apico-basal polarity and rearrange to form microlumina by fusion of apical membrane-containing vesicles with the cell membrane. During this process, the asynchronous apical constriction of individual polarized cells generates rosettes with a central lumen that later expand and eventually fuse to generate an immature, highly interconnected tubular plexus, consisting of stratified epithelial cells surrounded by an epithelial periphery [7]. Their reorganization will form the ductal system and primordial endocrine islets and the acinar exocrine cells, respectively (**Figure 1**) [5, 6].

In the salivary gland, lumen formation takes place and evolves along the forming branched structure, following branching progression. Initially, epithelial cell polarization results in multiple microlumens that fuse to form a contiguous lumen [20] (**Figure 1**). The signaling events controlling microlumen fusion to establish a common single lumen are just beginning to emerge [15].

As above indicated, the establishment of cell polarity, in which cues provided by neighboring cells and ECM play major roles, has particular relevance for epithelial tubulogenesis. These cues activate signaling pathways, particularly those mediated by Wnt ligands and their receptors [15], which modify the cytoskeleton, cell contractibility, and trafficking, as well as the transcription program. Wnt ligands and receptors arrange in the epithelial cells in a polarized manner. Wnt5a and 3a are released specifically throughout the basolateral cell surface, where their specific receptors, Fz2, LRP6, and Rer2 are expressed [21]. In the embryonic midgut, Wnt5a is produced by mesenchyme cells under the basement membrane and it activates Wnt5a receptor (Fz2, Rer2) on the basolateral domains of epithelial cells, resulting in Rac-dependent adhesion, establishment of apical/basal polarization, formation of cell junctions, and organization of intracellular molecule trafficking necessary to establish different apical and basal domains.

The developing submandibular gland expresses numerous Wnt ligands and receptors, as well as antagonists in both epithelium and mesenchyme and are accurately regulated spatially and temporally [13]. Wnt signaling promotes duct development by coordinating canonical and noncanonical pathways. Canonical activation through Wnt/β-catenin signaling inhibits end bud formation, whereas Wnt 5b activates the noncanonical Wnt pathway to determine duct formation with the concourse of the transcription factor, TFCP2L1. Inhibition of end bud formation is a consequence of the absence of Wnt distally, regulated by FGF signaling that represses Wnt5b expression and upregulates the Wnt inhibitor, SFRP1, (secreted related frizzled protein 1), which sequesters Wnt proteins [22].

Likewise, retinoid acid produced by foregut mesenchyme before lung specification [23] signals through retinoid acid receptor B in the mesoderm to regulate FGF expression [24]. Shh signaling in the mesoderm is also a regulator of the initial lung bud outgrowth [25].

Distinct members of the EGF family (EGF, TGFα) and their receptors (EGFR 1, 2, 3) as well as heparin-binding EGF (HBEGF) and neuregulin are differentially expressed in the salivary glandular epithelium and mesenchyme, and the activation of EGF receptors modulates ductal morphogenesis by governing progenitor cell differentiation and expansion [26].

Hedgehog proteins, mainly Shh and their receptors Patched1 and Smoothed, also participate in the organization of a salivary duct and a preacinar end bud (prostate, sebaceous glands, mammary glands, lung) [11], but its effects on these organs are indirect because Hh signals in the mesenchyme, whereas in the salivary gland, the action is directly exerted on duct epithelium [26]. On the other hand, overexpression of Gli-1, one effector of Hh pathway in keratin+ epithelial cells, results in large lumens, duct expansion, and loss of acini [27]. Again, Hh and FGF8 appear to cooperate in these processes. FGF is a Gli3-mediated target of Hh signaling pathway. Both FGF8 and Shh positively upregulate each other [28], and the former rescues defects in salivary gland development produced by cyclopamine, a blocker of Hh signaling [11]. Shh could collaborate with other molecules, such as ectodysplasin [29] or TGFβ [30] in the formation of the salivary gland duct, but results are contradictory.

2.3. Branching morphogenesis

Branching morphogenesis constitutes a developmental program that induces the building of an arborized network, in which new tubules arise from the pre-existing ones by repeated

rounds of sprouting [15]. Two morphological models can be distinguished: de novo branching from the surface of a primordial epithelium or the lateral side of a pre-existing branch (budding) and the splitting of a pre-existing branch tip into several tips (clefting) [31]. Moreover, branching morphogenesis can be stereotypic as occurs in the kidney branches [32] or stochastic, without a defined pattern, as reported in mammary gland or salivary gland [31]. At the cellular level, new branch formation can be driven by collective cell migration, patterned cell proliferation and differential growth, coordinated cell deformation or epithelial folding, and/or cell arrangement and matrix-driven branching [31]. Budding in blood vessels and Drosophila trachea follows an invasive form of collective cell migration, whereas in mammalian epithelial organs (i.e., mammary gland) budding appears to be powered by a noninvasive form of collective cell migration along with cell proliferation [33].

Cell proliferation is related to organ growth, and differential cell proliferation may be related to branched budding [31]. Blocking cell proliferation abolishes budding in cultured mouse lung [34] and mammary gland [33], whereas clefting in salivary gland still proceeds [35] mediated by cytoskeleton and ECM remodeling [36]. Clefting at the branch tip in lung and kidney requires proliferation to enlarge the tip, which deforms and splits [37]. In kidney, other factors contribute because less mesenchyme cells correlate with less branching [38], and studies on the 3D morphology of fetal organs demonstrate that the local geometry of the epithelial buds determine the pattern of branching [32].

In lung, branching involve cytoskeleton-mediated constriction of the apical surface of cells [39], with the concourse of Rho GTPases and the involvement of Wnt-dependent planar cell polarity pathway [15].

ECM elements also play an important role in branching morphogenesis. Thus, fibronectin accumulates at branch point constriction and its block inhibits cleft formation [40]. In addition, the loss of β1 integrin that interacts with fibronectin blocks the branching morphogenesis inducing a multilayered epithelium [41]. Degradation of collagen 1 and collagen 3 reduces cleft formation and, therefore, branching [42], and the blockade of laminin α1 or γ1 inhibits branching in culture [43], whereas laminin α5−/− embryos show reduced branching [44].

In many organs, branching occurs through repetitive clefting and elongation of epithelial end buds at distal ends, but whereas in some of them, such as the pancreas, lumen formation occurs concomitantly with branching [7]; in others (i.e., salivary glands), there is a substantive delay between the two processes [45] (**Figure 1**). In pancreas, lumen formation gives rise to a plexus and, at the same time, the epithelial bud is progressively transformed into a lobulated surface of multiple minor protruding tips interrupted by epithelial ridges. Progressive remodeling of the pancreatic plexus in an outside-in continuous manner, eventually leading to a single-layered epithelial network surrounding a single lumen [6, 46] (**Figure 1**).

In the same manner as previous stages of epithelium development, branching morphogenesis is controlled through epithelial-mesenchyme interactions mediated by a network of signaling pathways that includes largely Wnt, FGF, Shh, and TGFβ/BMP. Mammary glands undergo several processes of branching morphogenesis, associated with their physiological cycle, under control of Wnt signaling [15]. In virgin glands, Wnt2, Wnt5a, and Wnt7b

are strongly expressed but downregulated in pregnancy [47] and overexpression of Wnt 4 increases branching while lacking results in delayed ductal branching [48].

Both canonical and noncanonical Wnt signaling pathways are necessary for lung branching morphogenesis. Reduced canonical Wnt/β-catenin signaling in the pulmonary epithelium causes enlarged bronchioles and reduced epithelial branches and alveoli [49], and conditional deletion of β-catenin or overexpression of Wnt inhibitor Dickkopf 1 severely impairs branching morphogenesis [49, 50] by regulating FGFR2 and BMP4 effects on lung epithelium [50]. BMP4 seems to limit FGF10-mediated lung epithelial outgrowth [51]. Wnt5a appears to be a key for determining the effects of noncanonical Wnt pathway in lung branching morphogenesis. Wnt5a−/− mice exhibit increased formation of peripheral airways [52]. In this case, effects of Wnt5a are mediated through Shh: Wnt5a regulates Shh expression in the lung epithelium and, in turn, Shh regulates FGF10 signaling in the mesenchyme [52].

Several members of the FGF family and their receptors are expressed in the renal stroma whereas FGF stimulation induces the appearance of branched tubular structures [53], and the lack of FGFR2b generates significantly smaller kidneys with reduced branches [54].

FGFR1 and FGFR2 are expressed in pubertal and adult mammary glands, and the specific deletion of FGFR1 in keratin 14+ cells produces a transitional delay of the gland development with reduced ductal outgrowth and branch points [55], whereas the deletion of FGFR2 produces an incomplete branching [56]. In addition, FGF10 directs the early stages of epithelial migration and branching, whereas FGF2 is responsible for epithelial expansion and duct elongation [57].

FGF/FGFR signaling is also a key for generating new branches in the developing lung [58]. FGFR2b, which binds four ligands (FGF1, FGF3, FGF7, and FGF10) detected on mesenchymal cells [58] is largely expressed in the airway epithelium, and FGF signaling in lung is associated with Shh pathway [59]. Activation of FGFR2b on epithelial cells by FGF10 secreted by mesenchyme cells induces Shh expression that creates a negative feedback loop by regulating FGF10 levels [60].

Recently, results on the effects of TGFβ1 have been contradictory. TCFβ1 that accumulates in mesenchyme inhibits the branching by inducing components of ECM [61], but its in vivo elimination does not result in altered branching, perhaps due to the existence of other similar factors as TGFβ2 and TGFβ3 [62].

2.4. Cell differentiation

At the end of the development, specialized epithelial cell types appear and gradually mature. In the case of salivary glands, final differentiation of end buds into secretory acini is followed by further growth and functional differentiation [26] (**Figure 1**).

Complex signaling established between lung epithelium, mesenchyme, ECM and vasculature is essential for normal alveolar space organization. Between E16.5 and 3-5PN, lungs develop at the distal end of branches saccules that finally form alveoli (3-14PN in mice) establishing a proximal-distal polarity in the just formed branches (**Figure 1**). Thus, whereas Sox-2

expressing endoderm progenitors that differentiate into ciliated cells, secretory cells and basal cells concentrate in the proximal zone, pluripotent Sox9/Id2+ progenitor cells that will form types 1 and 2 alveolar cells do so in the distal zone [63].

Pancreatic progenitors simultaneously proliferate and differentiate into the endocrine, ductal and acinar cell lineages. In the E9.5, early primordium, multipotent, unipotent endocrine, and duct-endocrine bipotent precursor cells are present, while a wave of acinar precursor differentiation takes place at the peripheral portion around E11.5–12 as branching morphogenesis initiates and tip differentiation is induced [46] (**Figure 1**). Mesenchymal factors and ECM components increase acinar/tip formation, whereas the interconnection between epithelium and endothelial cells favors trunk development [46].

In both organs, lung and pancreas, notch signaling plays an essential role in the differentiation of distinct cell types. Its chemical inhibition in lung causes expansion of distal progenitor cells and decreased numbers of proximal precursors [64]. On the other hand, during development, increased notch signaling correlates with preferential production of secretory cells versus ciliated and neuroendocrine cells [65]. In addition, activation of Notch in keratin 5+ basal cells promotes secretory cell fate whereas its inhibition favors the differentiation toward ciliated cells [66]. In pancreas, Notch activity regulates tip-trunk patterning. Inducing trunk formation via Nkx6.1 activation and blocking tip fate through Ptf1a repression [6] and regulates the differentiation of Ngn3/Pdx1-positive endocrine progenitors versus Sox9/ Hnf1b-expressing ductal cells from trunk bipotent precursors. The specification, differentiation, and maintenance of acini from tips are regulated mainly by Ptf1a [6, 67].

After branching morphogenesis, there are changes in the epithelial cells and cap mesenchyme cells of the developing kidney [32]. Remarkably, Wnt ligands are asymmetrically distributed in the epithelial branches. Wnt 9d is extensively expressed in the ureteric epithelium but downregulated in the tips where Wnt 11 is expressed. Also, Six 2-expressing cells show zonation in the cap mesenchyme: a slow dividing Six 2^{hi} cell population occurs in the periphery of cap, whereas fast cycling Six 2^{lo} cells are intimately associated with the pretubular aggregate that will govern the nephron formation [32]. Moreover, at the beginning of branching morphogenesis, four Six 2+ cap cells exist for every one of the epithelial tip cells, but during branching, the ratio falls to 2:1 and continues to decrease until the end of nephron formation [32].

3. The development of the thyroid

The condition of endocrine tissues is special because they do not show a ductal system, and the secretion is closely associated with the vascular system. Thyroid fate is induced in the anterior endoderm by the concerted action of FGF2 and BMP4 [68], probably derived from cardiogenic mesoderm [69]. A thyroid initial bud is generated in the midline of the pharyngeal floor under control of Tbx1/FGF8 dependent signals [70]; later it detaches from endoderm, cells proliferate and the primordium bifurcates and grows laterally to generate a bilobulated organ with two lateral thyroid bodies formed by fusion with the paired ultimobranchial bodies (UBB), which provide C cell precursors to the embryonic thyroid [71].

Afterward, at a prefolicular growth stage, the thyroid grows by branching morphogenesis of epithelial cords radiating from the UBB remnant, reminding the pseudoglandular stage of salivary gland before duct generation [72]. Finally, cells polarize locally forming cystic lumens leading to cords of back-to-back connected follicles. This folliculogenesis occurs synchronously, not in a proximal/distal direction and is related to Sox9 expression, which is firstly expressed in some cells in the placode and finally accumulates in the distal portions as in other branching organs, remaining in mature follicular cells [72].

Therefore, thyroid development is equivalent to that of an exocrine gland (i.e., salivary gland) in which the ductal system is not fully differentiated but is regressed, and the endocrine portion detached. An initially forming continuous branching structure polarizes locally leading to isolated cystic lumens and to the generation of isolated follicles [72].

4. The early development of the thymus: phases and involved molecules

Similarly, the thymus follows a pattern of development whose stages resemble the specification, tubulogenesis, and branching morphogenesis previously described. Remarkably, they appear to be regulated by many molecular families reported to be involved in the early development of other branching epithelial organs. Although the thymus development has been profusely studied [73–75], few studies have highlighted its resemblance with a process of tubulogenesis and branching morphogenesis the way we do in this review. As known, thymus development occurs in two steps: an early organogenesis, independent of the transcription factor Foxn1, in which the pharyngeal endoderm is specified to thymus fate and a later organogenesis in which thymic epithelium differentiates and is organized under the control of Foxn1 and the lymphoid progenitor cells that seed the thymic epithelial primordium [76].

4.1. Early thymus development

The first step for the thymic rudiment formation is the segmentation of the posterior pharynx that culminates with the specification of endodermal cells into thymic epithelial cells (TECs) [75]. At these early stages, an inner sheet of endodermal tissue of the third pharyngeal pouch and an outer layer of ectodermal cells of the third branchial cleft contact and fuse [77]. Although pioneer morphological studies pointed out that the thymic epithelium derived from these two embrionary layers [78, 79], further experiments in birds and mice demonstrated that all TECs have an endodermal origin [80, 81]. Moreover, clonal analysis determined the existence of a bipotent common thymic epithelial progenitor cell capable of giving rise to both cortical (c) and medullary (m) TECs [82]. In fact, many of ectodermal cells die in the contact limits with the endoderm and they could just be inductors of thymus tissue or even not contribute to the thymus rudiment [80].

Thymic rudiment appears at E10–11 in mice constituting a simple epithelial structure surrounded by mesenchyme largely derived from the neural crests (NC). Earlier (E9.5), the endoderm evagination has formed a common primordium that expresses Glial cells missing

homolog 2 (Gcm2), the earliest marker of parathyroid, in the anterodorsal domain. In the ventral domain, Foxn1 expression will be detected at E11 [80, 83]. From E 11.5, the common primordium initiates the detachment from the lateral surface of the pharynx through apoptosis [80]. Presumably, NC-derived mesenchyme cells are actively involved in this process because Splotch mutants that lack NC cells show delayed or no pharyngeal detachment of parathyroid/thymus rudiment [84, 85]. Nevertheless, other molecules are also concerned because mutants deficient in either Shh, Pax 9, or Frs 2a also maintain the pharynx connection [86–88]. At E12, the rudiment is totally separated from the pharynx and begins to individualize into two different organs. Then, the lateral thymic lobes descend caudally and medially until the midline, above the heart and behind the sternum. NC-derived mesenchyme as well as BMP4, Ephrin B2, and Hoxa3 are involved in the migration of thymic lobes [84, 85, 89].

In the branchial arches, the mesenchyme derives from both mesoderm and neural crests [90], although presumably the role of NC-derived cells is more important [91]. NC-derived mesenchyme contributes to organize the outer connective tissue capsule and interlobular septae of developing thymus [92], but their relevance decreases in the adult thymus where mesenchyme could derive from mesoderm [91]. Accordingly, NC-derived mesenchyme is not required for the initial specification of endoderm but, as in other branching suffering epithelial organ, it is important for thymus development participating in the determination of the third pharyngeal pouches, the establishment of the limits between thymus and parathyroid domains, and the signaling necessary for the separation from common rudiment of the pharyngeal endoderm and later of the parathyroid and thymic lobes [85]. Finally, NC-derived cells are involved in the migration of thymic lobes into the thoracic cavity [93].

4.2. Molecules involved in early thymic development

It is difficult to establish the temporal sequence of functioning of distinct molecules, particularly because any defect in the formation and/or organization of pharyngeal pouches or arches will finally affect the thymus development, even though this development is not regulated directly by it. Furthermore, several molecules act at different stages of the thymus development even exerting opposite effects. Two main systems seem to govern the early thymus development: the one constituted by Hoxa3 and Pax1/9, together with other related molecules, Eya 1 and Six1/4 [73], and Tbx1. Tbx1 is related to human defects in chromosome 22q11.2, responsible of three phenotypes: Di George syndrome (DGS), velocardiofacial syndrome, (SCFS) and conotruncal anomaly face syndrome [94]. Both systems target morphogens of the families FGF, BMP/TGFβ, Shh, and Wnt, which in turn regulate transcription factor activity making it difficult to establish a conclusive picture. As in other branching organs, many of these molecules are regulated by retinoid acid that would diffuse from adjacent NC-derived mesenchyme specifying pharyngeal endoderm [95]. In support of this, treatment with retinoid acid antagonists or mutant deficient in retinoid acid signaling courses with thymus agenesis [95, 96].

4.2.1. The Tbx1 complex

Tbx1 is expressed in the third pharyngeal pouch endoderm and surrounding mesenchyme, and its lack produces thymic hypoplasia and defects in other derivatives of third and fourth

pharyngeal pouches [97]. Apart from retinoid acid, Pbx1, which acts in cooperation with several Hox proteins, regulates Tbx1 expression [98]. Also, BMPs appear to affect Tbx1 indirectly. Mice deficient in Chordin, a BMP antagonist, shows reduced Tbx1 expression in both pharyngeal endoderm and head mesenchyme [99]. In addition, FGF8 expression disappears in the pharyngeal endoderm of these mice, suggesting a relationship between Tbx1 and FGF8. Indeed, the FGF family is a target of Tbx1. The expression of Tbx1and FGF8 overlap within the secondary heart field [100] and Tbx1-deficient mice exhibit reduced FGF8 expression in the pharyngeal endoderm but not in tissue where Tbx1 is not expressed [101]. The lack of FGF8 courses with failure of mesoderm to migrate at the primitive steak and then absence of embryonic endoderm tissue [102]). Therefore, Tbx1 acts downstream of Chordin/BMPs but upstream of FGF8. Thus, specific deletion of FGF8 in Tbx1-expressing cells phenocopies the DG and VCF syndromes [103]. Presumably, FGF8 models pharyngeal arches and pouch-derived structures, additionally affecting survival of pouch endoderm and NC cell migration [104].

Consequently, Tbx1 homozygous mutants show thymus aplasia [94] but indeed, the lack of Tbx1 results in absence of pharyngeal pouches. As a result, the thymus absence seems to be rather a consequence of this defective pouch formation. More recent studies demonstrate that ectopic Tbx1 expression in the ventral third pharyngeal pouch, the domain in which thymic primordium will be formed, suppresses Foxn1 expression and inhibits TEC proliferation and differentiation but does not reverse thymus fate [105]. Moreover, Tbx1 is downregulated in the ventral domain of wt third pharyngeal pouch [98, 101] and ectopic activation of Shh signaling in the third pharyngeal pouch endoderm (see later) induces Tbx1 expression that results in Foxn1 blockade [105]. All these results suggest that actually Tbx1 negatively regulates TEC growth and differentiation and its disappearance from third pharyngeal pouch endoderm is a requisite for proper thymic organization.

4.2.2. The Eya/Hoxa/Pax complexes

There are nine Pax (Paired box) proteins in mammals, subdivided in four groups. Pax 1 and Pax 9, belonging to the same group, and Pax 3 are necessary for early thymus development [88, 106]. In addition, Pax function is closely related to that of Hoxa3, Eya1, and Tbx1, suggesting that they share common signaling pathways or follow parallel, complementary routes [107, 108].

Pax 3 specifies third pharyngeal pouch endoderm to TEC fate [109]. Pax3−/− mice (Splotch mutants), that have severe deficiency of NC cells, organize the thymus and the parathyroid normally but from E11.5 onward a change in the limits of parathyroid/thymus domains produces an enlarged thymus and a small parathyroid. In addition, the common rudiment does not detach from the pharynx [85].

Pax1 appears firstly in the foregut endoderm (E 8.5) and 2 days later in the endoderm of the third pharyngeal pouch remaining in the developing thymus. In the adult thymus, Pax1+ cells are restricted to a small group of cTECs [106]. Pax9 expression follows the same pattern but is also detected in NC-derived mesenchyme [110]. Pax1 mutants exhibit smaller thymic than those of wt mice and contain large cysts accumulating DP thymocytes [106], whereas Pax 9−/− embryos do not fold away from foregut and the thymus rudiment does not move

vetrocaudally remaining in the larynx. Although the primordium is colonized by lymphoid progenitors, it shows decreased proportions of proliferating cells and increased apoptosis finally resulting, as Pax1-deficient thymi, in small thymi [111].

The control exerted by Pax1, perhaps also by Pax 9, and Hoxa3 on early thymus development presumably follows a common pathway [107, 108]. Hoxa 3 is expressed in both endoderm of third pharyngeal pouch and NC-derived mesenchyme [107]. When this expression is downregulated in E10.5–11 Hoxa3−/− mice, the formation of parathyroid/thymus rudiment is blocked, increases the proportion of apoptotic endodermal cells and there is reduced proliferation of mesenchyme cells [112]. More importantly, the expression of both Pax1 and Pax9 decreases in the third pharyngeal pouch of E10,5 Hoxa3-deficient embryos [107], suggesting that Pax 1/9 act downstream of Hoxa3 but all three molecules have synergistic and dose-dependent effects on early thymus maturation [88, 113, 114]. Thus, Hoxa3+/− Pax1+/− double heterozygous mice have a similar phenotype as Pax1−/− mutants, but Hoxa3+/− Pax1−/− hypoplastic thymi exhibit a more severe phenotype than Pax1−/− [114].

Eya1 is involved in the regulation of genes controlling cell growth, activating the repressor Six (Sine oculis). The expression of Eya1, Six, and Pax genes colocalizes in the NC cells and the pharyngeal endoderm [115]. In the absence of Eya1, the third pharyngeal pouch does not detach from the pharyngeal endoderm, and consequently, the thymic primordium is not formed. Foxn1, Pax1, and Pax3 are not expressed in the thymic area, but Hoxa3, Pax1, and Pax3 appear in the E10.5 pouch endoderm [115]. On the other hand, endodermal Six expression is Eya1 dependent, and loss of Six1 in Eya1−/− embryos contributes to the induced thymic defects [116]. Accordingly, Six1 acts downstream of Eya1, whereas Hoxa3, Pax1, and Pax3 do it upstream or independently of Eya 1 [117].

4.2.3. FGF family

FGF is an extensive family of molecules that influences cell survival, proliferation, and differentiation of many epithelial organs, as repeatedly mentioned in this review. FGF8 is expressed in the pouch epithelium, whereas FGF10 is produced by underlying NC-derived mesenchyme both being involved in the maturation of endoderm [104]. After pouch formation, FGF7 and again FGF10, activate FGFR2iiib receptor on fetal TECs for inducing their proliferation. Accordingly, deficient mice either in the receptor or FGF10 show severe thymic hypoplasia and reduced TEC proliferation [118–120]. Likewise, removal of surrounding mesenchyme from E12 fetal thymus inhibits the growth but not the differentiation of epithelial cells [119, 121]. Other studies demonstrate that FGF7 produced by thymic blood vessels also promotes expansion but not differentiation of TECs [118].

4.2.4. Shh

Shh is a promoting factor for parathyroid development via Tbx1 [122], whereas negatively regulating the growth of thymus domain. Consequently, Shh functions as an antagonist of BMP4 signaling [87]. Shh is expressed early in the posterior endoderm of second pouch and then in the third arch endoderm, acting upstream of Tbx1 [123] and affecting the patterning of pharyngeal pouches [77].

4.2.5. BMP family

Particularly relevant is the role played by BMPs and Wnt molecules in the early thymic development, as direct controllers of Foxn1 expression, the key transcription factor mandatory for the late embryogenesis of thymus [124]. In addition, both signaling pathways constitute the major means for NC-derived mesenchyme to signal thymic epithelial rudiment [93, 124, 125]. Possibly, FGF8 produced by the primordial endoderm signals to the adjacent mesenchyme inducing BMP4 expression [126]. BMP4 and its antagonist Noggin govern the parathyroid/thymus individualization and the Foxn1-dependent TEC maturation. In general, BMP4 is essential for the early stages of thymus development prior to the onset of Foxn1 expression [93]. BMP4 is expressed in the ventral domain of the pouch and Noggin in the dorsal area colocalizing with Gcm2 in the parathyroid domain [83]. Furthermore, BMP4 seems to be also involved in the full parathyroid/thymus separation, as BMP4 deletion delays the process [93]. Inhibition of BMP signaling provokes decline of Foxn1 expression in the zebrafish thymic primordium [83, 125], and BMP4 signaling promotes Foxn1 expression in early chicken thymus [126], as well as in mouse FTOCs [127]. Loss of BMP4 from pharyngeal endoderm and underlying mesenchyme prior to the onset of Foxn1 expression does not affect patterning, separation from the pharynx, or initial organ formation, although it alters some important morphogenetic processes such as lumen closure, organ separation and migration, initial lymphoid seeding, and formation of mesenchyme thymic capsule [93]. The sequence established between BMP and Foxn1 is the following: FGF8-mediated mesenchymal BMP signaling initiates the expression of both Foxn1 and BMP4 in the endodermal cells [126]. Then, endodermal BMP4 expression targets a regulatory feedback loop [128] for maintaining BMP4 and Foxn1 expression in the future thymic epithelium rather to directly affect Foxn1 [129]. In these conditions, if BMP signaling is blocked, the expression of both molecules ceases and nonfunctional Foxn1-TECs would remain in the thymus. If this occurs during concrete periods of midgestation, thymopoiesis will irreversibly fail [129]. Therefore, the balance between BMP4 and its inhibitors (i.e., Noggin) becomes critical for a proper maturation of thymic epithelium.

4.2.6. Wnt family

Wnt family members are extensively expressed in developing and adult thymi in both TECs and fibroblasts [130], whereas their receptors are only detected on TECs [124]. Particularly, the noncanonical Wnt4 and Wnt5b, but also the canonical Wnt10b, coexpress with Foxn1 in third pharyngeal pouch and later in E13 and adult thymus [131] and are involved in its control [124]. Thus, overexpression of Dkk1, a Wnt4 inhibitor, in TECs induces thymic atrophy with reduced epithelial progenitors and TEC proliferation and appearance of TEC proliferation [132]. However, recent results indicate that a proper thymus development can only occur when β-catenin-dependent Wnt signaling is low or lacking [133]. Thus, β-catenin-deficient thymi exhibit Foxn1 expression, and stabilized β-catenin overexpression shows decreased rather than increased Foxn1 transcripts [133, 134]. Therefore, these results suggest that β-catenin is dispensable for Foxn1 expression in fetal TECs. Remarkably, during branching morphogenesis of lung and lacrimal glands, Wnt overexpression, stimulated Wnt signaling and conditional overexpression of β-catenin all result in decreased branching morphogenesis [135]. However, it is important to remark that sustained Wnt signaling promotes the production of secreted

Wnt antagonisms [136] that block thymocyte development in FTOCs [137]. On the other hand, other signaling pathways involved in TEC differentiation, such as those mediated by BMPs, modulate the effects produced by Wnt4 overexpression [133].

5. After acquisition of thymus fate, thymic primordium undergoes tubulogenesis and branching morphogenesis

E11.5 thymic primordium consists of a bi/pluristratified epithelium polarized with respect to a ramified central lumen resulting from the evagination of pharyngeal epithelium where K5+ Cld 3/4+ cells line the lumen [138, 139]. In the following days, the thymus grows and the K5+ Cld 3/4 + cell cords increase their total length and branching degree. At the same time, external clefts determine an incipient lobulation that became clearly evident by day E14.5. Beyond E12.5, the initial lumen is almost totally closed although a central lumen is still visible at E12,5 and to some extent at E13,5 [139]. Secondary forming lumens can be observed in the K5 + Cld 3/4+ branching cell cords up to E13.5 (**Figure 2**) [139]. Thus, in these initial steps of thymus development, its histological organization is quite similar to that of organs undergoing branching morphogenesis in which the lumen formation and elongation take place within a proliferating bud (**Figure 2**) [20, 140]. These results indicate that between E11.5 and E13.5, a primary lumen connects with secondary and growing order lumens through branched microlumens or polarized canals, giving rise to a continuous formed or forming luminal structure that grows hierarchically (**Figure 2**). Therefore, in the thymus, clefting/branching and lumen formation seems to be more synchronic and not as regionally separated as in the salivary gland, similar to the pancreas condition (**Figure 2**).

However, in the thymus, a definitive duct is not developed, nor is terminal end buds, acini or other differentiated distal secreting structures, but instead the thymus remains as a concentric structure in which the central Cld + K5+ cells will differentiate into the thymic medulla [138, 139]. This central medulla does not apparently present lumen and is surrounded by the thymic cortex differentiated from Cld 3/4- cells (**Figure 2**) [139]. On the other hand, the fact that the branching pattern of the K5 + Cld 3/4+ cell cords appears to be similar between different mice [139] and that rat adult thymic medulla has also been described as a 4–5 order ramified structure in which the ratio of branches sizes is mathematically constant [141], suggesting that thymus development follows a programmed branching pattern.

If, as above indicated, the branching morphogenesis of the developing thymus has some particular features, as the lack of a definitive duct or terminal end buds or acini, the early lymphoid seeding introduces in the thymus development other important differences with respect to other epithelial organs inducing the specific three-dimensional network formed by dendritic-shaped TECs. Thymocyte precursors enter the thymus at around E11.5 through the surrounding mesenchyme [142], and at E12.5 $CD45^{+}$, lymphoid progenitors appear associated with nonpolarized TECs that express little or no K5 [139]. This 3D arrangement of thymic epithelium is, to some extent, precluded in the absence of thymocytes [143] in which the presence of medullary luminal or cystic structures becomes more evident, presumably representing a default pathway of epithelial differentiation when thymocytes are missing [143].

http://dx.doi.org/10.5772/intechopen.81193

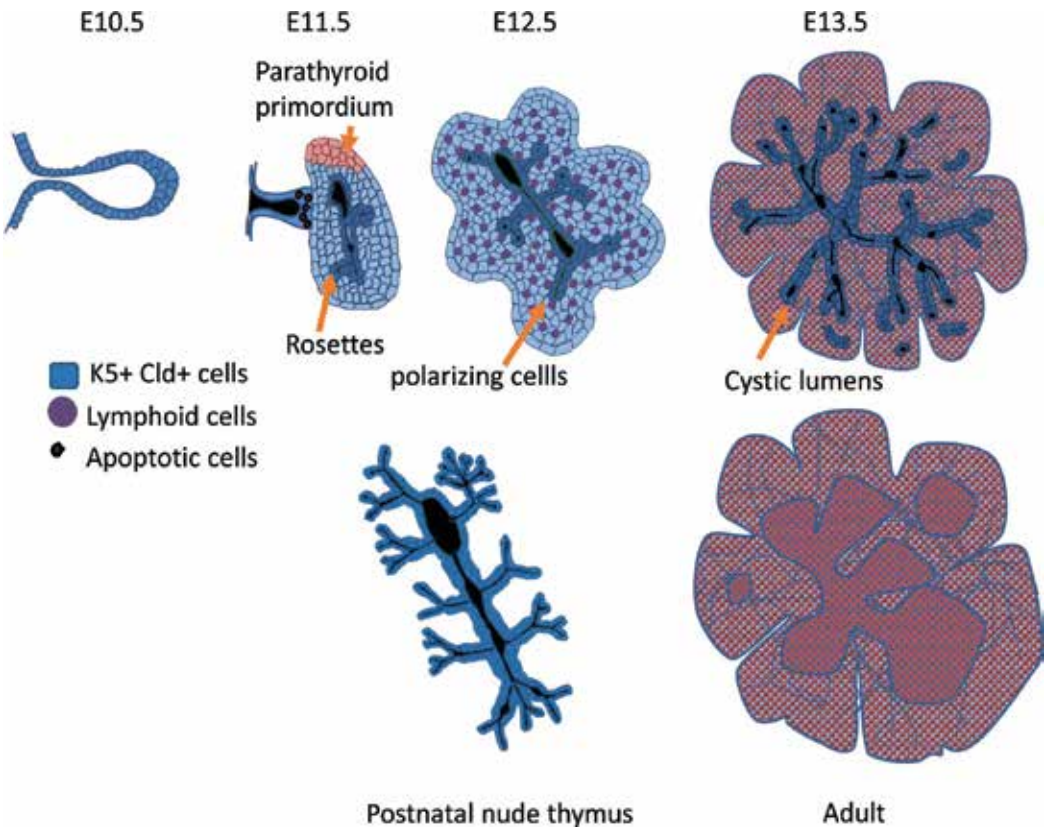

Figure 2. Thymus development follows a branching morphogenesis process similar to those of salivary gland and pancreas (see **Figure 1**).

On the other hand, in the absence of Foxn1, the existence of a tubular-branched structure in which both ductal and acinar components can be distinguished [144] and that cannot be colonized by lymphoid progenitors [76] is clearly evident. This is the situation of Nude (Foxn1−/−) thymi, in which the transcription factor Foxn1 central for thymic epithelial differentiation, lacks. The earliest stages of Foxn1−/− thymus development appear to occur in the same way as those of wt thymus, and the expression of claudin 3/4 and wt thymus takes place in similar ways [145], suggesting that wt thymus organogenesis might be considered as a modification of the tubulogenesis and epithelial branching morphogenesis, which occur in the nude thymus (**Figure 2**). Thus, FoxN1 expression would preclude lumen formation and generate concentric layers of distinct TEC subsets (Muñoz et al., 2018 submitted). Moreover, the conditioned removal of FoxN1 in K14+ epithelial cells results in the progressive polarization of medullary cells, Cld3/4 expression, and lumen formation [146]. Other defects affect mainly thymic branching morphogenesis without importantly altering thymic-specific differentiation. Transgenic expression of Noggin under the control of a FoxN1 promoter leads to a hypoplastic spheric thymus always containing big cystic structures [125]. These structural alterations seem to be the result of a branching defect in consonance with the known role of BMP signaling in regulating branching morphogenesis of different organs [26] and to affect Foxn1 expression [147].

Acknowledgements

This work was supported by grants BFU2013-41112-R from the Spanish Ministry of Economy and Competitiveness and Cell Therapy Network (RD12/0019/0007) from the Spanish Ministry of Health and Consume and Avancell-CM (S2017/BMD-3692) from Community of Madrid.

Conflict of interest

Authors declare no competing or financial interests.

Author details

Juan José Muñoz[1] and Agustín G. Zapata[1,2]*

*Address all correspondence to: zapata@ucm.es

1 Center for Cytometry and Fluorescence Microscopy, Complutense University of Madrid, Madrid, Spain

2 Department of Cell Biology, Complutense University of Madrid, Madrid, Spain

References

[1] Knosp WM, Knox SM, Hoffman MP. Salivary gland organogenesis. Wiley Interdisciplinary Reviews: Developmental Biology. 2012;**1**:69-82. DOI: 10.1002/wdev.4

[2] Harunaga J, Hsu JC, Yamada KM. Dynamics of salivary gland morphogenesis. Journal of Dental Research. 2011;**90**:1070-1077. DOI: 10.1177/0022034511405330

[3] Ober EA, Verkade H, Field HA, Stainier DY. Mesodermal Wnt2b signalling positively regulates liver specification. Nature. 2006;**442**:688-691. DOI: 10.1038/nature04888

[4] Bort R, Signore M, Tremblay K, Martinez Barbera JP, Zaret KS. Hex homeobox gene controls the transition of the endoderm to a pseudostratified, cell emergent epithelium for liver bud development. Developmental Biology. 2006;**290**:44-56. DOI: 10.1016/j.ydbio.2005.11.006

[5] Larsen HL, Grapin-Botton A. The molecular and morphogenetic basis of pancreas organogenesis. Seminars in Cell & Developmental Biology. 2017;**66**:51-68. DOI: 10.1016/j.semcdb.2017.01.005

[6] Bastidas-Ponce A, Scheibner K, Lickert H, Bakhti M. Cellular and molecular mechanisms coordinating pancreas development. Development. 2017;**144**:2873-2888. DOI: 10.1242/dev.140756

[7] Villasenor A, Chong DC, Henkemeyer M, Cleaver O. Epithelial dynamics of pancreatic branching morphogenesis. Development. 2010;**137**:4295-4305. DOI: 10.1242/dev.052993

[8] Swarr DT, Morrisey EE. Lung endoderm morphogenesis: Gasping for form and function. Annual Review of Cell and Developmental Biology. 2015;**31**:553-573. DOI: 10.1146/annurev-cellbio-100814-125249

[9] Harris-Johnson KS, Domyan ET, Vezina CM. Sun X: Beta-catenin promotes respiratory progenitor identity in mouse foregut. Proceedings of the National Academy of Sciences of the United States of America. 2009;**106**:16287-16292. DOI: 10.1073/pnas.0902274106

[10] De Moerlooze L, Spencer-Dene B, Revest JM, Hajihosseini M, Rosewell I, Dickson C. An important role for the IIIb isoform of fibroblast growth factor receptor 2 (FGFR2) in mesenchymal-epithelial signalling during mouse organogenesis. Development. 2000; **127**:483-492

[11] Jaskoll T, Witcher D, Toreno L, Bringas P, Moon AM, Melnick M. FGF8 dose-dependent regulation of embryonic submandibular salivary gland morphogenesis. Developmental Biology. 2004;**268**:457-469. DOI: 10.1016/j.ydbio.2004.01.004

[12] Guo L, Yu QC, Fuchs E. Targeting expression of keratinocyte growth factor to keratinocytes elicits striking changes in epithelial differentiation in transgenic mice. The EMBO Journal. 1993;**12**:973-986

[13] Knosp WM, Knox SM, Lombaert IM, Haddox CL, Patel VN, Hoffman MP. Submandibular parasympathetic gangliogenesis requires sprouty-dependent Wnt signals from epithelial progenitors. Developmental Cell. 2015;**32**:667-677. DOI: 10.1016/j.devcel.2015.01.023

[14] Pearl EJ, Li J, Green JB. Cellular systems for epithelial invagination. Philosophical Transactions of the Royal Society of London. Series B, Biological Sciences. 2017;**372**. DOI: 10.1098/rstb.2015.0526

[15] Bernascone I, Hachimi M, Martin-Belmonte F. Signaling networks in epithelial tube formation. Cold Spring Harbor Perspectives in Biology. 2017;**9**. DOI: 10.1101/cshperspect.a027946

[16] Marciano DK. A holey pursuit: Lumen formation in the developing kidney. Pediatric Nephrology. 2017;**32**:7-20. DOI: 10.1007/s00467-016-3326-4

[17] Santiago-Martinez E, Soplop NH, Patel R, Kramer SG. Repulsion by slit and roundabout prevents shotgun/E-cadherin-mediated cell adhesion during Drosophila heart tube lumen formation. The Journal of Cell Biology. 2008;**182**:241-248. DOI: 10.1083/jcb.200804120

[18] Mailleux AA, Overholtzer M, Brugge JS. Lumen formation during mammary epithelial morphogenesis: Insights from in vitro and in vivo models. Cell Cycle. 2008;**7**:57-62. DOI: 10.4161/cc.7.1.5150

[19] Datta A, Bryant DM, Mostov KE. Molecular regulation of lumen morphogenesis. Current Biology. 2011;**21**:R126-R136. DOI: 10.1016/j.cub.2010.12.003

[20] Walker JL, Menko AS, Khalil S, Rebustini I, Hoffman MP, Kreidberg JA, et al. Diverse roles of E-cadherin in the morphogenesis of the submandibular gland: Insights into the formation of acinar and ductal structures. Developmental Dynamics. 2008;**237**:3128-3141. DOI: 10.1002/dvdy.21717

[21] Yamamoto H, Awada C, Hanaki H, Sakane H, Tsujimoto I, Takahashi Y, et al. The apical and basolateral secretion of Wnt11 and Wnt3a in polarized epithelial cells is regulated by different mechanisms. Journal of Cell Science. 2013;**126**:2931-2943. DOI: 10.1242/jcs.126052

[22] Yamaguchi Y, Yonemura S, Takada S. Grainyhead-related transcription factor is required for duct maturation in the salivary gland and the kidney of the mouse. Development. 2006;**133**:4737-4748. DOI: 10.1242/dev.02658

[23] Malpel S, Mendelsohn C, Cardoso WV. Regulation of retinoic acid signaling during lung morphogenesis. Development. 2000;**127**:3057-3067

[24] Desai TJ, Malpel S, Flentke GR, Smith SM, Cardoso WV. Retinoic acid selectively regulates Fgf10 expression and maintains cell identity in the prospective lung field of the developing foregut. Developmental Biology. 2004;**273**:402-415. DOI: 10.1016/j.ydbio.2004.04.039

[25] Motoyama J, Liu J, Mo R, Ding Q, Post M, Hui CC. Essential function of Gli2 and Gli3 in the formation of lung, trachea and oesophagus. Nature Genetics. 1998;**20**:54-57. DOI: 10.1038/1711

[26] Mattingly A, Finley JK, Knox SM. Salivary gland development and disease. Wiley Interdisciplinary Reviews: Developmental Biology. 2015;**4**:573-590. DOI: 10.1002/wdev.194

[27] Fiaschi M, Kolterud A, Nilsson M, Toftgard R, Rozell B. Targeted expression of GLI1 in the salivary glands results in an altered differentiation program and hyperplasia. The American Journal of Pathology. 2011;**179**:2569-2579. DOI: 10.1016/j.ajpath.2011.07.033

[28] Aoto K, Nishimura T, Eto K, Motoyama J. Mouse GLI3 regulates Fgf8 expression and apoptosis in the developing neural tube, face, and limb bud. Developmental Biology. 2002;**251**:320-332

[29] Pummila M, Fliniaux I, Jaatinen R, James MJ, Laurikkala J, Schneider P, et al. Ectodysplasin has a dual role in ectodermal organogenesis: Inhibition of bmp activity and induction of Shh expression. Development. 2007;**134**:117-125. DOI: 10.1242/dev.02708

[30] Hall BE, Zheng C, Swaim WD, Cho A, Nagineni CN, Eckhaus MA, et al. Conditional overexpression of TGF-beta1 disrupts mouse salivary gland development and function. Laboratory Investigation. 2010;**90**:543-555. DOI: 10.1038/labinvest.2010.5

[31] Wang S, Sekiguchi R, Daley WP, Yamada KM. Patterned cell and matrix dynamics in branching morphogenesis. The Journal of Cell Biology. 2017;**216**:559-570. DOI: 10.1083/jcb.201610048

[32] Short KM, Smyth IM. The contribution of branching morphogenesis to kidney development and disease. Nature Reviews. Nephrology. 2016;**12**:754-767. DOI: 10.1038/nrneph.2016.157

[33] Ewald AJ, Brenot A, Duong M, Chan BS, Werb Z. Collective epithelial migration and cell rearrangements drive mammary branching morphogenesis. Developmental Cell. 2008;**14**:570-581. DOI: 10.1016/j.devcel.2008.03.003

[34] Goldin GV, Hindman HM, Wessells NK. The role of cell proliferation and cellular shape change in branching morphogenesis of the embryonic mouse lung: Analysis using aphidicolin and cytochalasins. The Journal of Experimental Zoology. 1984;**232**:287-296. DOI: 10.1002/jez.1402320216

[35] Nakanishi Y, Morita T, Nogawa H. Cell proliferation is not required for the initiation of early cleft formation in mouse embryonic submandibular epithelium in vitro. Development. 1987;**99**:429-437

[36] Daley WP, Yamada KM. ECM-modulated cellular dynamics as a driving force for tissue morphogenesis. Current Opinion in Genetics & Development. 2013;**23**:408-414. DOI: 10.1016/j.gde.2013.05.005

[37] Schnatwinkel C, Niswander L. Multiparametric image analysis of lung-branching morphogenesis. Developmental Dynamics. 2013;**242**:622-637. DOI: 10.1002/dvdy.23961

[38] Cebrian C, Asai N, D'Agati V, Costantini F. The number of fetal nephron progenitor cells limits ureteric branching and adult nephron endowment. Cell Reports. 2014;**7**:127-137. DOI: 10.1016/j.celrep.2014.02.033

[39] Kim HY, Varner VD, Nelson CM. Apical constriction initiates new bud formation during monopodial branching of the embryonic chicken lung. Development. 2013;**140**:3146-3155. DOI: 10.1242/dev.093682

[40] Sakai T, Larsen M, Yamada KM. Fibronectin requirement in branching morphogenesis. Nature. 2003;**423**:876-881. DOI: 10.1038/nature01712

[41] Chen J, Krasnow MA. Integrin Beta 1 suppresses multilayering of a simple epithelium. PLoS One. 2012;**7**:e52886. DOI: 10.1371/journal.pone.0052886

[42] Grobstein C, Cohen J. Collagenase: Effect on the morphogenesis of embryonic salivary epithelium in vitro. Science. 1965;**150**:626-628

[43] Kadoya Y, Nomizu M, Sorokin LM, Yamashina S, Yamada Y. Laminin alpha1 chain G domain peptide, RKRLQVQLSIRT, inhibits epithelial branching morphogenesis of cultured embryonic mouse submandibular gland. Developmental Dynamics. 1998;**212**:394-402. DOI: 10.1002/(sici)1097-0177(199807)212:3<394::Aid-aja7>3.0.Co;2-c

[44] Menko AS, Kreidberg JA, Ryan TT, Van Bockstaele E, Kukuruzinska MA. Loss of alpha-3beta1 integrin function results in an altered differentiation program in the mouse submandibular gland. Developmental Dynamics. 2001;**220**:337-349. DOI: 10.1002/dvdy.1114

[45] Andrew DJ, Ewald AJ. Morphogenesis of epithelial tubes: Insights into tube formation, elongation, and elaboration. Developmental Biology. 2010;**341**:34-55. DOI: 10.1016/j.ydbio.2009.09.024

[46] Larsen HL, Martin-Coll L, Nielsen AV, Wright CVE, Trusina A, Kim YH, et al. Stochastic priming and spatial cues orchestrate heterogeneous clonal contribution to mouse pancreas organogenesis. Nature Communications. 2017;**8**:605. DOI: 10.1038/s41467-017-00258-4

[47] Bradbury JM, Edwards PA, Niemeyer CC, Dale TC. Wnt-4 expression induces a pregnancy-like growth pattern in reconstituted mammary glands in virgin mice. Developmental Biology. 1995;**170**:553-563. DOI: 10.1006/dbio.1995.1236

[48] Brisken C, Heineman A, Chavarria T, Elenbaas B, Tan J, Dey SK, et al. Essential function of Wnt-4 in mammary gland development downstream of progesterone signaling. Genes & Development. 2000;**14**:650-654

[49] Mucenski ML, Wert SE, Nation JM, Loudy DE, Huelsken J, Birchmeier W, et al. Beta-catenin is required for specification of proximal/distal cell fate during lung morphogenesis. The Journal of Biological Chemistry. 2003;**278**:40231-40238. DOI: 10.1074/jbc.M305892200

[50] Shu W, Guttentag S, Wang Z, Andl T, Ballard P, Lu MM, et al. Wnt/beta-catenin signaling acts upstream of N-myc, BMP4, and FGF signaling to regulate proximal-distal patterning in the lung. Developmental Biology. 2005;**283**:226-239. DOI: 10.1016/j.ydbio.2005.04.014

[51] Weaver M, Dunn NR, Hogan BL. Bmp4 and Fgf10 play opposing roles during lung bud morphogenesis. Development. 2000;**127**:2695-2704

[52] Li C, Hu L, Xiao J, Chen H, Li JT, Bellusci S, et al. Wnt5a regulates Shh and Fgf10 signaling during lung development. Developmental Biology. 2005;**287**:86-97. DOI: 10.1016/j.ydbio.2005.08.035

[53] Qiao J, Bush KT, Steer DL, Stuart RO, Sakurai H, Wachsman W, et al. Multiple fibroblast growth factors support growth of the ureteric bud but have different effects on branching morphogenesis. Mechanisms of Development. 2001;**109**:123-135

[54] Zhao H, Kegg H, Grady S, Truong HT, Robinson ML, Baum M, et al. Role of fibroblast growth factor receptors 1 and 2 in the ureteric bud. Developmental Biology. 2004;**276**:403-415. DOI: 10.1016/j.ydbio.2004.09.002

[55] Pond AC, Bin X, Batts T, Roarty K, Hilsenbeck S, Rosen JM. Fibroblast growth factor receptor signaling is essential for normal mammary gland development and stem cell function. Stem Cells. 2013;**31**:178-189. DOI: 10.1002/stem.1266

[56] Parsa S, Ramasamy SK, De Langhe S, Gupte VV, Haigh JJ, Medina D, et al. Terminal end bud maintenance in mammary gland is dependent upon FGFR2b signaling. Developmental Biology. 2008;**317**:121-131. DOI: 10.1016/j.ydbio.2008.02.014

[57] Zhang X, Martinez D, Koledova Z, Qiao G, Streuli CH, Lu P. FGF ligands of the postnatal mammary stroma regulate distinct aspects of epithelial morphogenesis. Development. 2014;**141**:3352-3362. DOI: 10.1242/dev.106732

[58] Peters K, Werner S, Liao X, Wert S, Whitsett J, Williams L. Targeted expression of a dominant negative FGF receptor blocks branching morphogenesis and epithelial differentiation of the mouse lung. The EMBO Journal. 1994;**13**:3296-3301

[59] Hirashima T, Iwasa Y, Morishita Y. Distance between AER and ZPA is defined by feed-forward loop and is stabilized by their feedback loop in vertebrate limb bud. Bulletin of Mathematical Biology. 2008;**70**:438-459. DOI: 10.1007/s11538-007-9263-4

[60] Herriges M, Morrisey EE. Lung development: Orchestrating the generation and regeneration of a complex organ. Development. 2014;**141**:502-513. DOI: 10.1242/dev.098186

[61] Zhou L, Dey CR, Wert SE, Whitsett JA. Arrested lung morphogenesis in transgenic mice bearing an SP-C-TGF-beta 1 chimeric gene. Developmental Biology. 1996;**175**:227-238. DOI: 10.1006/dbio.1996.0110

[62] Letterio JJ, Geiser AG, Kulkarni AB, Roche NS, Sporn MB, Roberts AB. Maternal rescue of transforming growth factor-beta 1 null mice. Science. 1994;**264**:1936-1938

[63] Rawlins EL, Clark CP, Xue Y, Hogan BL. The Id2+ distal tip lung epithelium contains individual multipotent embryonic progenitor cells. Development. 2009;**136**:3741-3745. DOI: 10.1242/dev.037317

[64] Tsao PN, Chen F, Izvolsky KI, Walker J, Kukuruzinska MA, Lu J, et al. Gamma-secretase activation of notch signaling regulates the balance of proximal and distal fates in progenitor cells of the developing lung. The Journal of Biological Chemistry. 2008;**283**: 29532-29544. DOI: 10.1074/jbc.M801565200

[65] Tsao PN, Vasconcelos M, Izvolsky KI, Qian J, Lu J, Cardoso WV. Notch signaling controls the balance of ciliated and secretory cell fates in developing airways. Development. 2009;**136**:2297-2307. DOI: 10.1242/dev.034884

[66] Guseh JS, Bores SA, Stanger BZ, Zhou Q, Anderson WJ, Melton DA, et al. Notch signaling promotes airway mucous metaplasia and inhibits alveolar development. Development. 2009;**136**:1751-1759. DOI: 10.1242/dev.029249

[67] Krapp A, Knofler M, Ledermann B, Burki K, Berney C, Zoerkler N, et al. The bHLH protein PTF1-p48 is essential for the formation of the exocrine and the correct spatial organization of the endocrine pancreas. Genes & Development. 1998;**12**:3752-3763

[68] Kurmann AA, Serra M, Hawkins F, Rankin SA, Mori M, Astapova I, et al. Regeneration of thyroid function by transplantation of differentiated pluripotent stem cells. Cell Stem Cell. 2015;**17**:527-542. DOI: 10.1016/j.stem.2015.09.004

[69] Serls AE, Doherty S, Parvatiyar P, Wells JM, Deutsch GH. Different thresholds of fibroblast growth factors pattern the ventral foregut into liver and lung. Development. 2005;**132**:35-47. DOI: 10.1242/dev.01570

[70] Lania G, Zhang Z, Huynh T, Caprio C, Moon AM, Vitelli F, et al. Early thyroid development requires a Tbx1-Fgf8 pathway. Developmental Biology. 2009;**328**:109-117. DOI: 10.1016/j.ydbio.2009.01.014

[71] Johansson E, Andersson L, Ornros J, Carlsson T, Ingeson-Carlsson C, Liang S, et al. Revising the embryonic origin of thyroid C cells in mice and humans. Development. 2015; **142**:3519-3528. DOI: 10.1242/dev.126581

[72] Liang S, Johansson E, Barila G, Altschuler DL, Fagman H, Nilsson M. A branching morphogenesis program governs embryonic growth of the thyroid gland. Development. 2018;**145**. DOI: 10.1242/dev.146829

[73] Gordon J, Manley NR. Mechanisms of thymus organogenesis and morphogenesis. Development. 2011;**138**:3865-3878. DOI: 10.1242/dev.059998

[74] Manley NR, Richie ER, Blackburn CC, Condie BG, Sage J. Structure and function of the thymic microenvironment. Front Bioscience (Landmark Ed). 2011;**16**:2461-2477

[75] Takahama Y, Ohigashi I, Baik S, Anderson G. Generation of diversity in thymic epithelial cells. Nature Reviews. Immunology. 2017;**17**:295-305. DOI: 10.1038/nri.2017.12

[76] Vaidya HJ, Briones Leon A, Blackburn CC. FOXN1 in thymus organogenesis and development. European Journal of Immunology. 2016;**46**:1826-1837. DOI: 10.1002/eji.201545814

[77] Graham A. The development and evolution of the pharyngeal arches. Journal of Anatomy. 2001;**199**:133-141

[78] Cordier AC, Haumont SM. Development of thymus, parathyroids, and ultimo-branchial bodies in NMRI and nude mice. The American Journal of Anatomy. 1980;**157**:227-263. DOI: 10.1002/aja.1001570303

[79] Cordier AC, Heremans JF. Nude mouse embryo: Ectodermal nature of the primordial thymic defect. Scandinavian Journal of Immunology. 1975;**4**:193-196

[80] Gordon J, Wilson VA, Blair NF, Sheridan J, Farley A, Wilson L, et al. Functional evidence for a single endodermal origin for the thymic epithelium. Nature Immunology. 2004;**5**:546-553. DOI: 10.1038/ni1064

[81] Le Douarin NM, Jotereau FV. Tracing of cells of the avian thymus through embryonic life in interspecific chimeras. The Journal of Experimental Medicine. 1975;**142**:17-40

[82] Rossi SW, Jenkinson WE, Anderson G, Jenkinson EJ. Clonal analysis reveals a common progenitor for thymic cortical and medullary epithelium. Nature. 2006;**441**:988-991. DOI: 10.1038/nature04813

[83] Patel SR, Gordon J, Mahbub F, Blackburn CC, Manley NR. Bmp4 and noggin expression during early thymus and parathyroid organogenesis. Gene Expression Patterns. 2006;**6**:794-799. DOI: 10.1016/j.modgep.2006.01.011

[84] Chen L, Zhao P, Wells L, Amemiya CT, Condie BG, Manley NR. Mouse and zebrafish Hoxa3 orthologues have nonequivalent in vivo protein function. Proceedings of the National Academy of Sciences of the United States of America. 2010;**107**:10555-10560. DOI: 10.1073/pnas.1005129107

[85] Griffith AV, Cardenas K, Carter C, Gordon J, Iberg A, Engleka K, et al. Increased thymus- and decreased parathyroid-fated organ domains in splotch mutant embryos. Developmental Biology. 2009;**327**:216-227. DOI: 10.1016/j.ydbio.2008.12.019

[86] Kameda Y, Ito M, Nishimaki T, Gotoh N. FRS2alpha is required for the separation, migration, and survival of pharyngeal-endoderm derived organs including thyroid, ultimobranchial body, parathyroid, and thymus. Developmental Dynamics. 2009;**238**:503-513. DOI: 10.1002/dvdy.21867

[87] Moore-Scott BA, Manley NR. Differential expression of sonic hedgehog along the anterior-posterior axis regulates patterning of pharyngeal pouch endoderm and pharyngeal endoderm-derived organs. Developmental Biology. 2005;**278**:323-335. DOI: 10.1016/j.ydbio.2004.10.027

[88] Peters H, Neubuser A, Kratochwil K, Balling R. Pax9-deficient mice lack pharyngeal pouch derivatives and teeth and exhibit craniofacial and limb abnormalities. Genes & Development. 1998;**12**:2735-2747

[89] Foster KE, Gordon J, Cardenas K, Veiga-Fernandes H, Makinen T, Grigorieva E, et al. EphB-ephrin-B2 interactions are required for thymus migration during organogenesis. Proceedings of the National Academy of Sciences of the United States of America. 2010;**107**:13414-13419. DOI: 10.1073/pnas.1003747107

[90] Jiang X, Rowitch DH, Soriano P, McMahon AP, Sucov HM. Fate of the mammalian cardiac neural crest. Development. 2000;**127**:1607-1616

[91] Manley NR, Blackburn CC. A developmental look at thymus organogenesis: Where do the non-hematopoietic cells in the thymus come from? Current Opinion in Immunology. 2003;**15**:225-232. DOI: 10.1016/s0952-7915(03)00006-2

[92] Le Lievre CS, Le Douarin NM. Mesenchymal derivatives of the neural crest: Analysis of chimaeric quail and chick embryos. Journal of Embryology and Experimental Morphology. 1975;**34**:125-154

[93] Gordon J, Patel SR, Mishina Y, Manley NR. Evidence for an early role for BMP4 signaling in thymus and parathyroid morphogenesis. Developmental Biology. 2010;**339**:141-154. DOI: 10.1016/j.ydbio.2009.12.026

[94] Baldini A. DiGeorge syndrome: An update. Current Opinion in Cardiology. 2004;**19**: 201-204

[95] Wendling O, Dennefeld C, Chambon P, Mark M. Retinoid signaling is essential for patterning the endoderm of the third and fourth pharyngeal arches. Development. 2000; **127**:1553-1562

[96] Begemann G, Schilling TF, Rauch GJ, Geisler R, Ingham PW. The zebrafish neckless mutation reveals a requirement for raldh2 in mesodermal signals that pattern the hindbrain. Development. 2001;**128**:3081-3094

[97] Lindsay EA, Vitelli F, Su H, Morishima M, Huynh T, Pramparo T, et al. Tbx1 haploinsufficieny in the DiGeorge syndrome region causes aortic arch defects in mice. Nature. 2001; **410**:97-101. DOI: 10.1038/35065105

[98] Manley NR, Selleri L, Brendolan A, Gordon J, Cleary ML. Abnormalities of caudal pharyngeal pouch development in Pbx1 knockout mice mimic loss of Hox3 paralogs. Developmental Biology. 2004;**276**:301-312. DOI: 10.1016/j.ydbio.2004.08.030

[99] Bachiller D, Klingensmith J, Shneyder N, Tran U, Anderson R, Rossant J, et al. The role of chordin/bmp signals in mammalian pharyngeal development and DiGeorge syndrome. Development. 2003;**130**:3567-3578

[100] Xu H, Morishima M, Wylie JN, Schwartz RJ, Bruneau BG, Lindsay EA, et al. Tbx1 has a dual role in the morphogenesis of the cardiac outflow tract. Development. 2004; **131**:3217-3227. DOI: 10.1242/dev.01174

[101] Vitelli F, Taddei I, Morishima M, Meyers EN, Lindsay EA, Baldini A. A genetic link between Tbx1 and fibroblast growth factor signaling. Development. 2002;**129**:4605-4611

[102] Sun X, Meyers EN, Lewandoski M, Martin GR. Targeted disruption of Fgf8 causes failure of cell migration in the gastrulating mouse embryo. Genes & Development. 1999;**13**:1834-1846

[103] Brown CB, Wenning JM, Lu MM, Epstein DJ, Meyers EN, Epstein JA. Cre-mediated excision of Fgf8 in the Tbx1 expression domain reveals a critical role for Fgf8 in cardiovascular development in the mouse. Developmental Biology. 2004;**267**:190-202. DOI: 10.1016/j.ydbio.2003.10.024

[104] Frank DU, Fotheringham LK, Brewer JA, Muglia LJ, Tristani-Firouzi M, Capecchi MR, et al. An Fgf8 mouse mutant phenocopies human 22q11 deletion syndrome. Development. 2002;**129**:4591-4603

[105] Reeh KA, Cardenas KT, Bain VE, Liu Z, Laurent M, Manley NR, et al. Ectopic TBX1 suppresses thymic epithelial cell differentiation and proliferation during thymus organogenesis. Development. 2014;**141**:2950-2958. DOI: 10.1242/dev.111641

[106] Wallin J, Eibel H, Neubuser A, Wilting J, Koseki H, Balling R. Pax1 is expressed during development of the thymus epithelium and is required for normal T-cell maturation. Development. 1996;**122**:23-30

[107] Manley NR, Capecchi MR. The role of Hoxa-3 in mouse thymus and thyroid development. Development. 1995;**121**:1989-2003

[108] Su D, Ellis S, Napier A, Lee K, Manley NR. Hoxa3 and pax1 regulate epithelial cell death and proliferation during thymus and parathyroid organogenesis. Developmental Biology. 2001;**236**:316-329. DOI: 10.1006/dbio.2001.0342

[109] Blackburn CC, Manley NR. Developing a new paradigm for thymus organogenesis. Nature Reviews. Immunology. 2004;**4**:278-289. DOI: 10.1038/nri1331

[110] Hetzer-Egger C, Schorpp M, Haas-Assenbaum A, Balling R, Peters H, Boehm T. Thymopoiesis requires Pax9 function in thymic epithelial cells. European Journal of Immunology. 2002;**32**:1175-1181. DOI: 10.1002/1521-4141(200204)32:4<1175::Aid-immu1175>3.0.Co;2-u

[111] Peters H, Wilm B, Sakai N, Imai K, Maas R, Balling R. Pax1 and Pax9 synergistically regulate vertebral column development. Development. 1999;**126**:5399-5408

[112] Chisaka O, Kameda Y. Hoxa3 regulates the proliferation and differentiation of the third pharyngeal arch mesenchyme in mice. Cell and Tissue Research. 2005;**320**:77-89. DOI: 10.1007/s00441-004-1042-z

[113] Neubuser A, Koseki H, Balling R. Characterization and developmental expression of Pax9, a paired-box-containing gene related to Pax1. Developmental Biology. 1995;**170**:701-716. DOI: 10.1006/dbio.1995.1248

[114] Su DM, Manley NR. Hoxa3 and pax1 transcription factors regulate the ability of fetal thymic epithelial cells to promote thymocyte development. Journal of Immunology. 2000;**164**:5753-5760

[115] Zou D, Silvius D, Davenport J, Grifone R, Maire P, Xu PX. Patterning of the third pharyngeal pouch into thymus/parathyroid by six and Eya1. Developmental Biology. 2006;**293**:499-512. DOI: 10.1016/j.ydbio.2005.12.015

[116] Laclef C, Souil E, Demignon J, Maire P. Thymus, kidney and craniofacial abnormalities in six 1 deficient mice. Mechanisms of Development. 2003;**120**:669-679

[117] Xu PX, Zheng W, Laclef C, Maire P, Maas RL, Peters H, et al. Eya1 is required for the morphogenesis of mammalian thymus, parathyroid and thyroid. Development. 2002; **129**:3033-3044

[118] Erickson M, Morkowski S, Lehar S, Gillard G, Beers C, Dooley J, et al. Regulation of thymic epithelium by keratinocyte growth factor. Blood. 2002;**100**:3269-3278. DOI: 10.1182/blood-2002-04-1036

[119] Jenkinson WE, Jenkinson EJ, Anderson G. Differential requirement for mesenchyme in the proliferation and maturation of thymic epithelial progenitors. The Journal of Experimental Medicine. 2003;**198**:325-332. DOI: 10.1084/jem.20022135

[120] Revest JM, Suniara RK, Kerr K, Owen JJ, Dickson C. Development of the thymus requires signaling through the fibroblast growth factor receptor R2-IIIb. Journal of Immunology. 2001;**167**:1954-1961

[121] Jenkinson WE, Rossi SW, Parnell SM, Jenkinson EJ, Anderson G. PDGFRalpha-expressing mesenchyme regulates thymus growth and the availability of intrathymic niches. Blood. 2007;**109**:954-960. DOI: 10.1182/blood-2006-05-023143

[122] Bain VE, Gordon J, O'Neil JD, Ramos I, Richie ER, Manley NR. Tissue-specific roles for sonic hedgehog signaling in establishing thymus and parathyroid organ fate. Development. 2016;**143**:4027-4037. DOI: 10.1242/dev.141903

[123] Garg V, Yamagishi C, Hu T, Kathiriya IS, Yamagishi H, Srivastava D. Tbx1, a DiGeorge syndrome candidate gene, is regulated by sonic hedgehog during pharyngeal arch development. Developmental Biology. 2001;**235**:62-73. DOI: 10.1006/dbio.2001.0283

[124] Balciunaite G, Keller MP, Balciunaite E, Piali L, Zuklys S, Mathieu YD, et al. Wnt glycoproteins regulate the expression of FoxN1, the gene defective in nude mice. Nature Immunology. 2002;**3**:1102-1108. DOI: 10.1038/ni850

[125] Bleul CC, Boehm T. BMP signaling is required for normal thymus development. Journal of Immunology. 2005;**175**:5213-5221

[126] Neves H, Dupin E, Parreira L, Le Douarin NM. Modulation of Bmp4 signalling in the epithelial-mesenchymal interactions that take place in early thymus and parathyroid development in avian embryos. Developmental Biology. 2012;**361**:208-219. DOI: 10.1016/j.ydbio.2011.10.022

[127] Soza-Ried C, Bleul CC, Schorpp M, Boehm T. Maintenance of thymic epithelial phenotype requires extrinsic signals in mouse and zebrafish. Journal of Immunology. 2008;**181**:5272-5277

[128] Metz A, Knochel S, Buchler P, Koster M, Knochel W. Structural and functional analysis of the BMP-4 promoter in early embryos of Xenopus laevis. Mechanisms of Development. 1998;**74**:29-39

[129] Swann JB, Krauth B, Happe C, Boehm T. Cooperative interaction of BMP signalling and Foxn1 gene dosage determines the size of the functionally active thymic epithelial compartment. Scientific Reports. 2017;**7**:8492. DOI: 10.1038/s41598-017-09213-1

[130] Heinonen KM, Vanegas JR, Brochu S, Shan J, Vainio SJ, Perreault C. Wnt4 regulates thymic cellularity through the expansion of thymic epithelial cells and early thymic progenitors. Blood. 2011;**118**:5163-5173. DOI: 10.1182/blood-2011-04-350553

[131] Ma D, Wei Y, Liu F. Regulatory mechanisms of thymus and T cell development. Developmental and Comparative Immunology. 2013;**39**:91-102. DOI: 10.1016/j.dci.2011.12.013

[132] Osada M, Jardine L, Misir R, Andl T, Millar SE, Pezzano M. DKK1 mediated inhibition of Wnt signaling in postnatal mice leads to loss of TEC progenitors and thymic degeneration. PLoS One. 2010;**5**:e9062. DOI: 10.1371/journal.pone.0009062

[133] Swann JB, Happe C, Boehm T. Elevated levels of Wnt signaling disrupt thymus morphogenesis and function. Scientific Reports. 2017;**7**:785. DOI: 10.1038/s41598-017-00842-0

[134] Zuklys S, Gill J, Keller MP, Hauri-Hohl M, Zhanybekova S, Balciunaite G, et al. Stabilized beta-catenin in thymic epithelial cells blocks thymus development and function. Journal of Immunology. 2009;**182**:2997-3007. DOI: 10.4049/jimmunol.0713723

[135] Dean CH, Miller LA, Smith AN, Dufort D, Lang RA, Niswander LA. Canonical Wnt signaling negatively regulates branching morphogenesis of the lung and lacrimal gland. Developmental Biology. 2005;**286**:270-286. DOI: 10.1016/j.ydbio.2005.07.034

[136] Niida A, Hiroko T, Kasai M, Furukawa Y, Nakamura Y, Suzuki Y, et al. DKK1, a negative regulator of Wnt signaling, is a target of the beta-catenin/TCF pathway. Oncogene. 2004;**23**:8520-8526. DOI: 10.1038/sj.onc.1207892

[137] Mulroy T, McMahon JA, Burakoff SJ, McMahon AP, Sen J. Wnt-1 and Wnt-4 regulate thymic cellularity. European Journal of Immunology. 2002;**32**:967-971. DOI: 10.1002/1521-4141(200204)32:4<967::Aid-immu967>3.0.Co;2-6

[138] Hamazaki Y, Fujita H, Kobayashi T, Choi Y, Scott HS, Matsumoto M, et al. Medullary thymic epithelial cells expressing Aire represent a unique lineage derived from cells expressing claudin. Nature Immunology. 2007;**8**:304-311. DOI: 10.1038/ni1438

[139] Munoz JJ, Cejalvo T, Tobajas E, Fanlo L, Cortes A, Zapata AG. 3D immunofluorescence analysis of early thymic morphogenesis and medulla development. Histology and Histopathology. 2015;**30**:589-599. DOI: 10.14670/HH-30.589

[140] Tucker AS. Salivary gland development. Seminars in Cell & Developmental Biology. 2007;**18**:237-244. DOI: 10.1016/j.semcdb.2007.01.006

[141] Ginda WJ, Jaroszewski J, Warchol JB, Brelinska R. Three dimensional analysis of thymic medulla. Folia Morphologica. 1994;**53**:157-164

[142] Masuda K, Itoi M, Amagai T, Minato N, Katsura Y, Kawamoto H. Thymic anlage is colonized by progenitors restricted to T, NK, and dendritic cell lineages. Journal of Immunology. 2005;**174**:2525-2532

[143] Vroegindeweij E, Crobach S, Itoi M, Satoh R, Zuklys S, Happe C, et al. Thymic cysts originate from Foxn1 positive thymic medullary epithelium. Molecular Immunology. 2010;**47**:1106-1113. DOI: 10.1016/j.molimm.2009.10.034

[144] Dooley J, Erickson M, Farr AG. An organized medullary epithelial structure in the normal thymus expresses molecules of respiratory epithelium and resembles the epithelial thymic rudiment of nude mice. Journal of Immunology. 2005;**175**:4331-4337

[145] Nowell CS, Bredenkamp N, Tetelin S, Jin X, Tischner C, Vaidya H, et al. Foxn1 regulates lineage progression in cortical and medullary thymic epithelial cells but is dispensable for medullary sublineage divergence. PLoS Genetics. 2011;**7**:e1002348. DOI: 10.1371/journal.pgen.1002348

[146] Guo J, Rahman M, Cheng L, Zhang S, Tvinnereim A, Su DM. Morphogenesis and maintenance of the 3D thymic medulla and prevention of nude skin phenotype require FoxN1 in pre- and post-natal K14 epithelium. Journal of Molecular Medicine (Berlin). 2011;**89**:263-277. DOI: 10.1007/s00109-010-0700-8

[147] Barsanti M, Lim JM, Hun ML, Lister N, Wong K, Hammett MV, et al. A novel Foxn1(eGFP/+) mouse model identifies Bmp4-induced maintenance of Foxn1 expression and thymic epithelial progenitor populations. European Journal of Immunology. 2017;**47**:291-304. DOI: 10.1002/eji.201646553

Chapter 3

Histology of Umbilical Cord in Mammals

Luis Manuel Barrios Arpi

Additional information is available at the end of the chapter

http://dx.doi.org/10.5772/intechopen.80766

Abstract

The histology is one of the most important disciplines for studying of organic tissues such as the placenta, umbilical cord and related structures which has been poorly studied in mammals, mainly in domestic animals. The umbilical cord, connection between fetus and mother, is one of the most important anatomical structures related to the development of the animal during their stage of formation due to its participation as responsible of the exchange of nutrients and protection of the structural vessels. There are several researches which have described anatomic, histological, immunohistochemical characteristics of the main constituents of the umbilical cord in wild and domestic animals due to its importance in the maintaining of the fetus during their development. The present chapter recompiles and describes the majority of researches about histological characteristics of the constituents of the umbilical cord included images and graphics that improve the understanding about the histological main differences found among mammals and also, this review aims to be a great helpful for the pathologist, surgeons and staff dedicated to reproduction and research about stem cells, this last considered one of the fields of special interest since some years ago in veterinary medicine.

Keywords: allantoic duct, histology, umbilical artery, umbilical cord, umbilical vein, mammals

1. Introduction

When an animal is born, it is necessary that several changes in the fetal circulation appear such as fast closure of some anatomical communication channels by coordinated mechanisms which arrows to autonomic life. The umbilical orifice permits the passage of the umbilical cord, being this characteristic a natural defect [1].

The majority of mammals have an umbilical cord and eventually an umbilicus, but sea shellfish, the whole animals, looks like an umbilicus [1].

The umbilical cord was originated from the embryonic stem which connects the bladder of both yolk sac and amniotic. This is discarded after birth in all species of mammals [2]. The umbilical cord forms a connection between placenta and the fetus. This structure is responsible for exchange of nutrients during the gestation. The main characteristic that umbilical cord shows is a specific gross morphology of vein and arteries surrounded of mucous connective tissue. It is known that fetus-mother nutrients exchange is very delicate and difficult to maintain; however, many morphological and functional alterations may produce changes in this mechanism of exchange easily.

In relation to the hematopoietic cells, these have been widely studied functionally, molecularly and structurally, but there are few studies about ultrastructural characterization [3]. The use of stem cells obtained from umbilical cord have originated a lot of expectative for use it in cell therapy and regeneration of organs [4]. Furthermore, it is known that the umbilical cord cells have been studied only in preclinical approaches [5].

The scarcity of bibliographic information about studies of optical microscopy of the umbilical cord in mammals and lack researches about these topics in mammalian species have motivated to execution of this type of reviews that reveal main characteristics in relation to the histology of umbilical cord and comparative aspects between different species of mammals of interest.

2. Umbilical cord

2.1. Structure

The umbilical cord is a structure discarded after the birth and the transplant of their cells may present less risks of causing reactions, resulting immune reactions, resulting in minimum for the recipient of its cells [4]. This structure has amniotic and allantoic segments. The amniotic segment of the umbilical cord contains two arteries and a vein that arborize into the amnion. These segments continue as multiple vessels in the allantoic segment of the cord with mainly two arteries and two veins with branches (**Figure 1**) [6]. The urachus courses within the cord from the fetus and empties into the allantoic cavity [6].

The umbilical cord is a unique mammalian fetal attachment and was attached to the center of the placental disk [7, 8]. This structure plays an important role in the transport of maternal nutrients for developing of fetus during gestation [1]. The umbilical cord shows distinct types of composition with respect to the number of blood vessels. There are many morphological changes that appear at the birth into local anatomical structures around the umbilical cord form a complex device to help the organism to severe relation with the placenta. The relation between anatomical structures that form the umbilical cord arrows the morphological support as basis of contraction to eliminate remnants that was inside the abdominal cavity [1, 6].

As has already been mentioned, this structure has a main function of making the connection between the fetus and placenta, ensuring its viability mainly during the later stages of pregnancy [9]. In relation to the umbilical vessels, these are not supplied by *vasa vasorum* and thus

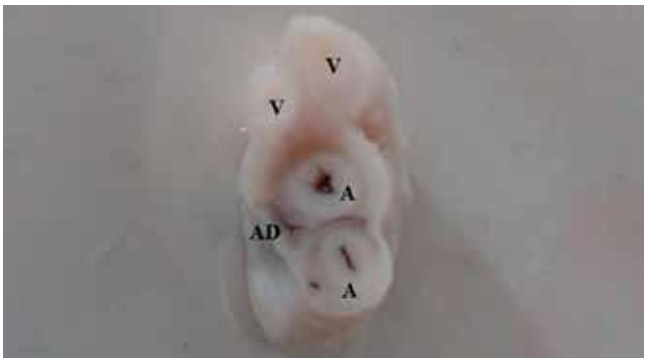

Figure 1. Photograph of umbilical cord of alpaca (*Vicugna pacos*) showing two umbilical veins (V) and umbilical arteries (a). Next to the umbilical arteries is located allantoid duct (AD). (adapted from barrios-Arpi et al. 2017. Histological characterization of umbilical cord in alpaca (*Vicugna pacos*).

depend on their oxygen supply making them more vulnerable to changes originated by hemodynamic disorders and similar conditions [10].

This structure is coated by amniotic epithelium (simple squamous epithelium) and the conjunctive layer is adhered closely to the fundamental substance of the umbilical cord majority known as fetal mesenchyme, which is constituted of mesenchymal connective tissue with stellate cells and amorphous ground substance which contains abundant glycogen. This gelatinous composition also called Wharton's jelly or mucous connective tissue has been of great interest and potential impact due to research about tissue repair and differentiation [10]. However, many of the investigations have not been able to continue due to the lack of an animal model that can be used in the preclinical studies [11]. This mucous connective tissue (Wharton's jelly) is an active metabolically tissue involved in fluid exchange between umbilical vessels and amniotic fluid [12].

In the majority of domestic species, two arteries and two veins wound spirally being immersed in a mucous connective tissue appears [13, 14]; however, it is known that in some species, appear the formation of anastomosis of arteries in middle third and proximal to the maternal part of the placenta appears [15].

There are important changes evidenced in the structure of umbilical cord in different animal species. It is indicated that from the beginning, vessels of umbilical cord are represented by two umbilical veins and arteries in species such as bovines and small ruminants [16], zebu-crossed bovines [17], buffaloes [18–20], pigs [21], African lions and gazelles [22], and Bactrian camels and dromedaries [23, 24] (**Figure 2**); however, it is known that in some species the disintegration of right umbilical vein appears without have a strong explanation about this feature [25] (**Figure 3**). Among these species are carnivores, horses, guinea pigs, nutrias, chinchillas, cavies and rock cavies [26–32].

Finally, as the stages of gestation, the tunica adventitia is becoming thicker in relationship to the tunica intima in both arteries and veins [23].

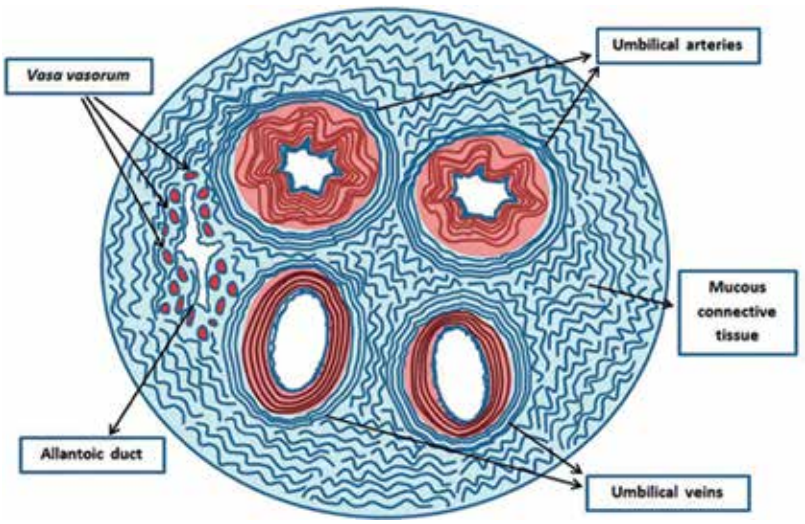

Figure 2. Schematic representation of structure of umbilical cord in cattle, sheep, goat, buffalo, alpaca, canine and feline showing two arteries and two veins. Furthermore, this figure shows the localization of allantoic duct and their relation with blood vessels.

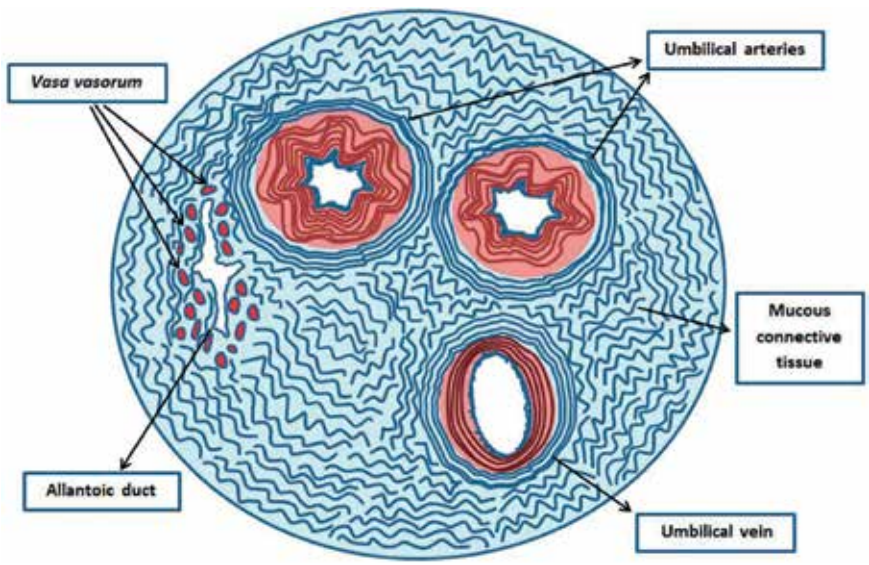

Figure 3. Schematic representation of structure of umbilical cord in horses, pigs and humans showing two arteries and only one vein. Furthermore, this figure shows the localization of allantoic duct and their relation with blood vessels.

2.2. Umbilical artery

At parturition the umbilical arteries retract into the abdomen and close by smooth muscle contraction. This process appears in response to the increased partial pressure of oxygen in the blood [33].

There are some characteristics that differ between lumens of umbilical arteries in different mammalian species. In the majority of mammals, umbilical arteries show a very large lumen and irregular shape. In some species such as buffaloes, bovines and zebu cows, the umbilical arteries show a lumen of star-shaped lumen [17, 18, 34–36]; however, in species as South American Camelids, the animals present a lumen of slightly star-shaped [37]. In mammals, the umbilical artery is constituted by tunicas intima, media and external/adventitia (**Figure 4**).

2.2.1. Intima

The intima layer consists of elongated endothelium to the long axis of the blood vessel. The endothelium of tunica intima corresponds to the thinnest layer comprised of simple squamous

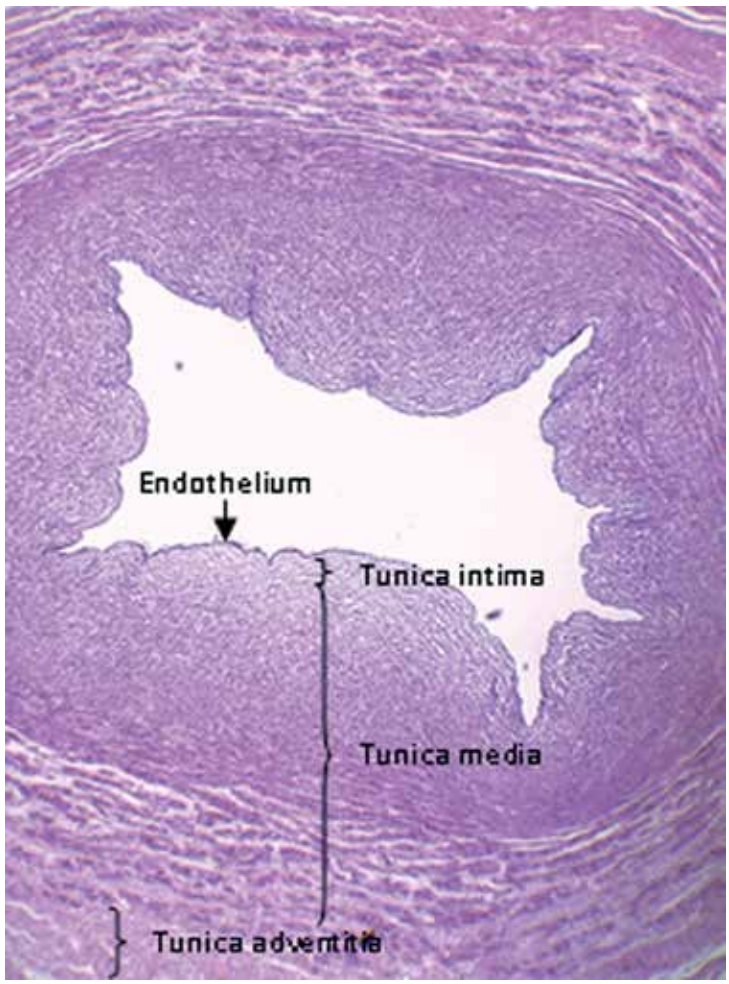

Figure 4. Umbilical artery, light microscopy, H-E stain. The tunica intima is constituted by endothelium and a small endothelial space. The tunica media is formed mainly by smooth muscle and has double size of tunica adventitia. The abundant collagen and elastic fibers of the tunica adventitia contrasts with muscular tissue and collagen fibers of the tunica media. 40 x.

epithelium. Most animals, the internal elastic lamina is discontinuous and thin [17, 18, 32–38] with exception of humans and camels which the umbilical arteries possess no internal elastic lamina [10, 23]. In some species as alpacas is possible to observe a very small sub endothelial space which consisted of muscular fibers (non-differentiated muscular cells) cross and cut diagonally (circular disposition), and connective tissue fibers [37] (**Figure 5**).

2.2.2. Media

The media layer is located below to the sub endothelial space and the thickness of this layer is double the size of the external/adventitia. The tunica media is constituted by a double layered muscular of smooth muscle bundles, characterized for inner circular muscular layer (collagen and reticular fibers) and outer longitudinal layer (**Figure 6**). Another characteristic of the media layer is absence of elastic lamina, a presence of reticular fibers and both collagen and elastic fibers and presence of capillaries [10, 17, 32–38].

2.2.3. Adventitia

The tunica adventitia is the most outer layer that forms the umbilical cord wall in all mammals. The tunica adventitia consists of collagen, smooth muscle and elastic fibers. This layer is constituted by smooth muscular fibers which invade part of tunica media and muscle fibers cross-sectional [10, 17, 18, 32, 34–36, 38].

Unlike other mammals, in alpacas, the inner layer is not well defined [37]. In alpacas, the concentration of collagen fibers is increased towards longitudinally oriented muscular fibers and towards periphery. The elastic fibers are abundant between the tunicas media and

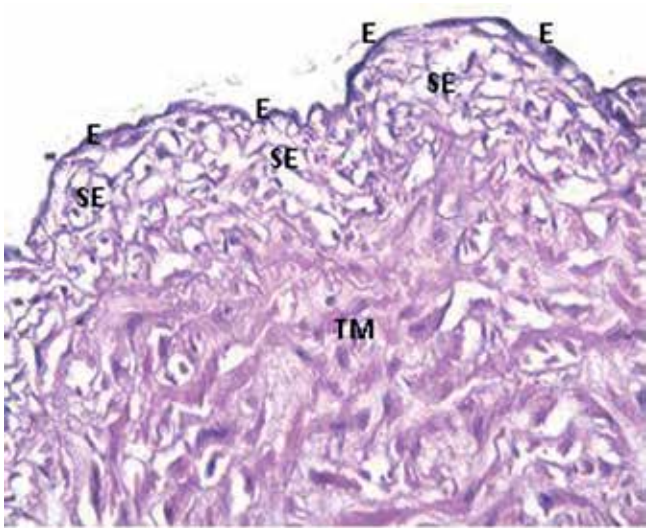

Figure 5. Umbilical artery, light microscopy, H-E stain. The tunica intima is comprised of a simple squamous epithelium (E) and a small endothelial space (SE) characterized by elastic and reticular fibers. Note that the internal elastic lamina is not well-defined. TM: Tunica muscular. 400 x.

adventitia. Finally, the tunica adventitia is constituted by small blood vessels denominated *Vasa vasorum*, non-myelinated nerves cross-sectional and clearly separated from mucous connective tissue (**Figure 7**) [10, 17, 18, 32, 34–38].

2.3. Umbilical vein

At parturition the umbilical vein and urachus remain outside the abdomen. In relation to the vein, this structure closes soon by smooth muscle contraction and the urachus shrinks and dries within a day [1].

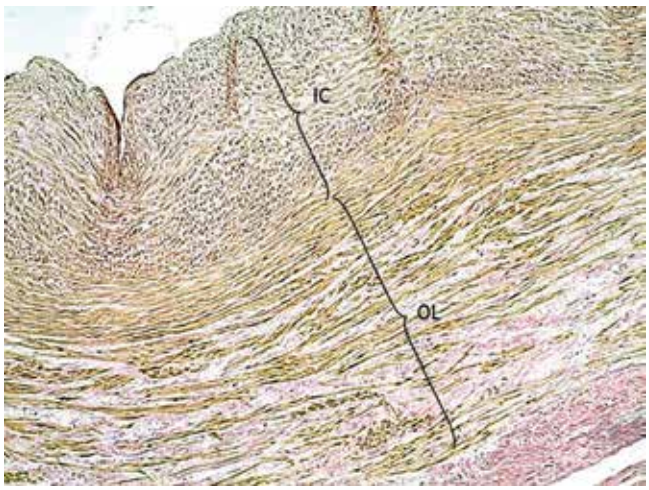

Figure 6. Umbilical artery, light microscopy, van Gieson stain. The tunica media is constituted by a double layered muscular of smooth muscle bundles, characterized for inner circular (IC) and outer longitudinal muscular (OL) layers. 100 x.

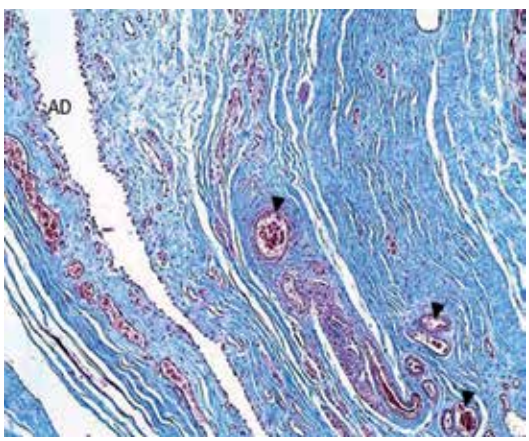

Figure 7. Umbilical artery, light microscopy, Masson's trichrome stain. The tunica adventitia/external is the most external layer of umbilical cord and is constituted by small blood vessels denominated *Vasa vasorum* (short arrows). AD: Allantoic duct. 100 x.

Similar to the umbilical artery, there are some characteristics that differ between lumen of umbilical arteries in different mammalian species. In some mammals such as buffaloes, carnivores, horses, guinea pigs, nutrias, chinchillas, cavies and rock cavies, umbilical vein shows a lumen in elliptic shape with wall thinner than umbilical artery [26–32]; however, in species as South American Camelids and horses, the umbilical vein displays a lumen obliterated into star-shaped [29, 37, 38]. In mammals, umbilical vein is constituted of tunicas intima, media and external/adventitia (**Figure 8**).

2.3.1. Intima

The tunica intima consists of endothelium but lack of external elastic lamina with less organization line compared to the umbilical artery. However, in general, endothelium showed similar characteristics as observed in the umbilical artery.

There are several studies that confirm this conformation of the tunica intima which is thin and lack internal elastic lamina [10, 17, 23, 34–38]. Similar to alpacas, is possible to observe a small

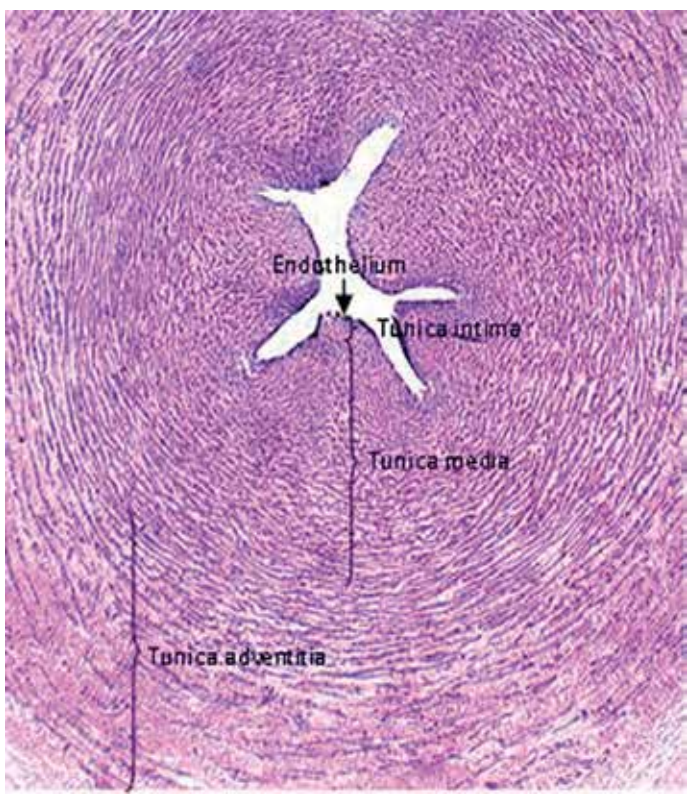

Figure 8. Umbilical vein, light microscopy, H-E stain. The tunica intima is constituted by endothelium and a very small endothelial space. The tunica media is formed mainly by smooth muscle and has a thickness similar to the tunica adventitia. The abundant collagen and elastic fibers of the tunica adventitia is slightly invaded by muscular tissue and collagen fibers of the tunica media. 40 x.

sub endothelial space which consist of muscular fibers (non-differentiated muscular cells) cross and cut diagonally (circular disposition), and connective tissue fibers [37] (**Figure 9**).

2.3.2. Media

The media layer is located below to the sub endothelial space and the thickness of this layer is variable in relation to the external/adventitia in different mammalian species. Most animals display a tunica media which is smaller than tunica adventitia including species such as buffaloes, carnivores, horses, guinea pigs, nutrias, chinchillas, cavies and rock cavies [26–32]. Additionally, the South American camelids present a tunica media which is larger in dimension than the tunica adventitia [37], however, the cause of this morphologic evidence is not known.

This tunica is constituted by a double layered muscular of smooth muscle bundles, characterized for inner circular muscular layer (collagen and reticular fibers) and outer longitudinal layer (**Figure 10**). The tunica media comprises the inner circular and outer longitudinal muscular layers, with an absence of outer elastic lamina and presence of reticular fibers. Also, it presented a small amount of collagen and elastic fibers [10, 17, 23, 34–38]. Furthermore, in alpacas is known that smooth, cross-sectional muscle fibers invade part of the tunic adventitia consisting in muscular fibers cross-transverse, abundant collagen fibers, collagen and muscular fibers arranged longitudinally [37].

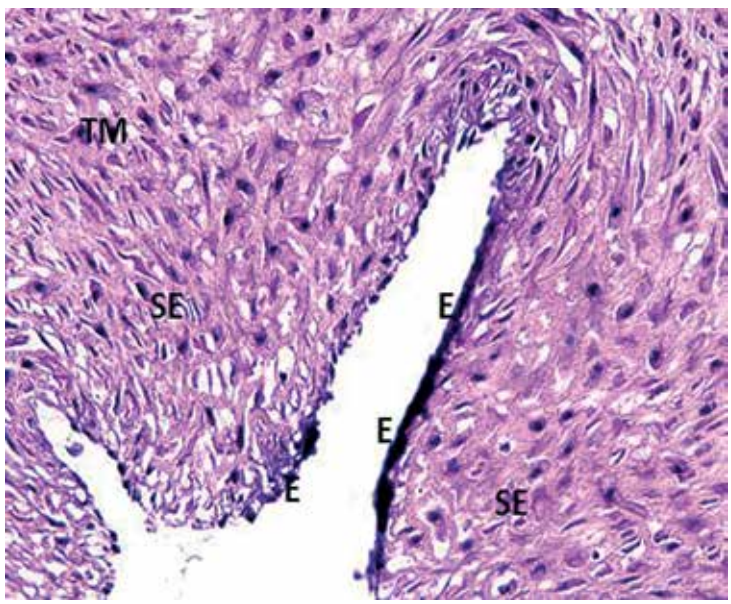

Figure 9. Umbilical vein, light microscopy, H-E stain. The tunica intima is comprised of a simple squamous epithelium (E) and a small endothelial space (SE). TM: Tunica muscular. 400 x.

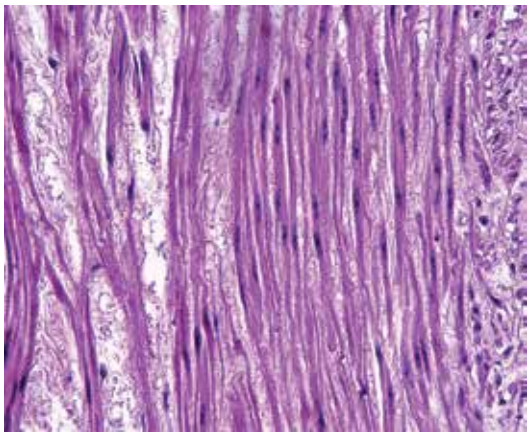

Figure 10. Umbilical vein, light microscopy, H-E stain. The tunica media is constituted by abundant muscular fibers separated by elastic and fibrous tissue. 400 x.

2.3.3. Adventitia

In the majority of mammalian species, the tunica adventitia is larger than the tunica media [26–32] and this layer consists of collagen and elastic fibers, and small blood vessels called *Vasa vasorum* (**Figure 11**). Additionally, the tunica adventitia is slightly smaller than the tunica media in alpacas [37]. Generally, this tunica not is clearly separated of the mucous connective tissue also called Wharton's Jelly, however, is species as alpacas, it is possible observe a clear separation among both structures [37]. This tunica displays variations in their thickness where most mammalian species present a great number of transversal nerves in all thickness fibers [10, 17, 23, 34–38].

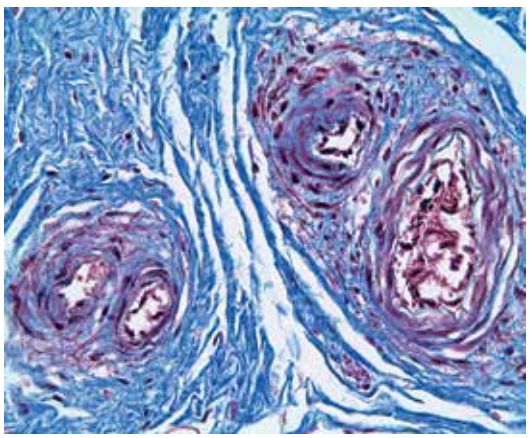

Figure 11. Umbilical vein, light microscopy, Masson's trichrome stain. The tunica adventitia/external is constituted by small blood vessels denominated *Vasa vasorum.* Note the presence abundant collagen and elastic fibers. 400 x.

2.4. Mucous connective tissue (Wharton jelly)

The mucous connective tissue surrounding the umbilical artery is almost the same in thickness and share histological features with that of umbilical vein region except that smaller blood vessels and blood capillaries are more numerous towards periphery (**Figure 12**). Moreover, small nerve bundles cut in different profiles (and some structures resembling to ganglion) have been also observed towards periphery of the mucous connective tissue [10, 17, 18, 32, 34–38].

In alpacas has been observed some larger cells that had triangular or star-shaped with less basophilic nuclei and strongly eosinophilic cytoplasm, probably mesenchymal stem cells. A few round cells with differently stained nuclei were also observed which showed similar features to lymphoid cells [37].

2.5. Allantoic duct

The allantoic duct present irregular lumen and is comprised by simple cuboidal to columnar epithelium [10, 17, 18, 32, 34–38]. In alpacas has been recognized some characteristics such as the less basophilic nuclei of varying shapes that are oriented in mid portion of the epithelium, and eosinophilic dense and finely granular cytoplasm [37].

Most animals display the outer layer consisting of band of smooth muscle bundles arranged in different directions; oblique, circular and longitudinal [10, 17, 18, 32, 34–38].

In alpacas, this structure presents abundant fine blood vessels between arterioles, venules and capillaries which have been reduced to adjacent portion of the mucous connective tissue (**Figure 13**) [37].

Umbilical cord is covered by simple squamous epithelium in all mammalian species [10, 17, 18, 32, 34–38].

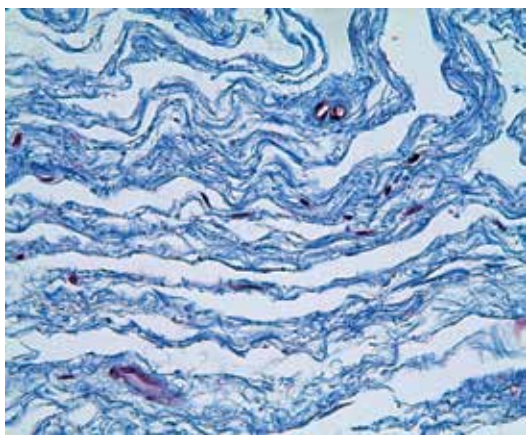

Figure 12. Mucous connective tissue, light microscopy, Masson's trichrome stain. In the most periphery part is observed great number of blood vessels that alternate with abundant reticular, elastic and collagen fibers. 400 x.

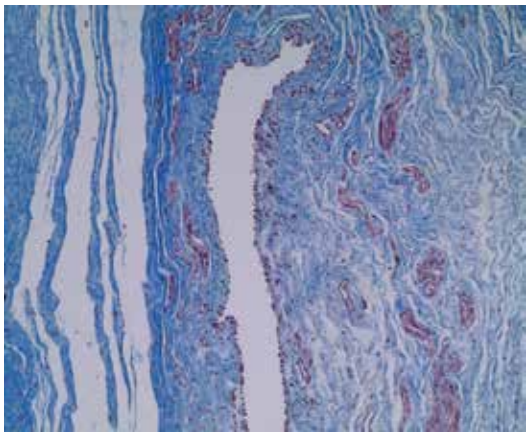

Figure 13. Allantoic duct, light microscopy, Masson's trichrome stain. Note the irregular shape lumen with plane epithelium and presence of abundant small blood vessels located near to this structure immersed in abundant connective tissue. 100 x.

Conclusions

Histology plays an important role in the characterization of umbilical cord in mammals. There are many structures which enable to be recognized through of this method and furthermore, allow compares and differentiate among different animal species. According with the presence of certain structures and characteristics that comprise the wall of arteries and veins is possible a well-characterized description of the umbilical cord in mammals.

Acknowledgements

The present chapter contains several details obtained of article entitled "Histological characterization of umbilical in alpaca (*Vicugna pacos*)" which was published by Jose Luis Rodríguez Gutierrez, Bernardo Lopez Torres and me as corresponding author and main author. As author, I want to recognize the contribution of these authors for presentation of this book chapter.

Author details

Luis Manuel Barrios Arpi

Address all correspondence to: lbarriosa@unmsm.edu.pe

Animal Physiology Laboratory, San Marcos University, Lima, Peru

References

[1] Fahmy M. Umbilicus and Umbilical Cord. 1st. ed. Springer; 2018. p. 264. DOI: 10.1007/978-3-319-62383-2

[2] Bydlowski OP, Debes AA, Maselli LMF, Janz FL. Características biológicas das células-troncos mesenquimais. Revista Brasileira de Hematologia e Hemoterapia. 2009;**31**(Supl. 1): 25-35. DOI: 10.1590/S1516-84842009005000038

[3] Deliliers LG et al. Ultrastructural features of CD 34+ hematopoetic progenitor cells from bone marrow, peripheral blood and umbilical cord blood. Leukemia and Lymphoma. 2001. 2001;**42**(4):699-708. DOI: 10.3109/10428190109099332

[4] Zucconi E, Vieira NM, Bueno DF. Mesenchymal stem cells derived from canine umbilical cord vein—A novel source for cell therapy studies. Stem Cells and Development. 2019;**19**: 395-402. DOI: 10.1089/scd.2008.0314

[5] Niemeyer GP, Hudson J, Bridgman R, Spano J, Richard AN, Lathrop CD. Isolation and characterization of canine hematopoetic progenitor cells. Experimental Hematology. 2001; **29**:686-693. DOI: 10.1016/S0301-472X(01)00638-5

[6] Bradley LN. Diagnosis of Abortion and Neonatal Loss in Animals. 4th ed. Wiley-Blackwell; 2012. p. 241. DOI: 10.1002/9781119949053

[7] Blanchette H. The rising cesarean delivery rate in America: What are the consequences? Obstetrics and Gynecology. 2011;**118**:687-690. DOI: 10.1097/AOG.0b013e318227b8d9

[8] Favaron et al. Placentation in Sigmodontinae: A rodent taxon native to South America. Reproductive Biology and Endocrinology. 2011, 2011;**9**(55):1-14. DOI: 10.1186/1477-7827-9-55

[9] Caughey AB et al. Maternal and neonatal outcomes of elective induction of labor. Evidence Report/Technology Assessment. 2009;**176**:247-257. DOI: 10.1007/s00404-017-4354-4

[10] Barnwal M, Rathi SK, Chhabra S, Nanda S. Histomorphometry of umbilical cord and its vessels in pre eclampsia as compared to normal pregnancies. Nepal Journal of Obstetrics and Gynaecology. 2012;**7**(1):28-32. DOI: 10.3126/njog.v7i1.8832

[11] Sousa AF, Andrade PZ, Pirzgalska RM, Galhoz TM, Azevedo AM. A novel method for human hematopoietic stem/progenitor cell isolation from umbilical cord blood based on immunoaffinity aqueous two-phase partitioning. Biotechnology Letters. 2011;**33**:2373-2377. DOI: 10.1007/s10529-011-0727-0

[12] Tavares-Fortuna LF, Lourdes-Pratas M. Coarctation of the umbilical cord: A cause of intrauterine fetal death. International Journal of Gynaecology and Obstetrics. 1978;**15**(5): 469-473. DOI: 10.1002/j.1879-3479.1977.tb00735.x

[13] Ribeiro AACM. Pesquisa anatômica sobre o funículo umbilical em bovinos azebuados [thesis]. São Paulo: Universidade de São Paulo; 1995

[14] Whitwell KE, Jeffcott LB. Morphological studies on the fetal membranes of the normal singleton foal at term. Research in Veterinary Science. 1975;**19**(1):44-45 PMID: 1153897

[15] Carambula SF, Filho AT, Miglino MA, Didio LJA, Souza WM. Research on anatomical branchingand arrangement of arteries and veins of the placenta of zebu cattle. Brazilian Journal of Veterinary Research and Animal Science. 1997;**34**:131-137

[16] Neves WC. Pesquisa anatômica sobre a ramificação e distribuição das artérias e veias da placenta em caprinos [thesis]. São Paulo: Universidade de São Paulo; 1996

[17] Ribeiro AACM, Miglino MA. O funículo umbilical em bovines azebuados. Brazilian Journal of Veterinary Research and Animal Science. 1997;**34**(5):266-269. DOI: 10.11606/issn.2318-3659.v34i5

[18] Feitosa FS Jr. Pesquisa anatômica sobre a ramificação e distribuição das artérias e veias da placenta em búfalos [thesis]. São Paulo: Universidade de São Paulo; 1997

[19] Ferreira GJ et al. Morphological aspects of buffaloes (*Bubalus bubalis*) umbilical cord. Pes Vet Bra. 1997;**29**(10):788-792. DOI: 10.1590/S0100-736X2009001000002

[20] Singh J et al. Cell morphology and Mucopolysaccharides in early gestation buffalo umbilical cord. The Indian Veterinary Journal. 2012;**89**(11):36-38

[21] Barclay AE, Franklin KJ, Prichard MML. The Foetal Circulation and Cardiovascular System, and the Changes that they Undergo at Birth. Oxford, UK: Oxford Blackwell Scientific Publications, Ltd. 1945;**92**(1):93-95. DOI: 10.1002/ar.1090920111

[22] Benirschke K, Miller CJ. Anatomical and functional differences in the placenta of primates. Biology of Reproduction. 1982;**26**(1):29-53. DOI: 10.1095/biolreprod26.1.29

[23] Elgozouli SO, Osman DI. Histology of the constituents of the umbilical cord and Ductus arteriosus and Ductus Venosus of the dromedary camel. J Vet Adv. 2012;**2**(9):449-456

[24] Tibary A, Anouassi A. Theriogenology in Camelidae: Anatomy, Physiology, Pathology and Artificial Breeding. 1st ed. Actes ed1997. p. 489

[25] Dos Santos HSL, Azoubel R. Embriologia Comparada (Texto eAtlas). 1st ed. FUNEP; 1996. p. 189

[26] Hillemann HH, Gaynor AI. The definitive architeture of the placenta of nutria, Myocastor coypus (Molina). The American Journal of Anatomy. 1961;**109**:299-317. DOI: 10.1002/aja.1001090306

[27] Leiser R, Kaufmann P. Placental structure: in a comparative aspect. Experimental and Clinical Endocrinology. 1994;**102**(3):122-134. DOI: 10.1055/s-0029-1211275

[28] Zanco NA. Pesquisa anatômica das artérias e veias do funículo umbilical, suaramificação e disposição na placenta de cães (*Canis familiaris*, Linnaeus, 1758). São Paulo: Universidade de São Paulo; 1998

[29] Carvalho FSR, Miglino MA, Severino RS, Ferreira FA, Santos TC. Aspectos morfológicos do funículo umbilical em eqüinos (*Equus caballus*, Linnaeus, 1758). Brazilian Journal of Veterinary Research and Animal Science. 2001;**38**:214-219. DOI: 10.1590/S1413-95962001000500003

[30] Silva WN. Aspecto morfológico da placenta e anexos fetais da paca (*Agouti paca*, L. 1766). São Paulo: Universidade de São Paulo; 2001

[31] Dantas CHG, Rodrigues MN, Oliveira GB, Chaves HSA, Albuquerque JFG, Oliveira MF. Cordão Umbilical do Preá Gálea Spixii. In: Anais do 36° CONBRAVET. Brasil; 2009

[32] Rodrigues MN et al. Microscopy of the umbilical cord of rock cavies—Kerodon rupestris Wied, 1820 (Rodenta, Caviidae). Microscopy Research and Technique. 2013;**76**:419-422. DOI: 10.1002/jemt.22182

[33] Anderson DE, Rings DM. Food Animal Practice. 5th ed. Saunders; 2008. p. 736. DOI: 10.1016/B978-141603591-6.10134-4

[34] Barone R. Anatomie comparée des mammiféres domestiques. In: Splanchnologie 1: appareil digestif et appareil respiratoire. 4e éd ed. Vigot; 1996. p. 853. DOI: 10.1111/j.1439-0264.2005.00619.x

[35] Miglino MA, LJA D, Teofilovski-Parapid G. Allantoid duct, arteries and veins of the Funiculus umbilicalis in bovines. Revta Chilena Anat. 1994;**12**(1):61-64

[36] Miglino MA. Placentation in cloned cattle: Structure and microvascular architecture. Theriogenology. 2007;**68**(4):604-617. DOI: 10.1016/j.theriogenology. 2007.04.060

[37] Barrios-Arpi LM, Rodríguez Gutiérrez J-L, Lopez-Torres B. Histological characterization of umbilical cord in alpaca (*Vicugna pacos*). Anatomia, Histologia, Embryologia. 2017; **46**(6):533-538. DOI: 10.1111/ahe.12298

[38] Kumar P. Gross anatomy, histomorphology and histochemistry of equine umbilical cord. IJVA. 2013;**25**(2):65-68

Chapter 4

Salivary Glands

Sonia Gupta and Nitin Ahuja

Additional information is available at the end of the chapter

http://dx.doi.org/10.5772/intechopen.81213

Abstract

Saliva is a fluid secreted by the salivary glands that keeps the oral cavity moist and also coats the teeth along with mucosa. The salivary gland possesses tubuloacinar units, and these are merocrine. The functional unit of the salivary glands is the terminal secretory piece called acini with a roughly spherical or tubular shape. It also consists of branched ducts for the passage of the saliva and also plays an important role in the production and modification of saliva. Each type of duct is lined by different types of epithelia, on the basis of its location. Myoepithelial cells are contractile cells with respect to intercalated and secretory endpieces. Parotid, submandibular, and sublingual glands are the major salivary glands. The minor salivary glands are labial and buccal gland, glossopalatine gland, and palatine and lingual glands. Saliva plays an important role in mastication, speech, protection, deglutition, digestion, excretion, tissue repair, etc. Secretion stimulated in response to sympathetic stimulation will differ in protein and electrolyte from that due to parasympathetic stimulation. The concentration of saliva depends only on the rate of flow and not on the nature of stimulus. Saliva guides the clinician toward the optimal mode of treatment and guides the patient toward ultimate prognosis.

Keywords: saliva, serous gland, mucous gland, myoepithelial cells, acini, striated duct

1. Introduction

The human salivary glands are a group of compound exocrine glands that produce saliva, an important fluid required for lubrication, immunity, mastication, deglutition, taste, speech, etc. The salivary glands consist of a series of branched ducts which terminate in a spherical or tubular endpieces or acini; a correlation can be made to a bunch of grapes, with the stems analogous to the ducts and the grapes indicating the secretory endpieces. Serous and mucous cells (**Figure 1**) are the two main types of secretory cells present in salivary

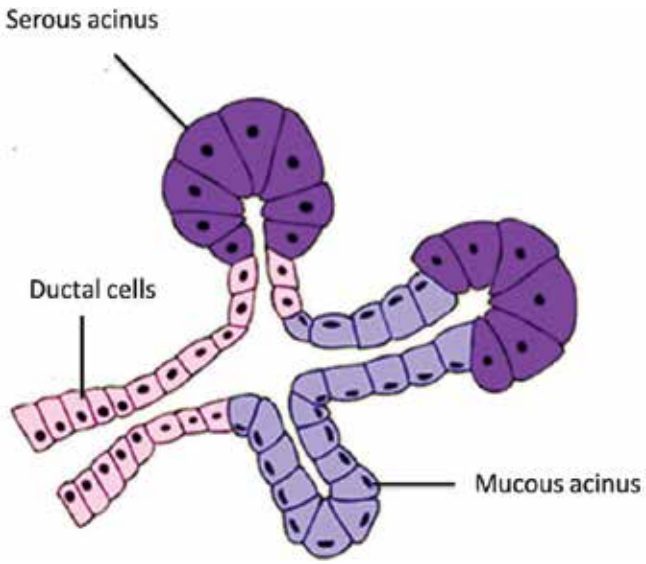

Figure 1. Structural organization of salivary gland [3].

gland and divided into two main groups. The major salivary glands include the paired parotid, submandibular, and sublingual glands. Additionally, the mucosa of the upper aerodigestive tract is lined by hundreds of small, minor salivary glands. The connective tissue forms a capsule around the gland and extends into it, dividing groups of secretory units and ducts into lobes and lobules. Blood vessels, lymphatic vessels and nerves that supply the gland, are present within the capsule [1].

The salivary glands are compound glands as they have more than one tubule entering the main duct, and the architectural arrangement is tubuloacinar, where acini are secretory units. These secretory units are merocrine as they release only the secretion of the cell from the secreting units. Myoepithelial cells are contractile cells associated with the secretory end-pieces and intercalated ducts of the salivary gland [2].

2. Classification, structure, and anatomy of salivary glands

- On the basis of size and location, salivary glands are classified as [1, 2]:
  - **a.** Major salivary glands
    - Parotid
    - Submandibular
    - Sublingual

b. Minor salivary glands

- Labial and buccal
- Glossopalatine
- Palatine
- Lingual
  - **i.** Anterior lingual gland (glands of Blandin and Nuhn)
  - **ii.** Posterior lingual serous gland (von Ebner's glands)
  - **iii.** Posterior lingual mucous gland

- On the basis of secretion [3], they are classified as:
  - Serous
  - Mucous

2.1. Major salivary glands

These are the largest, bilaterally paired, and situated extraorally, but their secretion reaches the oral cavity by variable long ducts.

2.1.1. Parotid gland

The parotid gland is the largest of all the salivary glands and weighs about 15–30 g. It is located below the external acoustic meatus between the ramus of the mandible and the sternocleidomastoid. It is divided by facial nerve into a superficial and deep lobe. The superficial lobe, overlying the lateral surface of the masseter, is defined as the part of the gland lateral to the facial nerve. The deep lobe is medial to the facial nerve and located between the mastoid process of the temporal bone and the ramus of the mandible. An accessory parotid gland may also be present lying anteriorly over the masseter muscle between the parotid duct and zygomatic arch [4].

The parotid duct, also known as Stensen's duct, secretes serous saliva and opens into the vestibule of the mouth (gingiva-buccal vestibule) opposite the crown of the upper second molar tooth [2].

2.1.2. Submandibular gland

It is the second largest salivary gland, also known as submaxillary salivary gland, weighs about 7–16 g and is almost the size of a walnut. It is situated in the submandibular triangle, which has a superior boundary formed by the inferior edge of the mandible and inferior boundaries formed by the anterior and posterior bellies of the digastric muscle. The gland is approximately J-shaped being indented by the posterior border of the mylohyoid which

divides into a larger part superficial to the muscle and a smaller part lying deep to the muscle [4]. The submandibular gland duct, also known as Wharton's duct, is thin-walled, about 5 cm long, and runs forward above the mylohyoid muscle lying just below the mucosa of the floor of the mouth in its terminal portion. The duct opens on the floor of the mouth, on the summit of the sublingual papilla also called the caruncula sublingualis, lateral to the lingual frenulum [2].

2.1.3. Sublingual gland

It is the smallest of all the three major salivary glands that is almond shaped and weighs about 3–4 g. The gland lies above the mylohyoid, below the mucosa of the floor of the mouth, medial to the sublingual fossa of the mandible, and lateral to the genioglossus [4]. It comprises of one main gland duct with various small ducts. The main duct, Bartholin's duct, opens with or near the submandibular duct. Several smaller ducts, duct of Rivinus, open independently along the sublingual fold [2].

2.2. Minor salivary glands

The minor salivary glands are placed below the epithelium in almost all parts of the oral cavity. These glands comprise numerous small groups of secretory units opening via short ducts directly into the mouth. They lack a distinct capsule, instead mixing with the connective tissue of the submucosa or muscle fibers of the tongue or cheeks [2].

2.2.1. Labial and buccal glands

These glands are present on the lips and cheeks and comprise of mucous tubules with serous demilunes [1, 2].

2.2.2. Glossopalatine glands

These are located to the region of the isthmus in the glossopalatine fold but may extend from the posterior extension of the sublingual gland to the glands of the soft palate [1, 2].

2.2.3. Palatine glands

These are located in the glandular aggregates present in the lamina propria of the posterolateral aspect of the hard palate and in the submucosa of the soft palate and uvula [1, 2].

2.2.4. Lingual glands

The glands of the tongue can be divided into various groups [1, 2]. The anterior lingual glands (glands of Blandin and Nuhn) are present near the apex of the tongue. The ducts open on the ventral surface of the tongue near the lingual frenulum. The posterior lingual mucous glands are present lateral and posterior to vallate papillae and in association with lingual tonsil. The ducts of these glands open on the dorsal surface of the tongue. The posterior lingual serous glands (von Ebner's glands) are located between the muscle fibers of the tongue below the vallate papillae, and the ducts open into the trough of circumvallate papillae and at the rudimentary folate papillae on the sides of the tongue.

http://dx.doi.org/10.5772/intechopen.81213

3. Development of the salivary glands

The development of the glandular tissue involves the interaction of the epithelium with the underlying mesenchyme to form the functional part of the tissue [5, 6]. These epithelial-mesenchymal interactions are also known as secondary induction in which the mesenchyme is in close proximity with the epithelium and is required for the normal development of the epithelium. For example, epithelial-mesenchymal interactions regulate both the initiation and growth of the glandular tissue and the eventual cytodifferentiation of cells within the salivary glands. The mesenchyme, therefore, is required for normal development as well as formation of the supporting part of the adult gland.

All salivary glands follow a similar development pattern. The functional glandular tissue (parenchyma) develops as an epithelial outgrowth (glandular bud) of the buccal epithelium that invades the underlying mesenchyme. The connective tissue stroma (capsule and septa) and blood vessels form from the mesenchyme. The mesenchyme is composed of cells derived from neural crest and is important for the normal differentiation of the salivary glands.

As the bud formation begins during development, the portion of the bud closest to the stomodeum eventually differentiates into the main excretory duct of the gland, while the most distal portion of the bud forms the secretory endpieces or acini. The origin of the epithelial buds is believed to be ectodermal in the parotid and minor salivary glands but endodermal in origin in the submandibular and sublingual glands. The parotid gland originates near the corners of the primitive oral cavity by the sixth week of prenatal life. The submandibular glands arise from the floor of the mouth at the end of the sixth or the beginning of the seventh week in utero. The sublingual gland forms lateral to the submandibular primordium at about eighth week. All the minor salivary glands bud from buccal epithelium but start after their 12th prenatal week.

Stages of development [5, 6]

I. **Bud formation, i.e., induction of oral epithelium by underlying mesenchyme:** The mesenchyme underlying the oral epithelium induces the proliferation in the epithelium which results in tissue thickening and bud formation.

II. **Formation and growth of epithelial cord:** A solid cord of cells forms from the epithelial bud through cell proliferation. Condensation and proliferation occur in the surrounding mesenchyme which is closely associated with the epithelial cord. The basal lamina plays a role in influencing morphogenesis and differentiation of the salivary glands throughout the development.

III. **Initiation of branching in terminal parts of epithelial cord and continuation of glandular differentiation:** The epithelial cord proliferates rapidly and branches into terminal bulbs.

IV. **Dichotomous branching of epithelial cord and lobule formation:** The branching continues at the terminal portion of the cord forming an extension treelike system of bulbs. As branching occurs, the connective tissue differentiates around the branches, eventually

producing extensive lobulation. The glandular capsule forms from mesenchyme and surrounds the entire glandular parenchyma.

V. **Canalization of presumptive ducts:** Canalization of the epithelial cord, with the formation of a hollow tube or duct, usually occurs by the sixth month in all the major salivary glands.

   The two main theories to explain the mechanism of canalization are:

   - Different rates of cell proliferation between the outer and inner layers of the epithelial cord.
   - Fluid secretion by the duct cells which increases the hydrostatic pressure and produces a lumen within the cord. Further branching of the duct and structure and growth of the connective tissue septa continues at this stage of development.

VI. **Cytodifferentiation:** The final stage of salivary gland development is the histodifferentiation of the functional acini and intercalated ducts. Myoepithelial cells arise from the epithelial stem cells in the terminal tubules and develop in concert with acinar cytodifferentiation.

Parasympathetic nerves play an important role in epithelial tubulogenesis in the developing salivary gland which involve epithelial-mesenchymal interaction. The neurotransmitter, i.e., vasoactive intestinal peptide (VIP) and its receptor VIPR1, regulates various steps like epithelial proliferation, duct elongation, and lumen formation through cAMP or protein kinase A (PKA) pathway, thus linking epithelial tubulogenesis with parasympathetic neuronal function. Neurotrophic factor neurturin (NRTN), secreted by the buds, binds its receptor GFR alpha 2 and promotes functional nerve outgrowths to ensure parallel development of nerves and epithelium. Cystic fibrosis transmembrane conductance regulator (CFTR) causes lumen expansion during development [7].

4. Structure

4.1. Terminal secretory units

The functional unit of a salivary gland is the terminal secretory unit called acini [1, 2]. Regardless of size and location, the terminal secretory unit is made up of epithelial secretory cells, namely, serous and mucous acini. The serous and mucous cells along with myoepithelial cells are arranged in an acinus or acini with a roughly spherical or tubular shape and a central lumen.

Serous cells: They are pyramidal in shape with a broad base on the basement membrane, and the apex faces the lumen. The serous cells have a spherical nucleus placed at the basal region of the cell along with numerous secretory granules in which macromolecule components of saliva are stored and are present in the apical cytoplasm. The granules are zymogen granules and are formed by glycosylated proteins which are released into a vacuole. The serous cells show acid phosphates, esterases, glucuronidase, glucosidase, and galactoside activity. The central lumen usually has fingerlike extensions located between adjacent cells called intercellular canaliculi that increase the size of the luminal surface of the cells [2].

Mucous cells: The secretory endpieces that are composed of mucous cells typically have a tubular configuration; when cut in cross section, these tubules appear as round profiles with mucous cells surrounding central lumen of larger size than that of serous endpieces. The nucleus is oval or flattened in shape and located above the basal plasma membrane. Sometimes, mucous cells have bonnet- or crescent-shaped appearance, which is made up of serous cells and are also known as demilunes first described by Giuseppe Oronzo Giannuzzi in 1865. The presence of demilunes is not clearly known, but these demilunes occur as a result of artifact during tissue preparation. Nowadays, recent studies like rapid freezing, freeze substitution, and three-dimensional reconstruction techniques have shown that serous cells align with mucous cells to surround a common lumen. The mucous cells show accumulation of large amounts of secretory product that pushes the nucleus and endoplasmic reticulum against the basal cell membrane.

The mucous secretion differs from secretion of serous in two important aspects:

- The secretion of mucous cells has little or no enzymatic activity and is responsible mainly for lubrication and protection of the oral tissues.
- The ratio of carbohydrates to protein is greater, and large amount of sialic acid and occasionally sulfated sugars are present [2].

  In routine histological sections, the secretion of mucous cell appears unstained, and they are strongly stained when special stains like PAS, alcian blue, mucicarmine, etc. are used [1].

4.2. Myoepithelial cells

These are the contractile cells associated with secretory endpiece and intercalated duct of the salivary glands. These cells are present between the basal lamina and the secretory or duct cells and are joined to the cells by desmosomes. They appear similar to smooth muscle but are derived from the epithelium. They are also known as basket cells or octopus sitting on a rock. The myoepithelial cells located around the secretory endpieces have stellate-shaped, numerous branching processes with a flattened nucleus and scanty perinuclear cytoplasm, but the cells associated with intercalated ducts have more fusiform shape and are elongated with fewer processes. These cells accelerate the initial flow of saliva from the acini, reduce luminal volume, support the underlying parenchyma, reduce the back permeation of fluid, and also help to maintain the patency. They maintain the cell polarity and structural organization of cells. They secrete various tumor suppressor proteins such as protease inhibitors and antiangiogenesis factors which provide a barrier against invasive epithelial neoplasm.

4.3. Ducts

It consists of hollow tubes that connect initially with the acinus, i.e., secretory endpieces, and extends to the oral cavity. It is not a pipeline or conduit for the passageway for the saliva, but it actively participates in the production and modification of saliva.

On the basis of location, ducts are of two types:

- **Intralobular ducts**: Those ducts which are within the lobule. The intercalated and striated ducts are intralobular ducts.

- **Interlobular ducts**: Those ducts which lie within the connective tissue within the lobules of the gland. The excretory ducts are interlobular ducts.

4.3.1. Intercalated duct

These are lined by single layer of cuboidal epithelium and are surrounded by myoepithelial cell bodies, and their processes typically are found along the basal surface of the duct. Under the light microscope, the intercalated ducts are difficult to identify as they are compressed between the secretory units. Under the electron microscope, the intercalated ducts have centrally placed nuclei and a small amount of cytoplasm containing some rough endoplasmic reticulum and a small Golgi complex. A few secretory granules may be found in the apical cytoplasm, especially in the cells located near the endpieces. The apical cell surface has a few short microvilli projecting into the lumen, and lateral surfaces are joined by junctional complexes. The macromolecule components, i.e., lysozyme and lactoferrin, are stored in the secretory granules of the intercalated duct and contribute to the saliva.

4.3.2. Striated ducts

The striated ducts receive the primary saliva from the intercalated ducts which constitute the largest portion of the duct system and are lined by columnar cells with a centrally placed large, spherical nucleus and pale, acidophilic cytoplasm. Under the electron microscope, the basal cytoplasm of the striated duct cells is partitioned by deep infoldings of the plasma membrane producing numerous sheetlike folds that extend beyond the lateral boundaries of the cell and interdigitate with similar folds of adjacent cells. Between the membrane infoldings, a large amount of radially oriented mitochondria are located in the portion of the cytoplasm. The combination of infoldings and mitochondria accounts for the striations seen in the light microscope. These ducts are involved in active transport and are considered as site of electrolyte reabsorption especially of sodium and chloride and secretion of potassium and bicarbonate. They also synthesize and secrete glycoproteins such as kallikrein and epidermal growth factor.

4.3.3. Excretory ducts

These ducts are located in the connective tissue septa between the lobules of the gland and are larger in diameter than striated duct. These ducts are lined by pseudostratified epithelium with columnar cells extending from the basal lamina to the ductal lumen and small basal cells that sit on the basal lamina. As the smaller ducts join to form large excretory ducts, the number of basal cell increases, and scattered mucous (goblet) cells may be present. The main excretory duct may become stratified near the oral opening. Tuft or brush cells with long stiff microvilli and apical vesicles are seen and are considered as receptor cells as they show nerve endings adjacent to the basal portion of the cell. Dendritic cells are also seen and play an important role in immune surveillance.

4.4. Connective tissue elements

The cells that are found in the connective tissue of the salivary glands are similar to those in other connective tissues of the body and include fibroblasts, macrophages, mast cells,

http://dx.doi.org/10.5772/intechopen.81213

occasional leukocytes, fat cells, and plasma cells. Collagen and reticular fibers are also embedded in a ground substance which is composed of proteoglycans and glycoproteins. It consists of a surrounding capsule that delineates the gland from the adjacent structures. Blood vessels and nerves are also present that supply the parenchymal components, i.e., glandular components and excretory ducts. The plasma cells present in the connective tissue produce immunoglobulins that are secreted into saliva by transcytosis.

5. Histology

5.1. Major salivary glands

- **Parotid glands:** The parotid gland is a purely serous gland, and all the acinar cells are similar in structure to the serous cells (**Figures 2** and **3**). Under the electron microscope, serous granules may have a dense central core, and the intercalated ducts are long branching along with pale-staining striated ducts, are numerous, and stand out evidently against the more densely stained acini. The connective tissue septa contain numerous fat cells which increase in number with age and leave an empty space in histologic sections.
- **Submandibular glands:** The submandibular gland is a mixed gland with both serous and mucous secretory units, but the serous units predominate. The mucous terminal portions are capped by demilunes of serous cells. Under the electron microscope, the intercalated ducts appear shorter in submandibular gland than those of the parotid, whereas the striated ducts are usually longer.
- **Sublingual glands:** The sublingual gland is also a mixed gland, but the mucous secretory units predominate. The mucous cells are present in tubular pattern along with serous

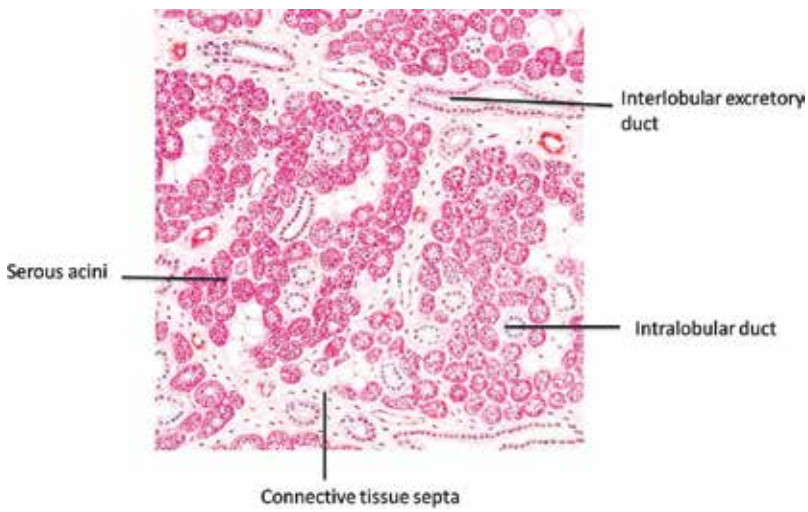

Figure 2. Histology of serous gland [3].

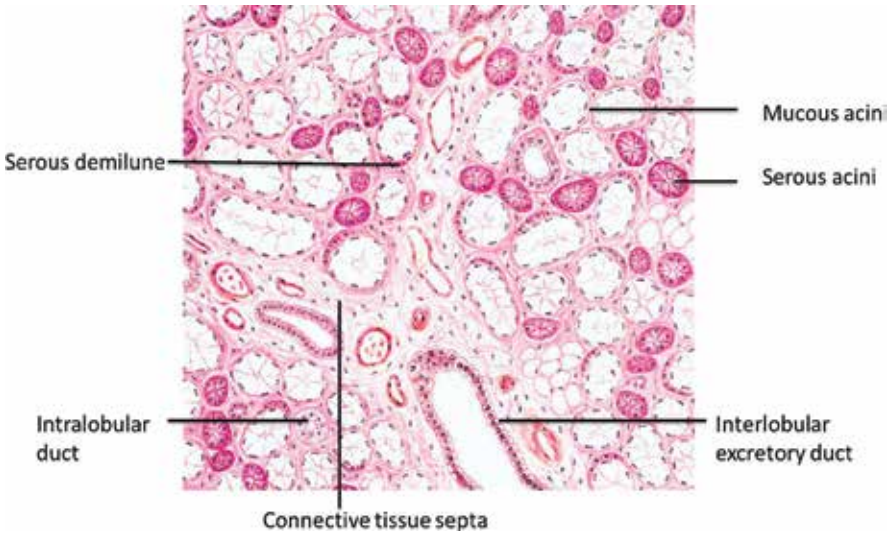

Figure 3. Histology of mixed gland [3].

demilunes and may be present at the blind ends of the tubules. The intercalated and striated ducts are poorly developed, and mucous tubules open directly into ducts lined with cuboidal or columnar cells without typical basal striations.

5.2. Minor salivary glands

- **Labial and buccal glands:** The glands of the lips and cheeks are a mixed gland consisting of mucous tubules with serous demilunes. The intercalated ducts appear variable in length, and the intralobular ducts possess only a few cells with basal striations.
- **Glossopalatine glands:** The glands present in the region of isthmus in the glossopalatine fold are purely mucous gland.
- **Palatine glands:** Palatine glands are a purely mucous gland, and the excretory ducts may have an irregular contour with large distensions as they course through the lamina propria.
- **Lingual glands:** In anterior lingual glands, the anterior portion of the glands is chiefly mucous in nature, whereas the posterior portions are mixed. The posterior lingual glands are purely mucous glands, but von Ebner's glands are purely serous gland.

6. Formation, secretion, and function of saliva

The oral cavity is kept moist by a film of fluid called saliva, which constantly coats its inner surfaces and occupies the space between the lining oral mucosa and the teeth [1, 2, 8–11]. It is a complex fluid, produced by the salivary gland, whose important role is maintaining the

http://dx.doi.org/10.5772/intechopen.81213

well-being of mouth. The whole saliva that bathes the oral cavity is primarily a mixture of secretions from the paired major (parotid, submandibular, sublingual) glands and the numerous minor (labial, buccal, palatine, and lingual) glands. The formation of saliva occurs in two stages:

1. **Formation of macromolecular components:** The structure of acinar cells consists of abundant RER, prominent Golgi complexes, and numerous secretory vesicles. Synthesis of secretory proteins begins with gene transcription and manufacture of mRNA to carry the sequence information from the nucleus to ribosome in the cytoplasm. Protein synthesized in the RER is settled to the Golgi complexes in transport vesicles. After fusion of their unit membrane with surface cell membrane, they rupture and they are released to the external environment. Rupture and rearrangement of the lipid layer of both permit the continuity of the granule membrane and cell membrane.
2. **Formation of fluid components:** After appropriate stimulation it is thought that the free Ca^{++} is released from storage site within the endoplasmic reticulum. Free cytoplasmic Ca^{2+} concentration can increase five- to tenfold in a second after such a stimulation which brings out significant compensatory changes that include the opening of the two membrane ion channels for passage of K^+ and Cl^-. When K^+ is released from the cell, a compensatory uptake of Na^+ and Cl^- occurs. The Cl^- exits the cell between the channels at luminal surface, and Na^+ enters the lumen through the paracellular pathway. The result of these ionic relocations is a flux of water into the lumen via the osmotic coupling of NaCl and H_2O.

The functions of saliva are:

- **Protection:** The protective functions of saliva is expressed as:
  - **a.** Lubricant
  - **b.** Mechanical washing
- **Buffering:** This occurs in two ways:
  - **a.** Many bacteria need a specific pH for growth; saliva prevents potential pathogens from colonizing in the mouth by denying them optimal environmental conditions.
  - **b.** Plaque microorganisms can produce acids from sugars, which if not rapidly buffered and cleared by saliva can demineralize enamel.
- **Digestion:** It provides taste acuity, neutralizes esophageal contents, and forms the food bolus.
- **Taste:** It dissolves substances to be carried to taste buds and also contains a protein, called gustin, which is necessary for growth and maturation of taste buds.
- **Antimicrobial action:** This occurs in various ways as:
  - **a.** Lactoferrin binds free iron and in doing so deprives bacteria of its essential element.
  - **b.** Lysozyme hydrolyzes the cell wall.

c. Histatin proteins with antibacterial property.

d. Immunoglobulin, i.e., secretory IgA, clumps or agglutinates microorganisms.

- **Maintenance of tooth integrity:** Saliva is saturated with calcium and phosphate ions, and interaction with saliva results in postoperative maturation through diffusion of such ions. This maturation increases surface hardness, decreases permeability, and increases the resistance of enamel to caries.
- **Tissue repair:** The rate of wound contraction is significantly increased in saliva due to the presence of peptides and proteins present in saliva.

7. Clinical considerations

a. Radiation caries: Radiation caries is a rampant form of dental decay that may occur in individuals who receive a course of radiotherapy that include exposure of salivary glands [1, 2, 11].

- Etiology

  Carious lesions are produced due to the exposure of salivary glands and reduced flow of saliva, decreased pH, decreased buffering capacity, and increased viscosity.

- Signs

  Superficial lesions attack the buccal, occlusal, incisal, and lingual surfaces. It includes cementum and dentin in cervical lesions. Lesions progress around the teeth circumferentially and resulting in loss of the crown.

b. Sjogren's syndrome: It consists of keratoconjunctivitis, xerostomia, and rheumatoid arthritis. The cause of the disease can be genetic, autoimmunological, etc.

- Features include dry mouth and dry eyes due to hypofunction of lacrimal and salivary glands. Most patients are treated symptomatically; ocular lubricants and salivary substitutes are given.

c. Xerostomia (dry mouth): It is defined as a subjective complaint of dry mouth that may result from a decrease in the production of saliva. It is not a disease but a symptom caused by many factors.

- Etiology
  - Sjogren's syndrome
  - Therapeutic radiation of head and neck
  - Surgical removal of salivary glands
  - Diabetes mellitus

http://dx.doi.org/10.5772/intechopen.81213

- Acute viral infections involving salivary glands result in temporary xerostomia
- Anxiety, mental stress, and depression may temporarily decrease salivary flow

- Symptoms
  - Oral dryness (most common)
  - Halitosis
  - Burning sensation
  - Loss of sense of taste or bizarre taste
  - Difficulty in swallowing
  - Tongue tends to stick to the palate
  - Decreased retention of denture
- Signs
  - Saliva pool disappears
  - Mucosa becomes dry
  - Tongue shows glossitis and fissured with papilla atrophy
  - Angular cheilitis
  - Rampant caries at the cervical or cusp tip
  - Periodontitis
  - Candidiasis

8. Conclusion

Salivary glands are compound, exocrine, and tubuloacinar in nature secreting saliva which keeps the oral cavity moist. The secretory units are acini, and saliva reached the oral cavity through ducts. Saliva is of great importance to diagnostic and prognostic pathology.

Author details

Sonia Gupta[1]* and Nitin Ahuja[2]

*Address all correspondence to: soniathegupta@gmail.com

1 Oral Pathologist, Jammu, J&K, India

2 Department of Oral Pathology, IDST College, Modinagar, UP, India

References

[1] Nanci A. Ten Cate's Oral Histology Development, Structure and Function. 8th ed. Elsevier; 2012. pp. 253-277

[2] Kumar GS. Orban's Oral Histology and Embryology. 13th ed. Elsevier; 2014. pp. 291-312

[3] Eroschenko VP. DiFiore's Atlas of Histology with Functional Correlations. 11th ed. Wolters Kluwer; 2006. pp. 251-258

[4] Chaurasia's BD. Human Anatomy Regional and Applied Dissection and Clinical: Head, Neck and Brain. 4th ed. Satish Kumar Jain; 2006. pp. 133-138; 157-162

[5] Cutler LS, Gremski W. Epithelial-mesenchymal interaction in the development of the salivary gland. Critical Reviews in Oral Biology and Medicine. 1991;**2**(1):1

[6] Avery JK. Oral Development and Histology. 3rd ed. BC Decker Inc; 1988. pp. 316-319

[7] Nedvetsky PI, Emmerson E, Finley JK, Ettinger A, Cruz-Pacheo N, et al. Parasympathetic innervation regulates tubulogenesis in the developing salivary gland. Developmental Cell. 2014;**30**:449-462

[8] Melvin JE, Yule D, Shuttleworth T, Begenisich T. Regulation of fluid and electrolyte secretion in salivary gland acinar cells. Annual Review of Physiology. 2005;**67**:445-469

[9] Egdar WM. Saliva: Its secretion, composition and function. British Dental Journal. 1992;**172**:305

[10] Dodds MW, DA J, Yeh CK. Health benefits of saliva: A review. Journal of Dentistry. 2005;**33**:223-233

[11] Spielmann N, Wong DT. Diagnostic and therapeutic perspectives. Oral Diseases. 2011;**17**:345-354

Section 3

Pathology and Repair

Chapter 5

A Study of the Correlation between Bacterial Culture and Histological Examination in Children with *Helicobacter pylori* Gastritis

Felicia Galoș, Gabriela Năstase, Cătălin Boboc, Cristina Coldea, Mălina Anghel, Anca Orzan and Mihaela Bălgrădean

Additional information is available at the end of the chapter

http://dx.doi.org/10.5772/intechopen.80257

Abstract

Helicobacter pylori (*H. pylori*) is one of the most common chronic bacterial infections in the world, and it is currently estimated that approximately half of the world's population is infected with the bacterium. The correct diagnosis and effective treatment of *H. pylori* gastric infection are essential in controlling this condition. The available diagnostic methods have advantages and limitations related to factors such as age of patients, technical difficulty level, costs and extensive accessibility in hospitals. The eradication therapy of *H. pylori* infection is still a challenge for gastroenterologists. One of the main causes of failure in *H. pylori* eradication is antibiotic resistance. Biopsy cultures are the most widely used methods among the antimicrobial susceptibility tests. In case of a negative culture, *H. pylori* can be clearly recognised in histological sections. The sensitivity and specificity of histology for the diagnosis depend on clinical settings, density of colonisation and the experience of the histopathologist. A prospective study was performed in order to analyse patients with *H. pylori* gastric infection with positive histology and positive culture versus positive histology and negative culture.

Keywords: *Helicobacter pylori* culture, histology, children

1. Introduction

Helicobacter pylori (*H. pylori*) is a Gram-negative spiral-shaped bacterium which colonises the gastrointestinal tract of nearly half of the world's population, causing local inflammation in

the stomach and duodenum and inducing a systemic humoral immune response [1]. *H. pylori* survival in the acidic gastric environment is mediated by mechanisms such as activity of the urease enzyme, which catalyses and hydrolyses urea to form carbon dioxide and ammonia, producing a neutral environment that is essential for its survival. The primary routes of transmission are considered to be faecal-oral and oral-oral, but some indirect evidences report that the infection can also be acquired by drinking water and by other environmental sources [2, 3].

H. pylori represents a key factor in the aetiology of various gastrointestinal diseases, ranging from asymptomatic chronic active gastritis to peptic ulceration, gastric adenocarcinoma and gastric mucosa-associated lymphoid tissue (MALT) lymphoma. Other diseases caused by the pathogen are iron deficiency anaemia, chronic idiopathic thrombocytopenic purpura and growth retardation. *H. pylori* was classified as a class I human carcinogen by the World Health Organization in 1994.

Numerous diagnostic tests are available for detecting *H. pylori* infection: invasive techniques, which means endoscopy with biopsies for a rapid urease test (RUT), histology and culture and noninvasive techniques, such as serology, ^{13}C-Urea breath test (^{13}C-UBT) and stool antigen test. There is no single method to detect *H. pylori* infection reliably and accurately. The choice of the diagnostic method depends on patients' age and complaints, technical difficulty level, costs and extensive accessibility in hospitals.

Two tests are recommended to define *H. pylori* status in children: bacterial culture of gastric biopsy and histology [4]. Bacterial culture of gastric biopsy has 100% specificity, but its sensitivity is low. *H. pylori* can be cultured from gastric biopsies, although this method often presents some difficulties. *H. pylori* soon loses viability when exposed to the environment, and biopsies should be cultured quickly. If it is not possible, a transport media may be used. Histology provides an excellent diagnostic accuracy, allowing for the detection of the bacteria as well as for the grading of gastritis. The sensitivity and specificity of histology for the diagnosis depend on clinical settings, density of colonisation and experience of the histopathologist [5].

The aims of our study were to assess the histological findings and to compare them with the results of bacterial cultures, obtained through gastric biopsy, in children with *H. pylori* gastritis. We also wanted to find out the possible factors that may influence bacterial culture outcomes.

2. Materials and methods

2.1. Patients

This was a prospective, single-centre study (in Maria Sklodowska Curie Children's Emergency Hospital Bucharest, Romania) that evaluated consecutive children referred by their physicians for an upper endoscopy because of dyspepsia. They were all screened for *H. pylori* and presented a positive stool antigen test.

Excluding criteria were the use of proton pump inhibitors or H2-receptor antagonists and antibiotics as well as non-steroidal anti-inflammatory drugs or steroidal treatment 2 weeks

http://dx.doi.org/10.5772/intechopen.80257

before the beginning of the study, previous intestinal surgery (except for polypectomy and appendectomy), concomitant severe disease (heart, lungs, kidney and endocrine diseases) and smoking or alcohol consumption among adolescents.

The study was approved by the ethics committee.

2.2. Endoscopy

All patients underwent endoscopy with biopsy specimens for histology (one for the antrum, one for the corpus). One sample from the antrum was used for rapid urease test. Two additional biopsies were taken from the antrum for bacterial culture. The samples were placed into separate vials, previously identified, containing the appropriate medium for each test. The first sample was used for bacterial culture.

This procedure was performed in patients with a minimum of 10 hours of fasting, under general anaesthesia or conscious sedation. Vital signs were continuously monitored for the entire procedure.

Written informed consent was obtained from the parent or guardian of each child included in the study.

2.3. Bacterial culture

The biopsy specimens collected for bacterial culture were transported in commercial selective transport *H. pylori* medium, Portagerm pylori (BioMérieux SA, Marcy l'Etoile, France), and were inoculated after a few hours onto selective medium pylori agar (BioMérieux Italia). The plates were incubated under microaerobic condition at 37° for 72 hours. Once incubated, the colonies resembling *H. pylori* were identified by Gram stain and by oxidase, catalase and urease tests. Suspensions from the primary plates were prepared in sterile solution to perform an E-test on pylori agar. An agar plate was streaked in three directions with a swab dipped into each bacterial suspension to produce a lawn of growth; an E-test strip (E-test; AB Biodisk, Solna, Sweden) was placed each onto separate plates, which was immediately incubated in a microaerobic atmosphere at 37° for 72 hours. Isolated strains were tested for amoxicillin, clarithromycin, metronidazole and levofloxacin resistance following the recommendations of the European Committee on Antimicrobial Susceptibility Testing.

2.4. Histology

A biopsy of the gastric body and antrum was fixed in a solution of formaldehyde 10%. Subsequently, the gastric mucosa samples were processed, following the usual steps of dehydration and paraffin embedding.

Two stains were used for histological study: haematoxylin-eosin and Giemsa. Haematoxylin-eosin stain was used to evaluate inflammatory cells and *H. pylori* (**Figure 1**). Giemsa stain was needed when haematoxylin-eosin stain failed to identify the bacterium (**Figure 2**). Giemsa stain is the preferred stain for detecting *H. pylori* because of its technical simplicity, high sensitivity and low cost.

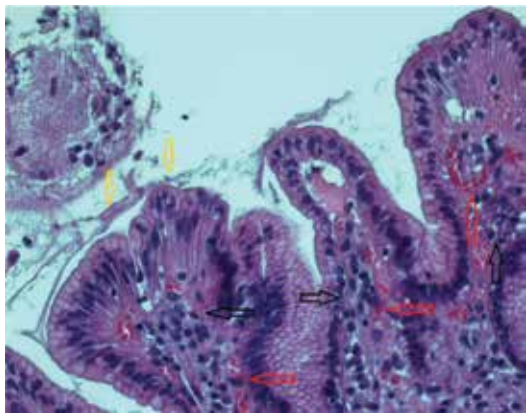

Figure 1. *Helicobacter pylori* in histological section of the gastric mucosa stained with haematoxylin-eosin. This figure represents a 200× histological section of haematoxylin-eosin-stained gastric mucosa. It is seen with diffuse inflammatory lymphoplasmacytic infiltrate (black arrows) and vascular congestion (red arrows). *Helicobacter pylori* is found at the surface of the gastric mucosa within the layer of mucus (yellow arrows).

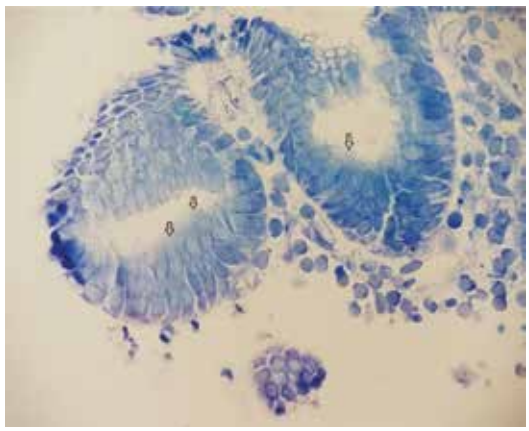

Figure 2. *Helicobacter pylori* in histological section of the gastric mucosa stained with Giemsa. This is a 400× histological section of Giemsa-stained gastric mucosa biopsy. There can be seen colonisation with *Helicobacter pylori* (white arrows) of the gastric glands, represented by small curved structures.

Gastritis was graded according to the Sydney system [6] that assesses the severity of inflammation, the level of activity (the degree of polymorph neutrophil inflammation) and the presence of atrophy and of intestinal metaplasia on a scale from 0 to 3.

In accordance with the Sydney system, the density of *H. pylori* infection was also graded semiquantitatively on a scale from 0 to 3 (mild, moderate and marked).

H. pylori was recognised in the histological section appearing as a short-curved or spiral bacillus resting on the epithelial surface or in the mucus layer.

2.5. Statistical analysis

The data was collected and analysed with Microsoft Excel 2013 and PSPP version 1.0.1. Continuous variables with a normal distribution were expressed as a mean with standard

http://dx.doi.org/10.5772/intechopen.80257

deviation (SD). Differences and relationships between variables were analysed using Fisher's exact for low expected frequencies. A $p < 0.05$ was considered statistically significant for all the analysed parameters.

We calculated the sensitivity and specificity for *H. pylori* culture and histology. Sensitivity and specificity may be defined, respectively, as the probability of having a positive test in a person with the disease (sensitivity) and the probability of having a negative test in a person without the disease (specificity).

3. Results

In the study, the culture findings and histological examination findings were accepted as "gold standard". The detection of *H. pylori* in at least one of the two tests was accepted as *H. pylori* positivity. Negative results in both culture and histology were accepted as *H. pylori* negativity.

Of the 38 patients who underwent upper endoscopy with biopsies by protocol (**Figure 3**), nine were excluded because of negative results in both culture and histology.

Twenty-nine cases (76.31%) were included in the final analysis, nineteen females (65.51%) and ten males (34.49%). The ages were between 3 years and 7 months and 17 years and 8 months (mean age 13, 5 ± 4.53 years).

The results for the diagnosis of *H. pylori* infection for each of the tests revealed that the haematoxylin-eosin and Giemsa stains of the antrum and body were the test that identified a higher number of *H. pylori* infection than the *H. pylori* culture.

Indeed, the histological examination of samples was able to identify the presence of *H. pylori* in 28 patients (96.55%), while the culture resulted to be positive in only six cases (21.42%).

We did not analyse separately the presence of the *H. pylori* in the antral mucosa compared with the gastric body mucosa; the result was recorded positive, if the bacterium was isolated in any of the histological examinations.

The histology also showed that 14/28 (50%) patients had mild *H. pylori* density, 11 (38.29%) had moderate density and 3 (10.71%) had marked density.

In one case, the culture was positive, but the bacterium was not identified through the histological exam. Among the other five cases with positive culture, two were associated with a mild score of *H. pylori* density, the other two with a moderate score and one with a marked score (**Table 1**).

We analysed the correlation between densities of *H. pylori* in histological exam and positive *H. pylori* culture: 14.28% (2/14) of patients with mild *H. pylori* density, 18.18% (2/11) of those with moderate density and 33.33% (1/3) of those with marked density had positive results in bacterial culture. There was not a statistically significant correlation between the degree of *H. pylori* density observed at histology and the positive result of bacterial culture ($p = 0.7$). The limited number of patients with positive bacterial culture may have influenced these results.

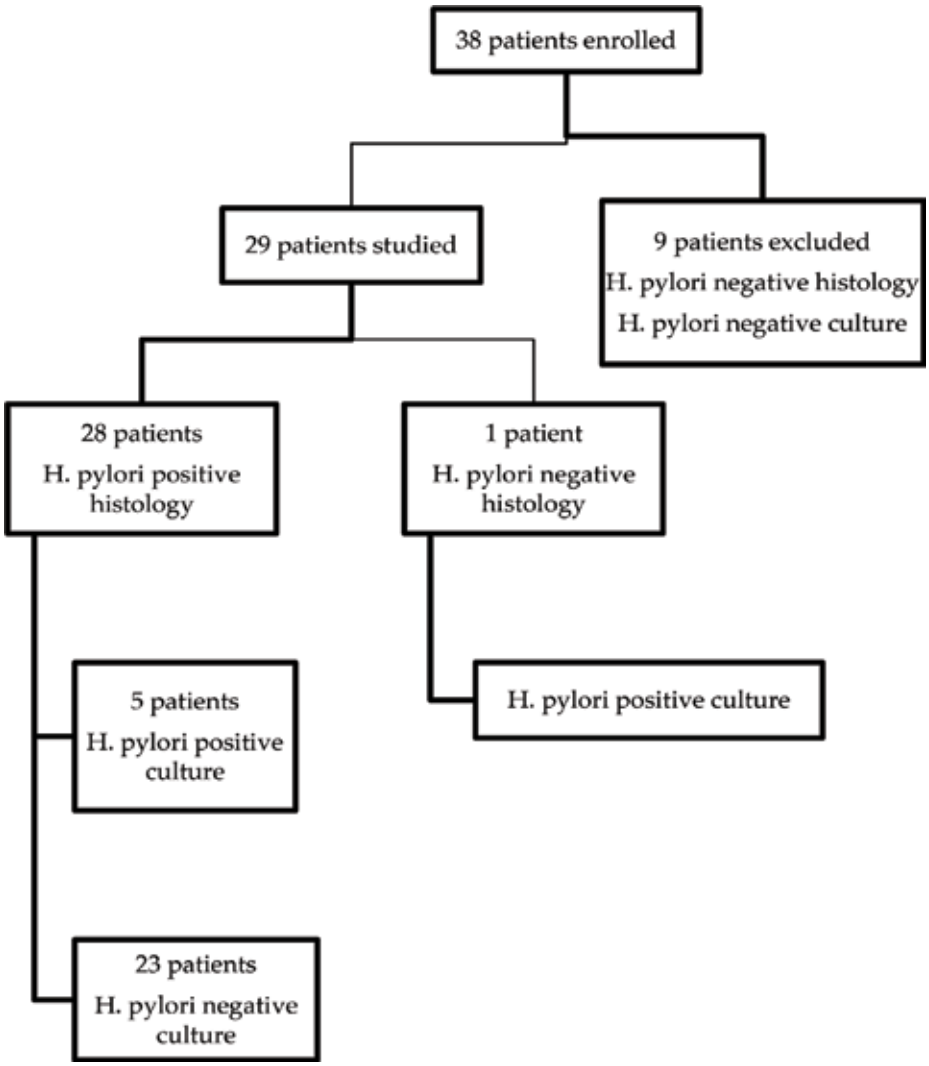

Figure 3. Flow chart of the study.

***Helicobacter pylori* density**	**Patients (n)**	***Helicobacter pylori* culture**	**Patients (n)**
Mild	14	Positive	2
		Negative	12
Moderate	11	Positive	2
		Negative	9
Severe	3	Positive	2
		Negative	1

Table 1. Correlations of *Helicobacter pylori* density and *Helicobacter pylori* culture.

http://dx.doi.org/10.5772/intechopen.80257

We used haematoxylin-eosin as the main staining method, while Giemsa stain was reserved for a few cases, not identified through haematoxylin-eosin staining, in which the suspect of infection was high.

We also tried to find out if there existed a relationship between the activity of gastritis and the density of *H. pylori* in the histological exam. Most of the patients with mild *H. pylori* density presented a mild gastritis activity (50%), while the other half showed a similar frequency of moderate gastritis activity (28.57%) and of no activity (21.43%); among patients with moderate *H. pylori* density, 54.54% had moderate activity, 36.36% a mild one and only 9.0% of them presented a marked gastritis activity. Those with marked bacterial density at histology displayed an identical frequency of absent, mild and moderate gastritis activity (33.33%). According to our results, there were not statistically significant differences between the groups that allow concluding that the severity of gastritis activity is related to *H. pylori* density at histology ($p = 0.3$) (**Table 2**).

The relationship between the degree of inflammation and *H. pylori* density was examined as well. Mild density was mostly associated with moderate (50.0%) and mild (42.80%) inflammation, while severe inflammation was demonstrated in only one case (7.20%). In patients with moderate *H. pylori* density, a moderate inflammatory process was identified in most of the cases (63.64%), together with a mild inflammation (36.36%), whereas nobody presented with a severe one. In children with marked density, mild inflammation was predominant (66.67%), followed by a moderate one in 33.33% of patients, while none of them was severely affected. Our findings do not show the evidence of a significant correlation between inflammation and *H. pylori* density at histology ($p = 0.7$) (**Table 3**).

The specificity for *H. pylori* culture in our study was 90.90%, but the sensitivity was low, 20.68%. The specificity for histology was 90.90%, and the sensitivity was 96.55%.

	Without activity n (%)	**Mild activity n (%)**	**Moderate activity n (%)**	**Marked activity n (%)**
Mild *H. pylori* density	3 (21.43%)	7(50%)	4(28.57%)	0
Moderate *H. pylori* density	0	4 (36.36%)	6 (54.54%)	1 (9.0%)
Marked *H. pylori* density	1 (33.33%)	1 (33.33%)	1 (33.33%)	0

Table 2. Correlations of activity of *Helicobacter pylori* gastritis and *Helicobacter pylori* density.

	Mild inflammation n (%)	**Moderate inflammation n (%)**	**Marked inflammation n (%)**
Mild *H. pylori* density	6 (42.80%)	7 (50.0%)	1 (7.20%)
Moderate *H. pylori* density	4 (36.36%)	7 (63.64%)	0
Marked *H. pylori* density	2 (66.67%)	1 (33.3%)	0

Table 3. Correlations of inflammation of *Helicobacter pylori* gastritis and *Helicobacter pylori* density.

4. Discussions

The enthusiasm beginning with the isolation of *H. pylori* from gastric biopsies by Warren and Marshall in 1982 has increasingly continued after the important role of this agent in the aetiology of gastric cancer has been established; consequently, the interest for *H. pylori* has increased. The association of gastric cancer, one of the most frequent causes of death worldwide, with a treatable aetiological factor has led to a profound impact on researchers [7, 8].

H. pylori infection is generally acquired in childhood, and it persists throughout life. Spontaneous resolution is rare, and a targeted therapy is needed [9].

The correct diagnosis and effective treatment of *H. pylori* gastric infection are essential. The recent guidelines for the management of *H. pylori* in children and adolescents recommend the initial diagnosis of *H. pylori* infection to be performed using invasive gastric biopsy methods including the following: obtaining a positive bacterial culture or demonstrating *H. pylori* gastritis on histopathology; using the updated Sydney classification, with at least one other positive test such as RUT or molecular-based assays where available; and including polymerase chain reaction or fluorescent in situ hybridisation. The initial diagnosis of *H. pylori* infection should not be based on noninvasive tests (i.e. ^{13}C-UBT and *H. pylori* stool antigen test) or other noninvasive methods. A positive noninvasive test, however, supports the diagnosis in cases in which positive histology is the only available invasive test [4].

76.31% of patients enrolled in the study were positive for *H. pylori* infection. The diagnosis was made in 96.55% by histology. In 17.25% of cases, both histology and bacterial culture were positive.

The *H. pylori* culture was positive in only six cases (21.42%). Our results are less significant if compared to other published data in which higher percentages of positive cultures were obtained, except one. Kaya et al. reported the sensitivity for *H. pylori* culture as 22.5%, and the specificity as 97.1% [10].

The specificity for *H. pylori* culture, in our study, was 90.90%, but the sensitivity was low, 20.68%.

A recent Israeli study, conducted in the paediatric population, reported 57.8% of positive *H. pylori* culture in 154 children with positive RUT [3]. In another study conducted on children and adolescents, the sensitivity for *H. pylori* culture was 79.3%, and the specificity was 100% [11].

The sensitivity of culture method to detect *H. pylori*, in adult population, ranges from 62.7% to 96.3% in the studies performed [8, 10, 12].

Although the culture method is accepted as a "gold standard" for the diagnosis, it is difficult to use alone as a routine diagnostic method. As the sensitivity of culture method is low, *H. pylori* positivity can be detected in case of growth. The absence of growth does not indicate *H. pylori* negativity.

Despite its long use, culture remains a challenge because of the fastidious nature of the bacterium, with particular growth requirements regarding environment and atmosphere [13]. Altering pH, the proton pump inhibitors (PPIs) indirectly interfere with *H. pylori* distribution

in the stomach. The antrum has been found to be the most affected part of the stomach by PPIs as *H. pylori* almost disappears from this niche. To avoid false-negative results, it is recommended not to consume these drugs 2 weeks prior to endoscopy [14, 15].

In our study, exclusion criteria were of inhibitory proton pump or H2-receptor antagonists and antibiotics 2 weeks before the beginning of the study, similarly with another study and recommendations [15].

The recent Maastricht V/Florence Consensus Report recommends discontinuation of antibiotics 4 weeks before the study to allow an increase of detectable bacterial load [2].

The number of biopsies necessary to diagnose *H. pylori* infection is a subject of controversy. A single biopsy specimen taken from the antrum (2 cm from the pylorus) gives good sensitivity, but it is not sufficient for a reliable diagnosis. Indeed, *H. pylori* may have a patch distribution, and the more biopsy specimens analysed, the higher the chance of detecting the organism. There are some rare cases where the infection lies only in the corpus, but usually, *H. pylori* is present in all sites. After consumption of antisecretory drugs, as pointed out before, the corpus may be the only site that remains positive [15].

We took two biopsies from the antrum for *H. pylori* culture, and maybe this could be adjusted by obtaining another one/two samples from the gastric body as well in order to try to improve the culture success rate, but this option is difficult to apply in children.

The usual recommendation derived from the Sydney system is to obtain two biopsy specimens from the antrum and two specimens from the corpus. Bacteria are usually present at both sites even if the lesions occur essentially in the antrum. When topographic studies of *H. pylori* distribution and gastritis were performed, the best site suitable from diagnosis was the lesser curvature of the midantrum, while for the corpus, there was a discrepancy between greater and lesser curvatures [15, 16]. Others showed that two antral biopsies only were sufficient to detect *H. pylori* [17].

We took the biopsy specimens for culture before specimens for histology, and we used an appropriate commercially transport medium, according to the recommendations.

We analysed the correlation between densities of *H. pylori* in histological exam and positive *H. pylori* culture: in 14.28% the *H. pylori* culture was positive in mild *H. pylori* density in histology, 18.18% in moderate *H. pylori* density and 33.33% in marked *H. pylori* score. We have not had a significant statistics correlation between densities of *H. pylori* in histological exam and positive *H. pylori* culture ($p = 0.7$). Similar results were reported by other authors [8].

We analysed the correlation between gastritis activity and density of *H. pylori* in histological exam, and we have not had a significant statistics correlation ($p = 0.30$).

The results of this study are in agreement with published work, suggesting that a strain of the organism may be a more important factor than the density of infection in determining the gastric inflammatory response to *H. pylori* [18].

In our study, we had four children with bleeding, and all of them had negative *H. pylori* culture.

Peptic ulcer bleeding and atrophic gastritis decreased the accuracy of *H. pylori* diagnostic test. The histology was found to be a reliable test in the presence of bleeding [19].

When atrophic changes occur in the gastric mucosa, a high percentage of endoscopic biopsy samples become negative at bacterial histology [20, 21]. During atrophy progression the density of *H. pylori* in the stomach mucosa decreases and may disappear completely during the late stages of atrophy [22]. This may explain the lower sensitivity of biopsy-based tests in the presence of atrophy: RUT, histology and culture. UBT and antigen stool detection can also give false-negative results in this situation. Serology is the only diagnostic method not influenced by a lower density of microorganism, being reliable even in advanced gastric body atrophy. Maastricht guidelines updates have reserved serology for special situations, including extensive atrophy of the stomach mucosa, in conditions in which the other tests may be negative because of low bacterial density.

In childhood, advanced gastric atrophy is rare. We found only one case with atrophy, but the *H. pylori* culture was positive. It was an adolescent, 17 years and 8 months old, with a long history of illness (2 years) and with previous treatment failure. We could not find, in this case, antibiotic resistance to amoxicillin, clarithromycin, metronidazole and levofloxacin, and we suppose that the noncompliance to therapy is the cause of failure for bacterial eradication. Successful eradication is important to prevent the development of antibiotic resistance, as well as to reduce the number of treatments and procedures. Among children receiving the triple standard therapy regimen, eradication rate is declining [23]. In part, this decrease can be attributed to increased antibiotic resistance. Other reasons for treatment failure are, among others, host genetic factors, *H. pylori* virulent factors, inadequate compliance to therapy or insufficient duration of therapy and, not in the last row, smoking and household crowding [23].

The sensitivity of histology in our study was 96.55%, while the specificity was 90.90%.

The sensibility and specificity of haematoxylin and eosin stain have been reported as 69–93% and 87–90%, respectively. The specificity can be improved to 90–100% by using special stains such as Giemsa stain, Warthin-Starry silver stain, Genta stain and immunohistochemical stain [15, 20, 21]. Immunohistochemical stain has a particular advantage in patients partially treated for *H. pylori* gastritis, a setting can result in atypical (including coccoid) forms, which may mimic bacteria or cell debris on haematoxylin and eosin preparation. The major advantages of immunohistochemical stain include shorter screening time and high specificity because it can exclude other similar-shaped organisms [15, 21].

In our study, we analysed the sensibility and specificity of histology in *H. pylori* infection, not focusing on the ones specific for the different types of stain. We used in all cases haematoxylin-eosin stain and in a few cases Giemsa stain.

5. Conclusions

Histology is an excellent method for detecting *H. pylori* infection. Haematoxylin-eosin, with or without Giemsa stains, is usually adequate. It is difficult to use culture method alone as routine diagnostic method. In our study, the specificity of histology in identifying *H. pylori* infection was 90.90%, and its sensitivity was 96.55%. Bacterial culture had the same specificity

as histology (90.90%), while its sensitivity was 20.68%. We did not find out a statistically significant positive correlation between *H. pylori* density observed at the histological exam and positive bacterial culture. This result may have been influenced by the limited number of patients and by the few cases with positive bacterial culture. Larger studies are needed in order to obtain relevant conclusions.

Acknowledgements

The authors thank Dr. Violeta Cristea and Dr. Augustina Enculescu for their laboratorial and histological support, respectively.

Conflict of interest

None declared.

Author details

Felicia Galoș[1,2*†], Gabriela Năstase[2†], Cătălin Boboc[2], Cristina Coldea[1,2], Mălina Anghel[2], Anca Orzan[1,2] and Mihaela Bălgrădean[1,2]

*Address all correspondence to: felicia_galos@yahoo.com

1 University of Medicine and Pharmacy Carol Davila, Bucharest, Romania

2 Maria Sklodowska Curie Children's Emergency Hospital, Bucharest, Romania

† These two authors contributed equally to this work.

References

[1] Sanders CJ, Yu Y, Moore DA, Williams IR, Gewirtz AT. Humoral immune response to flagellin requires T cells and activation of innate immunity. Journal of Immunology. 2006;**177**:2810-2818. DOI: 10.4049/jimmunol.177.5.2810

[2] Malfertheiner P, Megraud F, O'Morain C, Gisbert JP, Kuipers EJ, Axon AT, Bazzoli F, Gasbarrini A, Atherton J, Graham DY, Hunt R, Moayyedi P, Rokkas T, Rugge M, Selgrad M, Suerbaum S, Sugano K, El-Omar EM. Management of *Helicobacter pylori* infection—The Maastricht V/Florence consensus report. Gut. 2017;**66**:6-30. DOI: 10.1136/gutjnl-2016-312288

[3] Pastukh N, Peretz A, Brodsky D, Isakovich N, Azrad M, On A. Antimicrobial susceptibility of *Helicobacter pylori* strains isolated from children in Israel. Journal of Global Antimicrobial Resistance. 2018;**12**:175-178. DOI: 10.1016/j.jgar.2017.10.004

[4] Jones NL, Koletzko S, Goodman K, Bontems P, Cadranel S, Casswall T, Czinn S, Gold BD, Guarner J, Elitsur Y, Homan M, Kalach N, Kori M, Madrazo A, Megraud F, Papadopoulou A, Rowland M. Joint ESPGHAN/NASPGHAN guidelines for the management of *H. pylori* infection in children and adolescents (Update 2016). Journal of Pediatric Gastroenterology and Nutrition. 2017;**64**:991-1003. DOI: 10.1097/MPG.0000000000001594

[5] Ricci C, Holton J, Vaira D. Diagnosis of *Helicobacter pylori*: Invasive and non-invasive tests. Best Practice & Research. Clinical Gastroenterology. 2007;**21**:299-313. DOI: 10.1016/j.bpg.2006.11.002

[6] Sipponen P, Price AB. The Sydney system for classification of gastritis 20 years ago. Journal of Gastroenterology and Hepatology. 2011;**26**(1):31-34. DOI: 10.1111/j.1440-1746.2010.06536.x

[7] Drumm B, Day AS, Gold B, Gottrand F, Kato S, Kawakami E, Madrazo A, Snyder J, Thomas J. *Helicobacter pylori* and peptic ulcer: Working group report of second world congress of pediatric gastroenterology, hepatology, and nutrition. Journal of Pediatric Gastroenterology and Nutrition. 2004;**39**:S626-S631

[8] Cosgun Y, Yildirim A, Yucel M, Karakoc AE, Koca G, Gonultas A, Gursov G, Ustun H, Korkmaz M. Evaluation of invasive and noninvasive methods for the diagnosis of *Helicobacter pylori* infection. Asian Pacific Journal of Cancer Prevention. 2016;**12**:5265-5272. DOI: 10.22034/APJCP.2016.17.12.5265

[9] Fiorini G, Zullo A, Gatta L, Castelli V, Ricci C, Cassol F, Vaira D. Newer agents for *Helicobacter pylori* eradication. Clinical and Experimental Gastroenterology. 2012;**5**:109-112. DOI: 10.2147/CEG.S25422

[10] Kaya AD, Öztürk CE, Alcan Y, Behçet M, Karakoc AE, Yücel M, Misirlioglu M, Tuncer S. Prevalence of *Helicobacter pylori* in symptomatic patients and detection of clarithromycin resistance using melting curve analysis. Current Therapeutic Research, Clinical and Experimental. 2007;**68**(3):151-160. DOI: 10.1016/j.curtheres.2007.06.001

[11] Ogata SK, Kawakami E, Patricio FR, Pedroso MZ, Santos AM. Evaluation of invasive and non-invasive methods for the diagnosis of *Helicobacter pylori* infection in symptomatic children and adolescents. Sao Paulo Medical Journal. 2001;**119**:67-71. DOI: 10.159/S1516-31802001000200006

[12] Saracino I, Zullo A, Holton J, Castelli V, Fiorini G, Zaccaro C, Ridola L, Ricci C, Gatta L, Vaira D. High prevalence of primary antibiotic resistance in *Helicobacter pylori* isolates in Italy. Journal of Gastrointestinal and Liver Diseases (JGLD). 2012;**21**(4):363-365. DOI: PMID 2356118

[13] Patel SK, Pratap CB, Jain AK, Gulati AK, Nath G. Diagnosis of *Helicobacter pylori*: What should be the gold standard? Word Journal of Gastroenterology. 2014;**20**(36):12847-12859. DOI: 10.3748/wjg.v20.i36.12847

[14] Mégraud F, Boyanova L, Lamouliatte H. Activity of lansoprazole against *Helicobacter pylori*. Lancet. 1991;**337**:1486. DOI: 10.1016/0140-6736(91)93181-8

[15] Mégraud F, Lehours P. *Helicobacter pylori* detection and antimicrobial susceptibility testing. Clinical Microbiology Reviews. 2007;**20**:280-322. DOI: 10.1128/CMR. 00033-06

[16] Dixon MF, Genta RM, Yardley JH, Correa P. Classification and grading of gastritis. The update Sydney system international workshop on the histopathology of gastritis, Houston 1994. The American Journal of Surgical Pathology. 1996;**20**:1161-1181

[17] Genta RM, Graham DY. Comparison of biopsy sites for the histopathologic diagnosis of *Helicobacter pylori*: A topographic study of *H. Pylori* density and distribution. Gastrointestinal Endoscopy. 1994;**40**(3):342-345. DOI: 10.1016/S0016510(94)70067-2

[18] Phull PS, Price AB, Stephens J, Rathbone BJ, Jacyna MR. Histology of chronic gastritis with and without duodenitis in patients with *Helicobacter pylori* infection. Journal of Clinical Pathology. 1996;**49**:377-380. DOI: 10.1136/jcp.49.5.377

[19] Huang TC, Lee CL. Diagnosis, treatment, and outcome in patients with bleeding peptic ulcer and *Helicobacter pylori* infections. BioMed Research International. 2014;**2014**. DOI: 10.1155/2014/658108

[20] Lee JY, Kim N. Diagnosis of *Helicobacter pylori* by invasive test: Histology. Annals of Translational Medicine. 2015;**3**:1-10. DOI: 10.3978/j.issn.2305-5839.2014.11.03

[21] Lopes AI, Vale FF, Oleastro M. *Helicobacter pylori* infection – Recent developments in diagnosis. World Journal of Gastroenterology. 2014;**20**(28):9299-9313. DOI: 10.3748/wjg.v.i28.9299

[22] Lahner E, Vaira D, Figura N, Pilozzi E, Pasquali A, Severi C, Perna F, Delle Fave G, Annibale B. Role of noninvasive tests (C-urea breath test and stool antigen test) as additional tools in diagnosis of *Helicobacter pylori* infection in patients with atrophic body gastritis. Helicobacter. 2004;**9**:436-442. DOI: 10.1111/j.1083-4389.2004.0026.x

[23] Gold BD, Gilger MA, Czinn S. New diagnostic strategies for detection of *Helicobacter pylori* infection in paediatric patients. Gastroenterology & Hepatology. 2014;**10**(12 Suppl 7): 1-18. DOI: 05US14EBP1368

Chapter 6

Bone Marrow Mesenchymal Cell Contribution in Maintenance of Periodontal Ligament Homeostasis

Toshiyuki Kawakami, Keiko Kaneko, Tatsuo Takaya, Saeka Aoki, Rina Muraoka, Mihoko Tomida, Norimasa Okafuji, Masahito Shoumura, Naoto Osuga, Keisuke Nakano, Hidetsugu Tsujigiwa and Hitoshi Nagatuka

Additional information is available at the end of the chapter

http://dx.doi.org/10.5772/intechopen.80785

Abstract

In general, remodeling phenomenon of the periodontal ligament (PDL) is occurring in all times. Thus, in the chapter, the word "maintenance" was used, and the chapter title is "Maintenance of Periodontal Ligament Homeostasis." Our experimental data on the remodeling of the PDL with cell acceleration at the furcation area in this experimental model are recovered using the cells in situ and the bone marrow-derived cells (BMCs). BMC migration into the PDL tissues using green fluorescent protein (GFP) bone marrow-transplanted model mouse was examined. BMCs have abilities of cell migration and differentiation into tissues/organs in the body. The immunohistochemistry revealed that GFP-positive cells were detected in the PDL. GFP-positive cells were also positive to CD31, CD68, and Runx2 suggesting that fibroblasts differentiated into osteoclasts and tissue macrophages. In this way, Notch signaling involvement considered in our tentative examinations revealed that the experimentally induced periodontal polyp was examined; the cytological dynamics of the cells in granulation tissue are mainly from migration of undifferentiated mesenchymal cells of the bone marrow and differentiate into the tissue-specified cells. Furthermore, the data suggest that cell differentiation is due to Notch signaling.

Keywords: periodontal ligament (PDL), homeostasis, cell migration, bone marrow-derived cells, notch signaling

1. Introduction

In general, "homeostasis" of the periodontal ligament tissues (PDL) is occurring in any times, due to the mechanical stress to the tissue including the physiological and pathological occlusal stress and/or orthodontic mechanical stress, and so on. Thus, in the above sentences, the word "homeostasis" was used in the chapter. From a view point of developmental biology, there are well-known facts that the main component of PDL fibroblasts is from neural crest-derived neuroectodermal cells. From the point of the fact, at the period of the maintenance of the PDL, there are numerous cell proliferations that occurred in the regional tissues. It is a very important problem. Thus, at first, we introduce the chosed GFP bone marrowtransplanted model mouse (Tsujigiwa's model [1, 2]) shown in **Figure 1** (GFP mouse model: upper).

I used the ddY mouse as an experimental animal and chosed a histopathology in a periodontal ligament of the mouse that received mechanical stress by Waldo methods. The immunohistochemistry manifestation situation of heat shock protein 27 (HSP27) and phosphorylated HSP27 (p-HSP27) was investigated until that and at most 24 hours later. A periodontal ligament fibroblast was both low in HSP27 and p-HSP27 in the control group. But HSP27 was manifested 10 minutes later after a PDL fibroblast caused mechanical loading on the tension side of experimental group. The strongest appearance was detected 9 hours later after mechanical load was led. p-HSP27 was also weaker than HSP27, but it was manifested in a time-depending way. These results suggest that HSP27 and p-HSP27 are manifested by activation of a PDL fibroblast on the tension side for maintenance of the

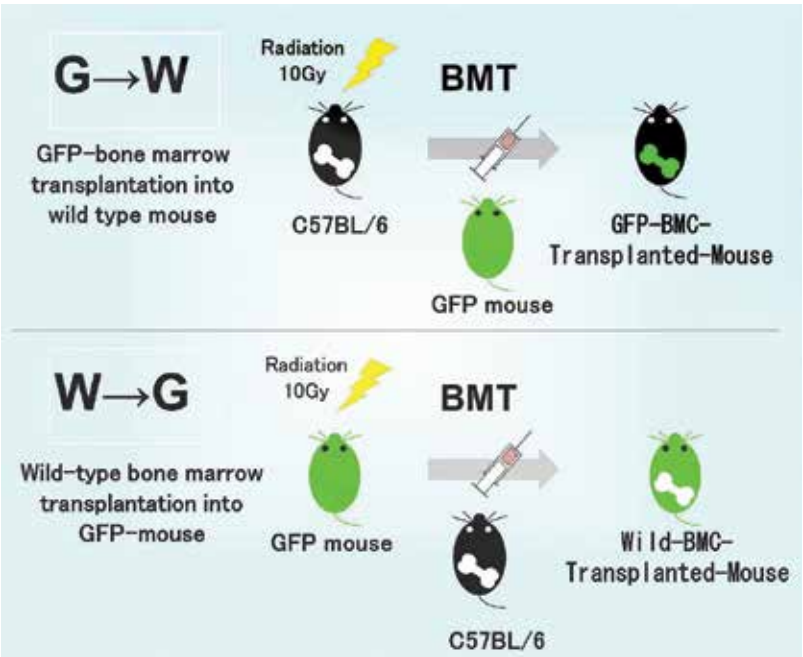

Figure 1. GFP-transplanted model mouse schematic diagram.

homeostasis of the periodontal ligament. Therefore, the facts suggest that these proteins will act on this as molecular chaperone for activation of an osteoblast and maintenance later.

We have investigated using the GFP mouse, the cell dynamics of the periodontal ligament in the past decade. The following experiments have been carried out: (1) Orthodontic mechanical stress causing injury of the periodontal ligament tissues. (2) Occlusal trauma of the periodontal ligament. In the examinations, histopathological changes were observed at the course of the experiments. Furthermore, we used the GFP bone marrow-transplanted mouse for examination of the cell supplying source to the regional periodontal ligament tissues from bone marrow-derived cells (BMDCs). (3) Experimentally induced periodontal polyp-contained cells are mainly from migration of undifferentiated mesenchymal cells of the bone marrow and differentiate into the tissue-specified cells. (4) Furthermore, the cell differentiation is due to the expression of Notch signaling. The result also suggests that the PDL fibroblasts in granulation tissue are differentiated in the periodontal ligament-specified cells from bone marrow-derived mesenchymal cells.

2. GFP-BMDCs into the PDL-received orthodontic mechanical stress

The periodontal ligament (PDL) is usually remodeling at physiological in condition. Furthermore, orthodontic treatment results to mechanical stress inducing reorganization of PDL collagen bundles. The examination results in "movement of an orthodontics tooth." The mechanical stress communicated to PDL causes a reaction of organization and causes "movement of a tooth." This reaction of PDL is the one for maintenance of a homeostasis. A histology-like reply and production of the copying factor which controls a cell differentiation and various morphogenesis phenomena are studied more widely in recent years [3, 4]. It becomes clear that it's able to bring manifestation of a remodeling of a periodontal tissue and the activated molecule which replies to various mechanical stress and inflammation to maintain a homeostasis [5–10]. Our experimental method was based on our previous reports [4, 5]. The Waldo method of inducing mechanical stress load in mouse periodontal tissues was followed. Under general anesthesia, the mouse was inserted between the maxillary molars to induce persistent mechanical stress. A separator was inserted between M1 and M2 of the right maxillary molars to ensure the mechanical stress due to pressure over a period of time. After each experimental time, the periodontal tissues of the left maxillary molar region (untreated side) were used as controls. In this experiment, the distal buccal root of the maxillary first molar was the observation part. The schematic diagram, macro-view, and histology are shown in **Figure 2**.

Therefore, we focused on the expression of various HSPs that maintain homeostasis during injury. HSPs are one of the factors recognized that is transiently enhanced by heat shock [11]. It is also called stress protein because it is not only enhanced by heat shock but also by ischemia; other pathological changes such as infections and inflammation and radiation; physical stress such as light; stress from enzymes, heavy metal ion, arsenic, arsenic acid, methanol, and active oxygen; and stress from chemical and various amino acid derivatives [12, 13]. When the chromosomes of the salivary gland of *Drosophila* were at high temperatures, HSP

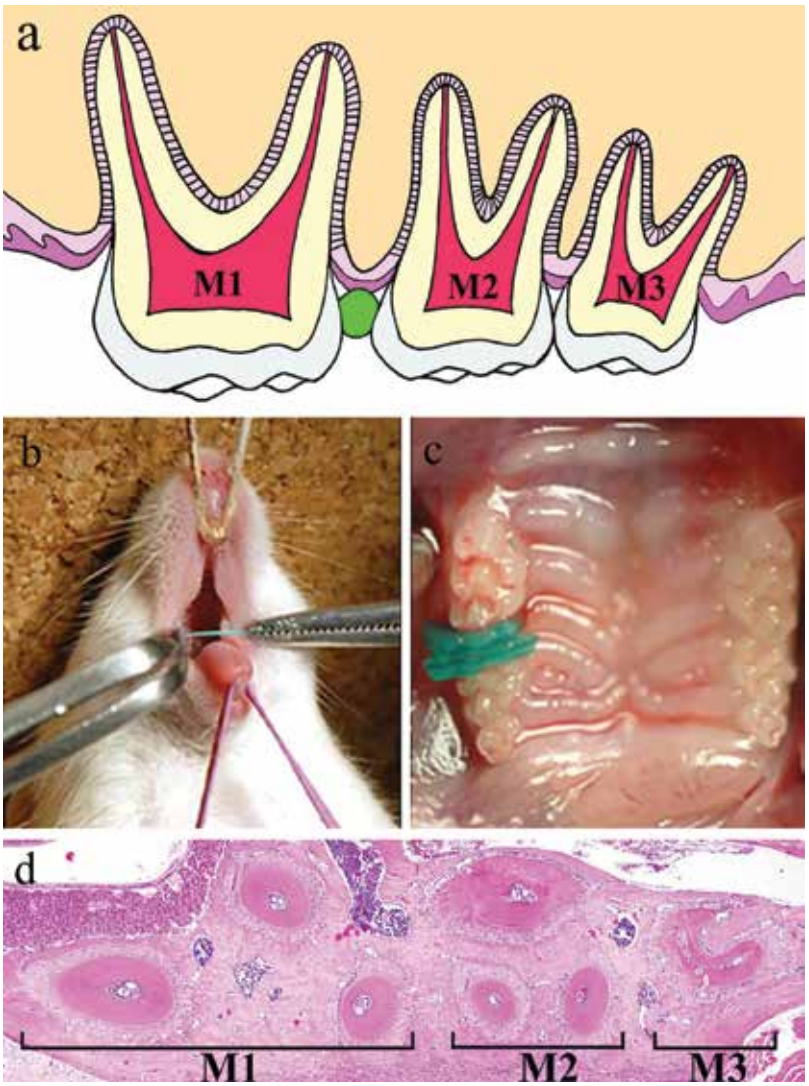

Figure 2. Experimental schema (a), macro-view (b, c), and histology (d). Quotation alteration of literature #5.

strongly expressed [14]. After that, the isolation of synthesized HSP by a SDS-polyacrylamide gel electrophoresis first by *Drosophila*. Some of the main protein which was also led by heat shock method of treatment in non-salivary glandular system was regarded as HSP together. A puff of the mRNA history of HSP was copied. After that a high study is reporting that the colon bacillus kept during the environment, leaven, and a gene of other mammalian cells are able to receive a heat stress and preserve a gene more than they are concerned with HSP [14]. The representation of these HSPs is then a common phenomenon [15]. HSPs have molecular ancillary and functional antiapoptotic capacity [16, 17] from ancient times. That is, it is a protein that develops to escape cell death in harsh conditions for cell survival. Many HSPs also

express many cells in response to stress, suppression, and repair of proteins whose properties have been altered. In addition, HSPs are essential proteins to maintain various cellular life functions between cell differentiation and growth and presence. It is a widely distributed intracellular equilibrium protein, which is regularly expressed under various conditions in in vitro and in vivo experiments. Depending on the molecular weight, HSP is classified into high molecular HSP (HSP 110, HSP 90, HSP 70, and HSP 40–60 families) and low molecular HSP (HSP 20 family). These are polypeptides of tens to hundreds of kDa. Many researches have been done on expression and function of these HSPs and various sites. That is, high molecular HSPs such as HSP 70 and HSP 90 have a role of assisting the maturation of proteins. That is, it temporarily binds to immature state protein and acts as a molecular chaperone. However, small molecular HSPs that function as molecular chaperones have not yet been reported [21]. HSP 27 belongs to the low molecular HSP family. Firstly, HSP 27 was found in the actin polymerization. HSP 27 is known to exist at high levels in non-stimulated vascular smooth muscle and skeletal muscle cells. From this, it is believed that HSP 27 plays a role in maintaining blood pressure and other physiological effects in the vascular system [18–20].

We reported that BMCs migrated into the PDL regions; PDL fibroblasts, hemendothelial cells,osteoclasts, and Langerhans cells migrated into the PDF regions. These cells differentiate into their tissue-specific cells [21–23]. The facts are that BMCs are not mesodermal cells and they are derived from neural crest cells. This differentiation into specialized cells may be done on the spot by expression of odontogenic genes [24]. According to a classical tissue engineering technique, the tooth-like structure is created based on biodegradable polymer scaffolds by transplantation of dental pulp cell pellets or BMC extracted directly from dental embryonic cells and dental pulp stem cells separated by enzyme treatment [25].

We examined the transplanted BMC migration into the PDL. The IHC revealed that GFP-positive cells were detected in the PDL tissues. A number of GFP-positive cells appeared on mechanically loaded periodontal tissue, especially on the tension side of the experimental group. On the other hand, little GFP-positive cells appeared in the control group. From the above results, we analyzed how they differ from the experimental group and control group [25]. Thus, these data indicated that orthodontic mechanical stress acts as a possible promoting factor of transplanted bone marrow-derived cell migration into periodontal tissues and of differentiation to fibroblasts [26].

On the other hand, mice transplanted with bone marrow cells of GFP transgenic mice were used to observe GFP-positive cells in dental pulp of mouse incisors, PLD, oral epithelial Langerhans cells, pulp fibroblasts, dental vascular endothelial cells, and osteoclasts. GFP-positive cells in the dental pulp are dendritic cell-like cells, and some odontoblast-like cells also showed a positive response to GFP. It is clear that BMCs have the ability to differentiate into teeth and related connective tissues. GFP-positive cells histopathologically differentiated into several cell types. Fluorescent immunohistochemistry (FIHC) and tartrate-resistant acid phosphatase (TRAP) staining techniques showed that these cells were detected as osteoclasts and macrophages. In addition, GFP-positive cells gathered in adjacent blood vessels. This data suggests that GFP-positive BMCs migrate to periodontal tissues and differentiate PDL tissue-specified cells.

GFP-positive cells were detected in PDL in both experimental and control groups in this study. In the experimental group, a number of GFP-positive cells were found in the PDL tissue and intermittently stimulated intermittent mechanical stress. However, there were few GFP-positive cells in the control group. This result was significantly larger between the experimental group and the control group. This suggests that orthodontic mechanical stress induces GFP-positive transplanted BMCs into the PDL tissues.

BMC migrate from bone marrow tissue and different types of tooth-related cell types including odontoblasts [27], osteoclasts [28], and PDL [29, 30]. Osteoblasts and osteoclasts maintain and reconstruct cancellous bone surrounding the marrow tissue. BMCs from the bone marrow are closely involved in the repair of tissues to maintain periodontal tissue homeostasis of PDL fibroblasts. Furthermore, mechanical stress strongly induces cellular activation of these PDLs. Teeth can be produced from non-odontogenic stem cells. This establishes the basic principle that bone marrow stem cells are also involved in tooth embryogenesis. As a future therapeutic possibility, these cells include transplantation to a tooth defect site or transplantation into a patient's bone marrow with developmental abnormality, which may lead to a new approach to tooth and jaw bone regeneration.

3. GFP-BMDCs into the PDL received occlusal trauma

Regarding the examination results of periodontal ligament in experimental occlusal trauma mouse model, we have reported the cytological behavior of the related regions. The experimental model diagram is shown in **Figure 3**. Periodontal connective tissue remodeling occurred due to traumatic occlusal overload [31]. In the remodeling course, the fibroblasts act as an important role. In the process of PDL remodeling phenomenon, fibroblasts make an important role such as collagen synthesis. Heat shock protein 47 (HSP 47) is a protein that acts as a molecular chaperone in procollagen biosynthesis and maturation. Type I collagen is a major component of PDL. Therefore, in our study, the expression of IHC of HSP 47 on the experimental-induced periodontal tissue of traumatic occlusion was investigated. That is, an experimental occlusal trauma model was developed and experimented. Expression of HSP in occlusal trauma periodontal tissue was performed using immunohistochemistry (IHC). The results indicated that fibroblasts had high HSP expression in response to excessive traumatic occlusion. HSP 47 is thought to play an important role in the maintenance of fibroblast homeostasis exposed to traumatic occlusion. HSP 27 and HSP 70 have detailed observation results on damaged periodontal tissue by Muraoka et al. [5–7]. Based on the experiments of Fujii et al. [31] and Takaya et al. [32], we carried out the IHC study on the histopathological changes of mouse dental tissue and on HSP.

The experimental outline is shown in **Figure 3**. After that, changes in the periodontal ligament were observed over time. Then after, the micro plus screw was removed at day 4 after implantation, and the subsequent tissue changes were observed. Histopathological examination: It was observed that a fibroblast and a spindle-shaped cell have high density in a periodontal ligament of the control group. An erythrocyte was filled by a capillary. Periodontal ligament

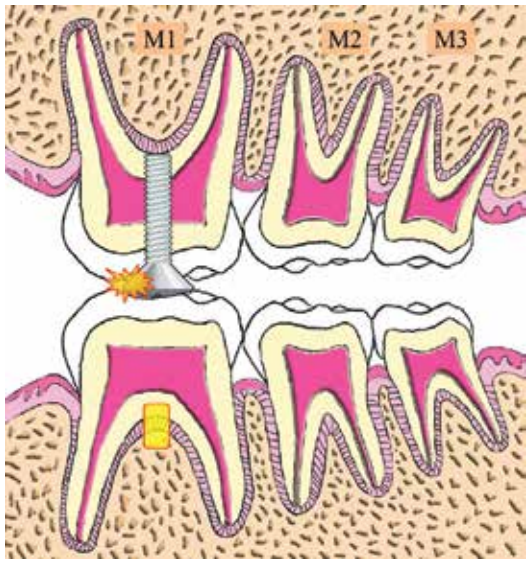

Figure 3. Diagram of the mouse traumatic model.

fiber was arranged irregularly. An osteoclast could see conspicuously in an alveolar bone. The furcation was lined by acellular cementum. At experimental group on day 1, the capillary which swelled was filled with an erythrocyte. The amount of deeply stained cells with round nuclei increased. More osteoclasts were observed on the glassy surface of the alveolar bone.

There are several kinds in a stem cell; a stem cell differentiates into various cells of a human body and has a special nature. The stem cell and a marrow-derived cells (BMCs) also possess the differentiation special quality of the plural. Many researchers reported that BMCs might relate into retinal vessels, myoblasts, hepatocytes in the liver, Purkinje neurons, cardiac muscle in the heart, and airway epithelial cells in recent years [33, 34]. A stem cell can be used in the field of the regenerative medicine; so to regenerate an organ, the stem cell is very important for treatment of various diseases [35]. For treatment of an end limb ischemia and an ischemia disease including myocardial infarction, a try at a local delivery of BMCs is studied [36, 37].

It is stated that occlusal trauma is defined as damage resulting from tissue changes within the PDL as a result of abnormal occlusion forces. It has been proven for many years by many researchers that occlusal trauma may cause various destructive biological reactions to the tissue of PDL [37–40]. A lot of researchers reported cytological kinetic examinations of PDL tissue regarding occlusal trauma PDL, but they have not been fully performed regarding establishing an experimental system with animals that can be used in a very versatile manner; we have constructed an experimental system with a mouse with respect to the occlusal trauma model. We reviewed the organization of PDL from the perspective of cytological kinetics [40]. We then performed a histopathological and also immunohistochemical study. **Figure 4** shows histopathology and IHC results.

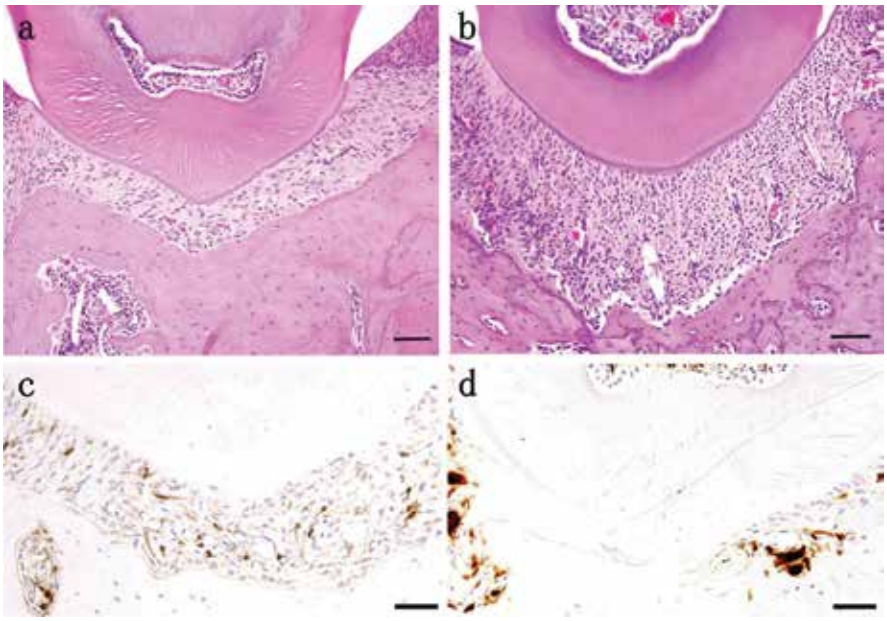

Figure 4. Histopathology of control region (a) and experimental region (b) of the day 4 specimen. Scale bar = 50 μm. IHC of GFP. Control specimen (c) and experimental day 7 specimen (d). Scale bar = 50 μm. Quotation alteration of literature #32.

Eleven 7-week-old ddY male mice and eight 7-week-old bone marrow-transplanted female C57BL/6 genealogy mice from GFP transgenic mice (GFP mice), for a total of 19 mice, were used in this study. Histopathological examination showed as followed. Control group specimens showed the PDL maintained a constant width; the major fibers arranged in orderly cementum and alveolar bone. Spindle-shaped fibroblasts that appeared in PDL were collagen fiber bundles. In the relatively dense cell nucleus, PDL, there was a congested capillary. Furthermore, the cellular cementum could be clearly confirmed. On day 4 of the experimental group, PDL was somewhat compressed, and evident capillary vessel filling was confirmed. In spindle-shaped fibroblasts, those with deeply stained circular nuclei of hematoxylin increased in number. Multinucleate giant cells appeared mainly on the alveolar bone surface. It gradually absorbed bone tissue and made some blanks. In the experimental group, the circular nucleus cells decreased considerably on day 7 from day 4. Vascular hypertrophy developed. Multinucleate giant cells were expressed on the alveolar bone surface of Howship's lacunae. On day 4 of the experimental group specimens, the regression of hyaline degeneration area had expanded. Furthermore, the cellular cementum destruction was evident in the expansion of PDL areas. On day 14 of the experimental group, the cementum absorption region by multinucleated giant cells and the alveolar bone surface rapidly expanded remarkably. There was a decrease in cells with circular nuclei. Cells in which both the nucleus and the cytoplasm are spindle-shaped are increasing again. The width of PDL became wider.

Using the cytological kinetics method, we analyzed the nuclear occupancy to compare all cell numbers. The area examining the occupancy rate analyzed related PDL experiments and

control groups in the histopathological photographs. The result was markedly increased on the day 4 of the experimental group. Compared with the experimental group, experimental group on day 7 and 14 decreased but mostly of the same degree share, and they were not significant to compare with the control group.

GFP-positive cells were sparse in the control group and the experimental group on days 4 and 14. These cellular contours are PDL cells with circular nuclei. According to the digital image analysis method, the number of GFP-positive cells increased in the experimental group day 7. The results of image analysis of GFP-positive cells of PDL on the day 7 of the experimental group showed a considerably larger increase in comparison with the control group.

In the progress of periodontal disease [41], things such as dental plaque and tartar caused by tooth deposits are common, but it is well-known that occlusion abnormalities such as traumatic occlusion are also important. Histopathological examination of PDL has been conducted [42–46] so far. These were done using rats, mice, macaque monkeys, and Beagle dogs. However, the report did not find a focus point at cytological kinetics of periodontal ligament due to excessive occlusal loading. Thus, we focused the cytological kinetics in the periodontal tissues by excessive occlusal loading.

GFP-IHC specimens shows, although the positive rate of GFP was considerably high on the day 7 of the experimental group, that there was almost no significant difference in the day 14 of the experimental group as compared with the control group. All cells constituting individual tissue cells of GFP transgenic mice have green fluorescent protein. Even if any types of cell differentiate transplanted bone marrow-derived cells, they can be traced by GFP. It is a technique of immunofluorescent staining. Such cells were identified from bone marrow-transplanted cells. At first it was osteoclasts and macrophages. It is reported later in the results of the previous experiment that many GFP-positive cells migrate to the PDL tissues in mice and differentiate into in situ specific cells. Furthermore, it is easy to imagine that dendritic cells and PDL fibroblasts, which migrate into the PDL, differentiate into PDL-specific cells.

In the experiment, bone marrow-derived cells showing GFP-positive cells in PDL of the root bifurcation region subjected to occlusal trauma on the day 7 of experimental group increased. It is clear that the majority of GFP-positive cells are osteoclasts and macrophages by previous studies. It is not only PDL damage due to continuous excessive occlusal trauma. It causes remodeling of alveolar bone and PDL and mobilization of bone marrow-derived cells is necessary for it.

According to many studies, PDL remodeling phenomenon due to acceleration of cell activation is caused by excessive traumatic occlusion stress on the day 4 of the experimental group on the tooth PDL damaged part in the root furcation region. In the experimental group day 7, PDL remodeling mechanism is done by osteoclasts and macrophages. The cells are present in the furcation area as GFP-positive BMDCs. Therefore, when gingivitis has not been caused at all or only very slightly, the PDL stressed with traumatic occlusion; it will be constructed by BMDCs.

4. Differentiation of BMDCs into the PDL peculiar cells

The IHC view is as follows. BMDC is GFP-positive except for an endothelial cell of micro-capillarity. PDL cells and/or cells spindle in shape on the alveolar bone surface are mostly GFP-positive (**Figure 5a**). Furthermore, the micro-capillaries are positive for GFP in some occasions of the periphery (**Figure 5b**).

Cells of various cell types could be identified by immunofluorescence double staining check for GFP. Green fluorescent GFP-positive cells as orange fluorescence by fluorescence immunohistochemical double staining of GFP-S100A4 (**Figure 5c**) and GFP-Runx2 were consistent with red fluorescent S-100 A 4-positive and Runx2-positive cells (**Figure 5d**). Fusiform cells toward the root direction were arranged in a bundle. When superimposing, the nucleus stained blue, and the cell of that cell was stained orange. The enlarged view of **Figure 6** also clearly shows both positive for GFP and CD 31 and proposes PDL capillaries (**Figure 5e**).

Recently, many studies using undifferentiated mesenchymal cells (UDMC) of the bone marrow are done in the repair and regeneration of tissues, bones, and other organs around the

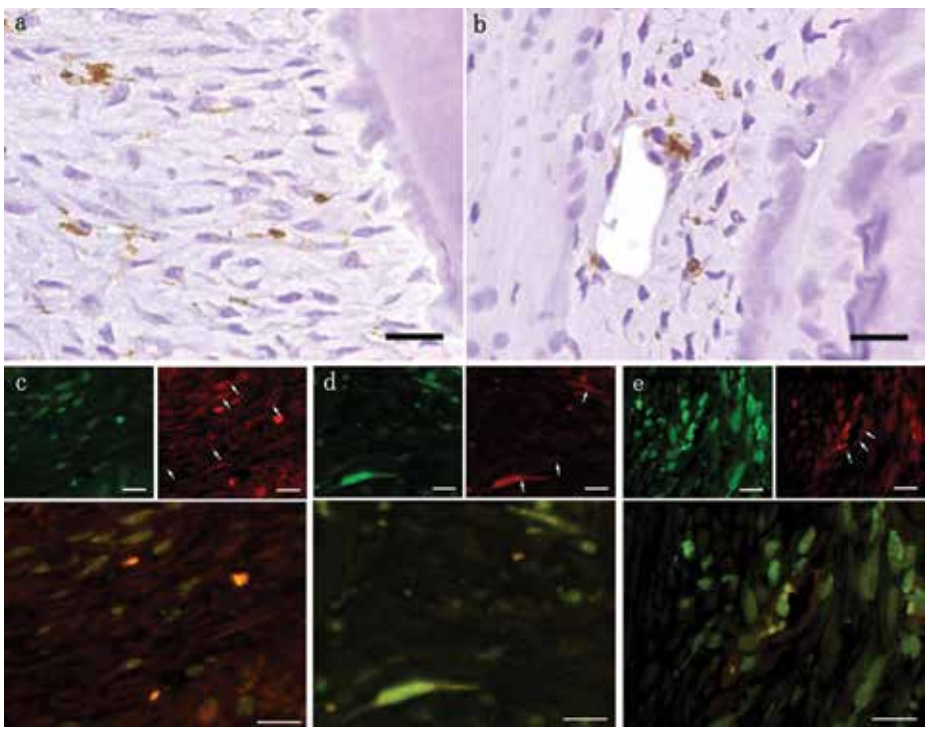

Figure 5. IHC results showing GFP-positive round- or spindle-shaped cells within the PDL tissues (a, scale bar = 50 μm) and GFP-positive products existing within the vascular endothelial cells (b, scale bar = 50 μm). Regarding the lower layer photographs (c–e), enlarged FIHC images of PDL, 6 months specimen. GFP (green) and merged image (c) of S-100 A4 (red) result fibroblast. GFP (green) and Runx2 (red) view (d) shows clearly both positive suggesting PDL fibroblasts, and GFP (green) and CD31 (red) image (e) suggests endothelial cells. Scale bar = 100 μm. Quotation alteration of literatures #26 and 43.

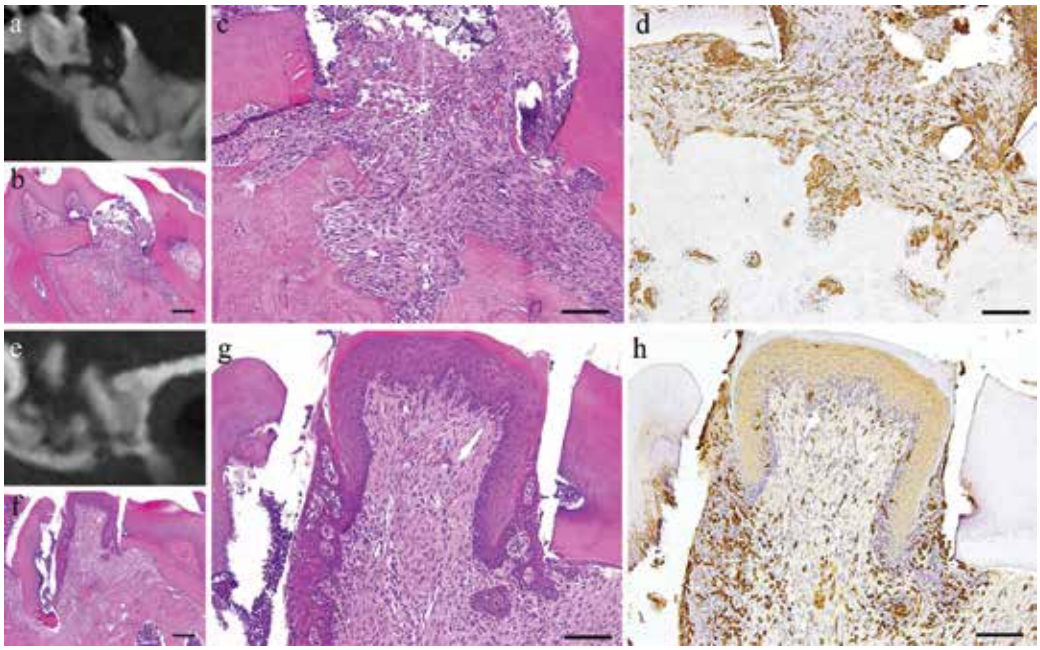

Figure 6. Micro-CT of day 4 specimen (a), histopathology view (b, c), and IHC of GFP (d). Micro-CT of day 7 specimen (e), histopathology view (f, g), and IHC of GFP (h). Scale bar = 50 μm. Quotation alteration of #44.

teeth. Regarding the alveolar bone and the PDL regenerations, it was described for the differentiation of UDMC from bone marrow into cartilage [11, 12]. Experiments on BMDCs using GFP mice showed that after cell transplantation, it differentiated into salivary gland epithelial cells and myoepithelial cells capable of playing a role not only of olfactory cells but also salivary gland tissue [13]. Histopathological examination of experimentally loaded mice in orthodontic treatment showed that bone marrow stem cells increase bone remodeling capacity [3].

Tomida et al. reported that PDL cells increased after 1–5 weeks of mechanical stress. In the current study, the cell number was calculated by counting GFP-positive cells in the control group and the experimental group [47]. The results showed that the number of GFP-positive cells in the experimental group was much higher than that in the control group. The increase in the number of cells in PDL after mechanical stress loading strongly suggests that it occurred because BMDCs were transferred to PDL. Using GFP mouse experiments, Tsujigiwa and others indicated that the transplanted BMDCs migrated to pulp and differentiated into cells constituting pulp tissue [1]. By using the same experiment, Muraoka et al. [48] showed that the transplanted BMDCs migrated to PDLs and later differentiated into PDL cells. However, the biological response of mesenchymal cells in response to mechanical stimuli also caused changes in cell morphology [48]. Movement of transplanted BMDCs using GFP mice was reported to be due to mechanical stress [49].

The results of the study showed that the mechanical stress promoted the increase in the number of cells in both pressure and tension sides of the PDL. Morphological changes of the

extracellular form were not detected, but the number of cells increased in a short period of 1 week. To determine if an increase in cell number is made by migration of BMDCs, using Tomida's method [47], GFP-positive cells were counted.

The number of GFP-positive cells immediately after stress load showed a gradual increase. It had increased over time until 6 months. It is certain that BMDCs were supplied to the PDF for a long period of time. Furthermore, when each cell was characterized by double immunofluorescence staining, Tsujigiwa et al. [1, 2] showed that the transplanted BMDCs, GFP-positive cells such as osteoclasts, were stained and identified. This confirmed that it moved and differentiated into the bone remodeling site.

Applying the method of Muraoka [48], cell identification by double immunofluorescence staining with GFP-CD31, GFP- CD68, and GFP- Runx2 were performed. As a result, it was possible to distinguish between osteoclasts and macrophages. Furthermore, since some GFP-positive cells expressing CD31 were found, they were derived from BMDCs and differentiated into hemangioendothelial cells. Similar results were obtained for macrophages by CD68. Furthermore, since Runx2 represented fibroblasts [3, 4], respectively, the expression of Runx2 was executed. As a result, it was clear that it was GFP-positive and expression of Runx2, and the cell morphology was a certain swimming; so it was a PLD fibroblast which strongly suggested that it had migrated from the bone marrow.

5. Notch signaling in cell differentiation of the BMDCs in the PDL

The GFP mouse model examination revealed that the cells were derived from mesenchymal cells of the bone marrow. Furthermore, these cells differentiated into the tissue-specific PDL fibroblasts, blood capillary endothelial cells, etc. Notch is a membrane-bounded protein, which regulates the differentiation gen for changing the cell type [49]. However, there have been no reports on the component cells of periodontal polyp-granulation tissues [9].

In usual dental clinical practice, perforation of the floor of the dental pulp suddenly occurred during a dental treatment. In case of a large perforation, it cause chronic granulomatous growth in the regional portions [9]. Granulation tissue grows in the periodontal ligament (PDL) region from the perforated dentin causing periodontal polyp. Regarding the PDL polyp, our previous histopathological and immunohistochemical examinations were done [4–6]. The data using an experimental system on GFP mouse bone marrow transplantation model revealed that the cells were derived from mesenchymal cells of the bone marrow. Furthermore, these cells differentiated into the tissue-specific PDL fibroblasts, blood capillary endothelial cells, etc. (**Figure 6**).

In general, Notch signaling is necessary for cell fate determination, cell proliferation, and differentiation [56, 57]. Therefore in this study, we examined using the method of Matsuda, et al. [9]. We examine the expression of Notch in the experimentally induced pulp polyp component cells, using observation of histopathology and immunohistochemistry methods. Histopathological observation of 2-week specimens, the spindle-shaped cell proliferation was evident with some neutrophils in the specimens. Within these cells, the relatively round nucleus-having cell and some capillaries were observed.

The IHC examination of Notch expression of the 2-week specimens, elongated, and spindle-shaped cells with spindle nucleus were positive to Notch1 (**Figure 7a, b**). From 1 to 6-month specimens, the spindle-shaped cells were also positive to Notch1. Notch1-positive reaction was continuously detected (**Figure 7c, d**). In contrast, as observed in the control, the dental pulpal tissues of the non-treated teeth were completely negative, although some nonspecific positive reactions existed (**Figure 7e, f**). Furthermore, the physiological PDL was slightly positive to Notch (**Figure 7e**).

Generally Notch is an important regulation signaling of morphogenesis. It was reported that Notch1 is a transmembrane protein necessary for cell fate determination, etc. [49]. Thus, we examined the relationship between the cell differentiation in the periodontal polyp component cells and Notch signaling in the present study. According to the present results: (1) spindle-shaped fibroblastic cell of the pulp polyp tissues was almost Notch1-positive reactive and (2)

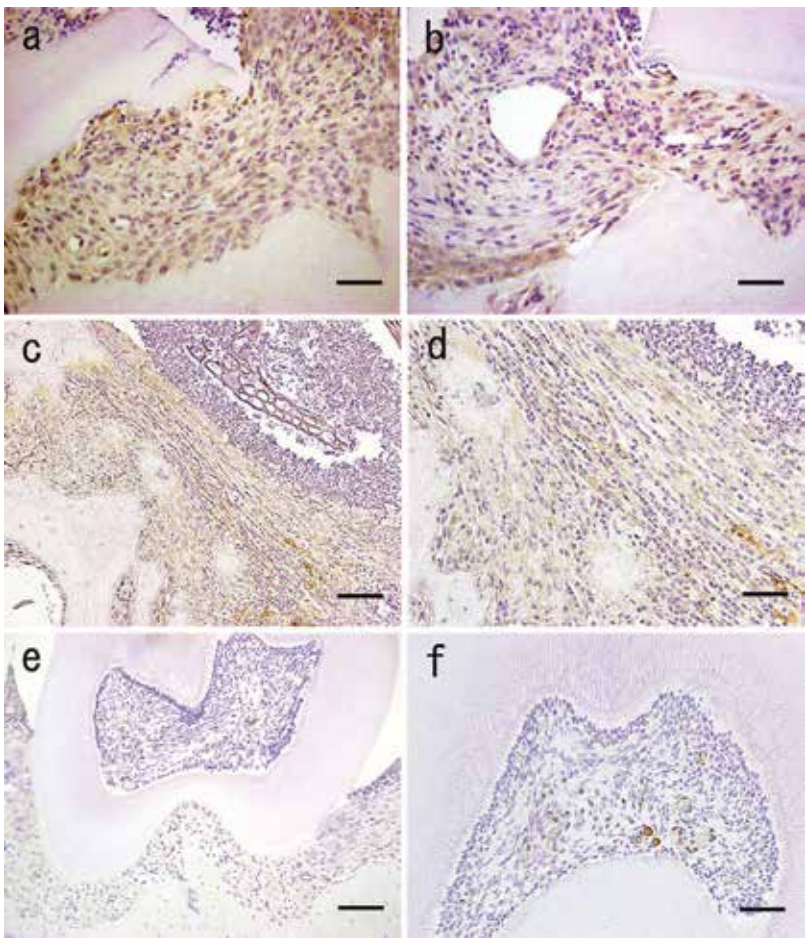

Figure 7. IHC images of notch expression. (a) Granulation tissue area, scale bar = 50 μm; (b) granulation tissue area, scale bar = 50 μm; (c) fibrous rich area, scale bar = 100 μm; (d) enlarged view of c, scale bar = 50 μm; (e) control areas (dental pulp and periodontal ligament tissues), scale bar = 100 μm; and (f) control areas (dental pulp and periodontal ligament tissues), scale bar = 50 μm. Quotation alteration of #44.

these reactions strongly suggested that the cell differentiation was caused by the Notch1 signaling. The reactions mean that the PDL is always received and controlled by Notch signaling.

6. Conclusions

In general, remodeling of the periodontal ligament (PDL) tissue is occurring in all times. Thus, in the above sentences, the word "remodeling" was used in the section "Maintenance of Periodontal Ligament Homeostasis." Our experimental data suggest that the remodeling of periodontal ligament with cell acceleration at the furcation area in this experimental model has recovered using the cells in situ and the bone marrow-derived cells (BMCs). BMC migration into the PDL tissues using BMC transplantation model was examined. BMCs have abilities of cell migration and differentiation into tissues/organs in the body. The immunohistochemistry revealed that GFP-positive cells were detected in the periodontal tissues, both in the experimental and control specimens. These results suggest that orthodontic mechanical stress accelerates transplanted BMC migration into the PDL tissues. GFP-positive cells were also positive to CD31, CD68, and Runx2 suggesting that fibroblasts differentiated into osteoclasts and tissue macrophages. In this way, Notch signaling involvement was considered in our tentative examinations.

Acknowledgements

We have received the supports for this study in parts of the Grants-in-Aid for Scientific Research (C) #23592951, #23593075, #25463204, #26463104, #26463031, #16K11817, 17H07211 and #17K11862 from the Japan Society for the Promotion of Science and have also been supported in part by 2016 Futokukai Grants-in-Aid for Scientific Research.

Conflict of interest

The authors have declared that there is no conflict of interest.

Author details

Toshiyuki Kawakami[1]*, Keiko Kaneko[1], Tatsuo Takaya[1], Saeka Aoki[1], Rina Muraoka[1], Mihoko Tomida[1], Norimasa Okafuji[1], Masahito Shoumura[1], Naoto Osuga[1], Keisuke Nakano[1,2], Hidetsugu Tsujigiwa[3] and Hitoshi Nagatuka[1,2]

*Address all correspondence to: kawakami@po.mdu.ac.jp

1 Graduate School, School of Dentistry and Hospital, Matsumoto Dental University, Shiojiri, Japan

2 Okayama University Graduate School of Medicine, Dentistry and Pharmaceutical Sciences, Okayama, Japan

3 Faculty of Science, Okayama University of Science, Okayama, Japan

References

[1] Tsujigiwa H, Hirata Y, Katase N, Buery RR, Tamamura R, Ito S, et al. The role of bone marrow-derived cells during the bone healing process in the GFP mouse bone marrow transplantation model. Calcified Tissue International. 2013;**92**:296-306

[2] Tsujigiwa H, Katase N, Sathi GA, Buerry RR, Hirota Y, Kubota M, et al. Transplanted bone marrow derived cells differentiated to tooth bone and connective tissues in mice. Journal of Hard Tissue Biology. 2011;**20**:147-152

[3] Saito Y, Yoshizawa T, Takizawa F, Ikegami M, Ishibashi O, Okuda K, et al. A cell line with characteristics of the periodontal ligament fibroblasts is negatively regulated for mineralization and Runx2/Cbfa1/Osf2 activity, part of which can be overcome by bone morphogenetic protein-2. Journal of Cell Science. 2002;**115**:4191-4200

[4] Yoshizawa T, Takizawa F, Iizawa F, Ishibashi O, Kawashima H, Matsuda A, et al. Homeobox protein Msx2 acts as a molecular defense mechanism for preventing ossification in ligament fibroblasts. Molecular and Cellular Biology. 2004;**24**:3460-3472

[5] Watanabe T, Nakano K, Muraoka R, Shimizu T, Okafuji N, Kurihara S, et al. Role of Msx2 as a promoting factor for Runx2 at the periodontal tension sides elicited by mechanical stress. European Journal of Medical Research. 2008;**13**:425-431

[6] Watanabe T, Okafuji N, Nakano K, Shimizu T, Muraoka R, Kurihara S, et al. Periodontal tissue reaction to mechanical stress in mice. Journal of Hard Tissue Biology. 2007;**16**:71-74

[7] Watanabe T, Nakano K, Shimizu T, Okafuji N, Kurihara S, Yamada K, et al. Immunohistochemistry of the periodontal ligament fibroblasts in orthodontic tension sides. Journal of Hard Tissue Biology. 2009;**18**:175-180

[8] Muraoka R, Nakano K, Matsuda H, Tomoda M, Okafuji N, Kurihara S, et al. Immunohistochemical observation of heat shock proteins expression in mouse periodontal tissues due to orthodontic mechanical stress. Journal of Hard Tissue Biology. 2009;**18**:193-197

[9] Matsuda H, Muraoka R, Tomoda M, Nakano K, Okafuji N, Yamada K, et al. Immunohistochemical observation of BMP in the mouse orthodontic periodontal tension sides. Journal of Hard Tissue Biology. 2009;**18**:181-184

[10] Kawakami T, Nakano K, Shimizu T, Kimura A, Okafuji N, Tsujigiwa H, et al. Histopathological and immunohistochemical background of orthodontic treatment. International Journal of Medical and Biological Frontiers. 2009;**15**(7/8):591-615

[11] Milton JS. Heat shock proteins. The Journal of Biological Chemistry. 1990;**265**:12111-12114

[12] Maeda T, Kameda T, Kameda A. Loading of continuously applied compressive force enhances production of heat shock protein 60, 70 and 90 in human periodontal ligament-derived fibroblast-like cells. Journal of Japan Orthodontic Society. 1997;**56**:296-302

[13] Okazaki M, Shimizu Y, Chiba M, Mitani H. Expression of heat shock proteins induced by cyclical stretching stress in human periodontal ligament fibroblasts. Tohoku University Dental Journal. 2000;**19**:108-115

[14] Ritossa F. A new puffing pattern induced by temperature shock and DNP in drosophila. Cellular and Molecular. 1962;**18**:571-573

[15] Miyagawa Y, Lee JM, Maeda T, Koga K, Kawaguchi Y, Kusakabe T. Differential expression of a *Bombyx mori* AHA1 homologue during spermatogenesis. Insect Molecular Biology. 2005;**14**:245-253

[16] Gething MJ, Sambrook J. Protein folding in the cell. Nature. 1992;**355**:33-44

[17] Miron T, Vancompernolle K, Vandekerckhove J, Wilchek M, Geiger B. A 25-kDa inhibitor of actin polymerization is a low molecular mass heat shock protein. The Journal of Cell Biology. 1991;**114**:255-261

[18] Craig EA, Weissman JS, Horwich AL. Heat shock proteins and molecular chaperones: mediators of protein conformation and turnover in the cell. Cell. 1994;**78**:365-372

[19] Arrigo AP, Landry J. Expression and function of the low molecular weight heat shock proteins. In: Morimoto RI, Tissières A, Georgopoulos C, editors. The Biology of Heat Shock Proteins and Molecular Chaperones. North America: Cold Spring Harbor Laboratory Press; 1994. pp. 335-373

[20] Lindquist S, Craig EA. The heat-shock proteins. Annual Review of Genetics. 1988;**22**: 631-677

[21] Shigehara S, Matsuzaka K, Inoue T. Morphohistological change and expression of HSP70, osteopontin and osteocalcin mRNAs in rat dental pulp cells with orthodontic tooth movement. The Bulletin of Tokyo Dental College. 2006;**47**:117-124

[22] Muraoka M, Tsujigiwa H, Nakano K, Tamura R, Tomida M, Okafuji N, et al. Transplanted bone marrow-derived cell migration into periodontal tissues and cell differentiation. Journal of Hard Tissue Biology. 2011;**20**:301-306

[23] Hratl FU. Molecular chaperone in cellular protein folding. Nature. 1996;**381**:571-579

[24] Ohazama A, Modino SA, Miletich I, Sharpe PT. Stem-cell-based tissue engineering of murine teeth. Journal of Dental Research. 2004;**83**:518-522

[25] Duailibi MT, Duailibi SE, Young CS, Bartlett JD, Vacanti JP, Yelick PC. Bioengineered teeth from cultured rat tooth bud cells. Journal of Dental Research. 2004;**83**:523-528

[26] Kaneko K, Matsuda S, Muraoka R, Nakano K, Iwasaki T, Tomida M, et al. International Journal of Medical Sciences. 2015;**12**:689-694

[27] Fromigue O, Hamidouche Z, Chateauvieux S, Charbord P, Marie PJ. Distinct osteoblastic differentiation potential of murine fetal liver and bone marrow stroma-derived mesenchymal stem cells. Journal of Cellular Biochemistry. 2008;**104**:620-628

[28] Mancino AT, Klimberg VS, Yamamoto M, Manolagas SC, Abe E. Breast cancer increases osteoclastogenesis by secreting M-CSF and upregulating RANKL in stromal cells. The Journal of Surgical Research. 2001;**100**:18-24

[29] Kinnaird T, Stabile E, Burnett MS, Epstein SE. Bone marrow-derived cells for enhancing collateral development. Circulation Research. 2004;**95**:354-363

[30] Feng W, Madajka M, Kerr BA, Mahabeleshwar GH, Whiteheart SW, Byzova TV. A novel role for platelet secretion in angiogenesis: Mediating bone marrow-derived cell mobilization and homing. Blood. 2011;**117**:3893-3902

[31] Fujii T, Takaya T, Mimura H, Osuga N, Matuda S, Nakano K. Experimental model of occlusal trauma in mouse periodontal tissues. Journal of Hard Tissue Biology. 2014;**23**: 377-380

[32] Takaya T, Mimura H, Matsuda S, Nakano K, Tsujigiwa H, Tomita M, et al. Cytological kinetics of periodontal ligament in an experimental occlusal trauma model. International Journal of Medical Sciences. 2015;**12**:544-551

[33] Popov BV, Serikov VB, Petrov N, Izusova TV, Guota N, Matthay MA. Lung epithelial cells induce endodermal differentiation in mouse mesenchymal bone marrow stem cells by paracrine mechanism. Tissue Engineering. 2007;**13**:2441-2450

[34] Zou H, Otani A, Oishi A, Yodoi Y, Kameda T, et al. Bone marrow-derived cells are differentially involved in pathological and physiological retinal angiogenesis in mice. Biochemical and Biophysical Research Communications. 2010;**391**:1268-1273

[35] Tsujigiwa H, Nishizaki K, Teshima T, Takeda Y, Yoshinobu J, Takeuchi A, et al. The engraftment of transplanted bone marrow-derived cells into the olfactory epithelium. Brain Research. 2005;**1052**:10-15

[36] Bobis S, Jarocha D, Majka M. Mesenchymal stem cells: Characteristics and clinical applications. Folia Histochemica et Cytobiologica. 2006;**44**:215-230

[37] Zhang HK, Zhang N, Wu LH, Jin W, Fenq H, Zhao HG, et al. Therapeutic neovascularization with autologous bone marrow CD34+ cells transplantation in hindlimb ischemia. Zhonghua Wai Ke Za Zhi. 2005;**43**:1275-1278

[38] Stahl SS. Accommodation of the periodontium to occlusal trauma and inflammatory periodontal disease. Dental Clinics of North America. 1975;**19**:531-542

[39] Lindhe J, Ericsson I. The influence of trauma from occlusion of reduced but healthy periodontal tissues in dogs. Journal of Clinical Periodontology. 1976;**3**:110-122

[40] Biancu S, Ericsson I, Lindhe J. Periodontal ligament tissue reactions to trauma and gingival inflammation. An experimental study in the beagle dog. Journal of Clinical Periodontology. 1995;**22**:772-779

[41] Waerhaug J. The Infrabony pocket and its relationship to trauma from occlusion and subgingival plaque. Journal of Periodontology. 1979;**7**:355-365

[42] Artavanis-Tsakonos S, Rand MD, Lake RJ. Notch signaling: Cell fate control and signal integration in development. Scince. 1999;**284**:770-776

[43] Matsuda S, Shoumura M, Osuga N, Tsujigiwa H, Nakano K, Okafuji1 N, et al. Migration and differentiation of GFP-transplanted bone marrow-derived cells into experimentally induced periodontal polyp in mice. International Journal of Medical Sciences. 2016;**13**:500-506

[44] Matsuda S, Nakayasu K, Tsujigiwa H, Takabatake K, Okafuji N, Shoumura M, et al. Overview of cytological dynamics of periodontal ligament inflammatory lesions. International Journal of Dentistry and Oral Science. 2016;**S9**:1-7

[45] Harada H, Mitsuyasu T, Toyono T, Toyoshima K. Epithelial stem cells in teeth. Odontología. 2002;**90**:1-6

[46] Hiraoka K, Grogan S, Olee T, Lotz M. Mesenchymal progenitor cells in adult human articular cartilage. Biorheology. 2006;**43**:447-454

[47] Tomida M, Tsujigiwa H, Nakano K, Muraoka R, Nakamura T, Okafuji N, et al. Promotion of transplanted bone marrow-derived cell migration into the periodontal tissues due to orthodontic mechanical stress. International Journal of Medical Sciences. 2013;**10**: 1321-1326

[48] Muraoka R, Nakano K, Kurihara S, Yamada K, Kawakami T. Immunohistochemical expression of heat shock proteins in the mouse periodontal tissues due to orthodontic mechanical stress. European Journal of Medical Research. 2010;**15**:475-482

[49] Noda Y, Nishizaki K, Yoshinobu J, Orita Y, Tsujigiwa H, Yamada M. The engraftment and differentiation of transplanted bone marrow-derived cells in the olfactory bulb after methimazole administration. Acta Oto-Laryngologica. 2013;**133**:951-956

Chapter 7

Discoid Meniscus-Histology and Pathology

Vaso Kecojević

Additional information is available at the end of the chapter

http://dx.doi.org/10.5772/intechopen.81242

Abstract

Discoid meniscus is an abnormality in which the cartilaginous meniscus is differently shaped, thick, and contains less collagen. It is mostly seen in children; and in the adult, it is rarely symptomatic. We have certain knowledge of discoid meniscus shape, its ultrastructure, epidemiology, and pathology. The discoid shape of the meniscus, which is seen mostly on the lateral meniscus, is described as an abnormality in which the cartilaginous meniscus, instead of the usual crescent type, is shaped like a full or partial disc, thickened, and covers more of the tibial lateral articular surface. The origin of the discoid shape is still not known. Some theories state that it is a normal finding during embryological development of the knee joint, some consider it as an atavism, and some consider it as a morphologic change during development. There are not many published studies on histological examinations. What is common is that the microstructure of the discoid meniscus differs in terms of the content and arrangement of collagen fibers. It is rarely symptomatic, so the true epidemiology of this abnormality is difficult to determine. In this chapter, we tried to make a cross-section of the current findings considering lateral discoid meniscus.

Keywords: discoid meniscus, histology, morphology, pathology

1. Introduction

Over 130 years have passed since the discoid lateral meniscus of the knee was described as a morphologic entity of the lateral meniscus. We have certain knowledge of discoid meniscus shape, its ultrastructure, epidemiology, and pathology. Yet, we still do not know its origin. The discoid shape of the meniscus, which is seen mostly on the lateral meniscus, is described as an abnormality in which the cartilaginous meniscus, instead of the usual crescent type, is shaped like a disc, thickened, and covers more of the tibial lateral articular surface. Young, in

1889, first described it in a paper after a cadaveric dissection [1]. Discoid meniscus is mostly located on the lateral side, although cases are also described in the medial compartment. In the adult, the lateral discoid meniscus is often found during knee arthroscopy. The reason is that it is rarely symptomatic, so the true epidemiology of this abnormality is difficult to determine.

2. Discoid meniscus

2.1. Epidemiology

Several studies have reported the incidence and prevalence of discoid meniscus. In the work of Sun and Jiang, the incidence of lateral discoid meniscus ranges from 0.4 to 17%, as compared with medial discoid meniscus. Medial discoid meniscus is a rather rare finding. In the work of Sun and Jiang, the incidence for medial discoid meniscus ranges from 0.06 to 0.3% [2]. Ikeuchi reported the incidence of discoid lateral meniscus (DLM) of about 16.6% [3], while Fukuta reported 10.6%, in Japanese populations [4]. Kim reported 10.9% in Korean populations [5], and Rao reported an incidence of 5.8% in India [6]. Greis in 2002 reported the incidence of discoid lateral meniscus to be 0.4–17% [7]. In white populations, according to the work of Papadopoulos, the incidence is quite low, 0.4–5% [8]. In a study on 1357 knee arthroscopies, Glisic et al. reported an incidence of 1.03% discoid lateral meniscus [9]. In our series, we found an incidence of 0.28% of discoid lateral meniscus out of 1071 knee arthroscopies. Regarding bilateral discoid lateral meniscus (DLM) in the Asian population, Bae et al. found out a high prevalence of 79% of symptomatic DLM [10]. There are also reports of anomalies of knee anatomy conjoined with DLM, such as high fibular head, hypoplasia of the lateral femoral condyle and fibular muscles [11, 12], osteochondritis dissecans of the lateral femoral condyle [13], and hypoplasia of the lateral tibial spine [14] and dipped lateral tibial plateau [15]. Thicker body, lack of blood vessels, and different ultrastructure make discoid lateral meniscus more susceptible to injury.

2.2. Histology

Meniscus of the knee has a specific microstructure. Most of the content is water, approximately 70%, and the remaining 30% belongs to organic residue. Organic matter is mostly collagen, approximately 60–70%, and the rest are noncollagenous proteins [16–19]. Collagen type I is predominant in normal meniscus (90%), in regard to articular cartilage where collagen type II is predominant, and that makes the major difference [20]. Collagen types II, III, V, and VI are present in smaller concentrations. The collagen and extracellular matrix are synthesizing in the fibrochondrocytes, which represented cellular components [21, 22]. Meniscus cells appear in two forms. Superficial cells are oval, and deeper cells are more rounded, both with a lot of endoplasmic reticula and Golgi complex, and with a few mitochondria [23]. The collagen fibers are set in three layers. Most superficial fibers are radial; in the middle, fibers run circumferentially, and in the deep layers, fibers are parallel to the periphery. Radial fibers seem to act like a connection to the circumferential ones, resisting splitting. Specific organization

of the collagen fibers transfers compressive loads to circumferential stress. The rest of the extracellular matrix is composed of proteoglycans. Chains of aggregate proteoglycans, the glycosaminoglycans, participate only by 1% of the meniscus wet weight, but their ability to retain and repel water during knee movement is essential to the stiffness and elasticity, and to resist compressive loads [24]. Also, water exudation from glycosaminoglycans has a role in joint lubrication. The highest concentrations of glycosaminoglycans are at the highest weight-bearing areas: anterior and posterior horns of the menisci and the inner half [25]. The ability of the meniscus to recover its form after deformation is small, probably because of low concentration of elastin, less than 0.6% [26].

The etiology of discoid meniscus is not known clearly. There are several explanations. Smillie in 1948 gave a theory that the lateral discoid meniscus is a normal fetal stage of development with the failure of resorption of the central area of the cartilage plate [27]. In several embryological studies, it was shown that the lateral meniscus does not have the discoid shape during development. Kaplan, on the contrary, demonstrated that the discoid meniscus is a pathological entity [28, 29]. Ross et al. reported that the plate of undifferentiated mesenchyme from which the meniscus develops resembles a disc at the very earliest phase during the embryonic period [30]. Several embryological studies showed that the lateral meniscus does not normally assume a discoid configuration during its development [28]. On the contrary, Kale et al. in the neonatal cadaver study found 77.27% discoid lateral meniscus and 22.72% of them were complete discoid menisci. They concluded that the primary shape of the lateral meniscus in the earlier intrauterine period is discoid, and it transforms to other shapes [31]. The rate of growth of both menisci is uniform; so is the ratio of the area of both menisci and corresponding tibial plateau. Another theory stated that the discoid shape may be the result of instability due to absence of the meniscofemoral attachment. The lateral meniscus covered 80–93% of the lateral tibial plateau, and it is thicker, so that fact may lead to increasing shearing forces in the knee joint [32]. At the end of embryological development, the meniscoligament complex is clearly defined (at 8 weeks by Streeter Stage 23) [33]. The blastema of human embryo does not have joint space. With chondrifying of mesenchyme in the region of the future knee joint can be identified intermediate zone of two parallel chondrogenic layers and one intermediate that has low density. By condensation in the intermediate layer, the menisci and cruciate ligaments show up. [33–35]. Both menisci are highly cellular, well vascularized, and have a characteristic shape. Vascularization of the menisci changes from the time of birth to 10 years of age: at birth, the whole meniscus is vascular; but by 9 months of age, the inner third becomes avascular; and at the age of 10, vascularity constantly decreases, and meniscus is similar to the meniscus of adults. Blood vessels are present only at the rim of the meniscus, according to Arnocky and Warren, in outer 10–25% of lateral and outer 10–30% of medial meniscus [36]. Meniscus vessels are branches of medial and lateral genicular arteries. A lot of studies show the ultrastructure of the normal menisci. Only a few published studies have investigated the histology of the lateral discoid meniscus. In the study of Atay et al. [37], by examination of partial-thickness biopsy of the symptomatic menisci, it is shown that the highly organized collagen matrix is not present in the discoid lateral meniscus. Collagen fibers are disorganized and decreased in number, and collagen concentration is low. Those facts lead to decreasing capability of the meniscus to act as stress absorber, similar to degenerated

menisci [25]. Papadopoulos et al. reported the histomorphological study of discoid lateral meniscus, taking samples during arthroscopy. They found out that there was no significant difference in the architecture of the radially arranged collagen, and significant distortion of the circumferential fibers, especially in whole high of anterior and posterior thirds, and on the medial and posterior thirds of discoid meniscus near the tibial surface. Also, the posterior third shows signs of extended myxoid degeneration, osseous metaplasia, and void spaces that make it the most disorganized part [38]. Choi et al. in his transmission electron microscopy study also stated low density and disorganization in the collagen ultrastructure of discoid lateral meniscus, that can lead to meniscal tear [39].

2.3. Discoid meniscus morphopathology

Discoid meniscus is a more common finding in children. Diagnosis is usually set on the basis of physical examination and MRI finding of the knee (**Figure 1**, **Figure 2**). Clinical findings varied from asymptomatic cases, often snapping and locking, and sometimes severe pain combined with swelling of the knee joint. Discoid meniscus is different by morphology. Normal meniscus is usually C-shaped and wedged from outer to inner edge, a form that increases the contact area between femur and tibia. In discoid meniscus, the central area is completely filled; in some cases, there is a very small aperture in the central part (**Figure 3**). The outer part that is connected to the joint capsule is much thicker than in normal meniscus. This variation disturbs normal mechanical loading and share stress and are predisponing factor to meniscal tears.

Classical classification of discoid meniscus was given by Watanabe in 1969, as complete, incomplete, and Wrisberg type, by the presence or absence of a normal posterior attachment of the meniscus, and the amount of tibial plateau coverage. According to Watanabe's classification, the most common is type I, complete discoid meniscus, which is a much thicker

Figure 1. An MRI sagittal view. Note the longitudinal rupture of lateral discoid meniscus.

http://dx.doi.org/10.5772/intechopen.81242

Figure 2. An MRI coronal view. Note the difference between thickness of the body of lateral and medial menisci.

lateral meniscus that covers the whole of the lateral tibial plateau, and is more vulnerable to tear during sports activities than normal meniscus. The next, type II, is incomplete discoid meniscus, which is smaller than type I, varies in size, structure, and shape and does not cover the whole of the lateral compartment. Common to both types are normal peripheral and posterior horn attachments and stability during arthroscopy probing. The least common is type III, the so-called Wrisberg type. The shape of this type is near to normal, not necessarily discoid, but with the absence of the posterior meniscal tibial attachments, including meniscotibial (coronary) ligament. The only attachment is the ligament of Wrisberg that connects the posterior horn of the lateral meniscus to the lateral surface of the medial femoral condyle. This leads to hypermobility of the posterior horn of the lateral meniscus during knee extension, displacement of the meniscus, and is probably the cause of the snapping. [40, 41]. Husson et al. in 1985 proposed a classification based on arthroscopic and clinical findings. They considered complete and incomplete discoid meniscus types as stable, because of the presence of firm anterior and posterior tibial and meniscofemoral attachments. Further, stable types were divided as symptomatic or asymptomatic, and torn or not torn. Unstable types were divided as unstable discoid or normal shape [32, 42]. Klingele et al. in 2004 proposed a newer classification based on the size, stability, and presence or absence of meniscal tear [43]. Kale et al. in 2006 based on a neonatal cadaver study, divided the lateral meniscus as discoid and undiscoid, and further divided discoid menisci as complete and incomplete. They stated that the primordial shape of the meniscus is discoid, and that transforms to other shapes [31].

Clinical findings differ discoid meniscus can be asymptomatic, and symptoms can be present regarding meniscal tear or meniscal instability. Typically, symptomatic discoid meniscus is presented in children between 5 and 10 years, by knee popping and snapping that can be heard or felt, with no trauma. Associated symptoms include pain, swelling, giving way,

Figure 3. An MRI axial view. Note the difference in the volume of the lateral meniscus.

decrease in range of motion, quadriceps atrophy, locking, and lack of knee extension. If tear of discoid meniscus occurs, symptoms can be severe pain, knee locking, and inability to bear weight, and snapping during knee flexion-extension. Sometimes, the patient complains of knee instability, due to posterior meniscofemoral ligament. In symptomatic types, the method of treatment choice is operative, which will be explained in other chapters.

3. Conclusion

Discoid meniscus, despite numerous studies, remains a great unknown. There is no conclusive evidence on the cause of discoid shape, or what causes its further design. The differences that exist with respect to normal histological meniscus are largely documented. The lack of histological study of the ultrastructure is reflected in the fact that the samples obtained during arthroscopic surgery were parts of symptomatic discoid meniscus. An undamaged and complete discoid meniscus that is asymptomatic is almost impossible to examine histologically, as this would lead to deterioration of the knee joint. Nevertheless, the first studies give us a guideline for further work.

Acknowledgements

I would like to thank Alma Brakus, MD, department of radiology, Clinical Center of Vojvodina, Novi Sad, for the MRI pictures of the discoid meniscus.

Conflict of interest

I have no conflict of interest.

Author note

The author is an orthopaedic surgeon; president of ASTAS (Association for Sports Traumatology and Arthroscopy of Serbia); former member of the ESSKA educational committee (2010–2014); former member of the ESSKA arthroscopy committee (2014–2016); as well as a member of EFORT, ISAKOS, SOTA (Serbian Orthopaedic and Traumatology Association), and the Serbian Medical Chamber.

Author details

Vaso Kecojević

Address all correspondence to: keckons@gmail.com

Department for Orthopaedic Surgery and Traumatology, Clinical Center of Vojvodina, Novi Sad, Serbia

References

[1] Young R. The external semilunar cartilage as a complete disc. In: Cleland J, Mackey JY, Young RB, editors. Memoirs and Memoranda in Anatomy. London: Williams and Norgate; 1889. pp. 179-187

[2] Sun Y, Jiang Q. Review of discoid meniscus. Orthopaedic Surgery. 2011;**3**:219-223

[3] Ikeuchi H. Arthroscopic treatment of the discoid lateral meniscus. Technique and long-term results. Clinical Orthopaedics and Related Research. 1982;**8**:19-28

[4] Fukuta S, Masaki K, Korai F. Prevalence of abnormal findings in magnetic resonance images of asymptomatic knees. Journal of Orthopaedic Science. 2002;**7**:287-291

[5] Kim SJ, Lee YT, Kim DW. Intraarticular anatomic variants associated with discoid meniscus in Koreans. Clinical Orthopaedics and Related Research. 1998:202-207

[6] Rao PS, Rao SK, Paul R. Clinical, radiologic, and arthroscopic assessment of discoid lateral meniscus. Arthroscopy. 2001;**17**:275-277

[7] Greis PE, Bardana DD, Holmstrom MC, et al. Meniscal injury: I. Basic science and evaluation. The Journal of the American Academy of Orthopaedic Surgeons. 2002;**10**:168-176.5

[8] Papadopoulos A, Karathanasis A, Kirkos JM, Kapetanos GA. Epidemiologic, clinical and arthroscopic study of the discoid meniscus variant in Greek population. Knee Surgery, Sports Traumatology, Arthroscopy. 2009;**17**:600-606

[9] Glisic M, Blagojevic Z, Ristic B, et al. Discoid lateral meniscus incidence during knee arthroscopy. Serbian Journal of Experimental and Clinical Research. 2015;**16**(2):129-134

[10] Bae JH, Lim HC, Hwang DH, Song JK, Byun JS, Nha KW. Incidence of bilateral discoid lateral meniscus in an Asian population: An arthroscopic assessment of contralateral knees. Arthroscopy. 2012;**28**:936-941

[11] Weiner B, Rosenberg N. Discoid medial meniscus: Association with bone changes in the tibia. A case report. The Journal of Bone and Joint Surgery. American volume. 1974;**56**:171-173

[12] Ha CW, Lee YS, Park JC. The condylar cutoff sign: Quantifying lateral femoral condylar hypoplasia in a complete discoid meniscus. Clinical Orthopaedics and Related Research. 2009;**467**:1365-1369

[13] Mitsuoka T, Shino K, Hamada M, et al. Osteochondritis dissecans of the lateral femoral condyle of the knee joint. Arthroscopy. 1999;**15**:20-26

[14] Nathan PA, Cole SC. Discoid meniscus. A clinical and pathologic study. Clinical Orthopaedics and Related Research. 1969;**64**:107-113

[15] Engber WD, Mickelson MR. Cupping of the lateral tibial plateau associated with a discoid meniscus. Orthopedics. 1981;**4**:904-906

[16] Fithian DC, Kelly MA, Mow VC. Material properties and structure-function relationships in the menisci. Clinical Orthopaedics. 1990;**252**:19-31.49

[17] Arnoczky SP, Warren RF, Spivak JM. Meniscal repair using exogenous fibrin clot: An experimental study in dogs. The Journal of Bone and Joint Surgery. American Volume. 1988;**70**:1209-1217

[18] Ingman A, Ghosh P, Taylor T. Variations of collagenous and non-collagenous proteins of human knee joint menisci with age and degeneration. Gerontology. 1974;**20**:212-233

[19] Peters TJ, Smillie IS. Studies on the chemical composition of the menisci of the knee joint with special reference to the horizontal cleavage lesion. Clinical Orthopaedics. 1972;**86**:245-252.48

[20] Mow VC. Structure and function relationships of the meniscus in the knee. In: Mow VC, Arnoczky S, Jackson D, editors. Knee Meniscus: Basic and Clinical Foundations. New York, NY: Raven Press; 1992. pp. 37-58

[21] Anatomy SS. Biology, and biomechanics of tendon, ligament, and meniscus. In: Simon S, Wilson J, editors. Orthopaedic Basic Science. Columbus, OH: American Academy of Orthopaedic Surgeons; 1994. p. 54

[22] Mginty JB, Geuss LF, Marvin RA. Partial or total meniscectomy. A comparative analysis. Journal of Bone and Joint Surgery. 1977;**59-A**:763-766

[23] McDevitt CA, Webber RJ. The ultrastructure and biochemistry of meniscal cartilage. Clinical Orthopaedics. 1990;**252**:8-18

[24] Adams M, Hukins D. The extracellular matrix of the meniscus. In: Mow VC, Arnoczky S, Jackson D, editors. Knee Meniscus: Basic and Clinical Foundations. New York, NY: Raven Press; 1992. pp. 15-28

[25] Herwig J, Egner E, Buddecke E. Chemical changes of the human knee joint menisci in various stages of degeneration. Annals of the Rheumatic Diseases. 1984;**43**:635-640

[26] Bullough P, Munuera L, Murphy J, Weinstein AM. The strength of the menisci of the knee as it relates to their fine structure. The Journal of Bone and Joint Surgery. British volume. 1970;**52**:564-570

[27] Smillie IS. The congenital discoid meniscus. Journal of Bone and Joint Surgery. 1948;**30B**:671-682

[28] Kaplan EB. The embryology of the menisci of the knee joint. Bulletin of the Hospital for Joint Diseases. 1955;**16**:111-124

[29] Kaplan EB. Discoid lateral meniscus of the knee joint: Nature, mechanism, and operative treatment. Journal of Bone and Joint Surgery. JaIL 1957;**39-A**:77-87

[30] Ross JA, Tough ICK, English TA. Congenital discoid cartilage: Report of a case of discoid medial cartilage, with an embryological note. Journal of Bone and Joint Surgery. 1958;**40-B**(2):262-267

[31] Kale A, Kopuz C, Edýzer M, Aydin ME, Demýr M, Ýnce Y. Anatomic variations of the shape of the menisci: A neonatal cadaver study. Knee Surgery, Sports Traumatology, Arthroscopy. 2006;**14**(10):975-981.0

[32] Kelly BT, Green DW. Discoid lateral meniscus in children. Current Opinion in Pediatrics. 2002;**14**(1):54-61

[33] Gardner E, O'Rahilly. Ronan: The early development of the knee joint in staged human embryos. Journal of Anatomy. 1968;**102**:289-299

[34] Ogden JA. The development and growth of the musculoskeletal system. In: Albright JA, Brand RA, editors. The Scientific Basis of Orthopaedics. New York: Appleton-Century-Crofts; 1979. pp. 41-103

[35] Ogden JA. Chondro-osseous development and growth. In Fundamental and Clinical Bone Physiology . M. R. Urist, editors. Philadelphia, J. B. Lippincott, 1980. pp. 108-171

[36] Arnoczky SP, Warren RF. Microvasculature of the human meniscus. The American Journal of Sports Medicine. 1982;**10**:90-95

[37] Atay OA, Pekmezci M, Doral MN, Sargon MF, Ayvaz M, Johnson DL. Discoid meniscus: An ultrastructural study with transmission electron microscopy. The American Journal of Sports Medicine. 2007;**35**(3):475-478

[38] Papadopoulos A, Kirkos JM, Kapetanos GS. Histomorphologic study of discoid meniscus. Arthroscopy. 2009;**25**:262-268

[39] Choi YH, Seo YJ, Ha JM, Jung KH, Kim J, Song SY. Collagenous ultrastructure of the discoid meniscus: A transmission electron microsopy study. The American Journal of Sports Medicine. 2017;**45**(3):598-603

[40] Kramer DE, Micheli LJ. Meniscal tears and discoid meniscus in children: Diagnosis and treatment. The Journal of the American Academy of Orthopaedic Surgeons. 2009;**17**(11): 698-707

[41] Watanabe M, Takada S, Ikeuchi H. Atlas of Arthroscopy. Tokyo: Igaku-Shoin; 1969

[42] Husson JL, Meadeb J, Cameau J, Blouet JM, Masse A, Duval JM. Aspect discoide des menisques externe et interne d'un meme genou a proposd'un cas. Bulletin de l'Association des Anatomistes. 1985;**69**:201-208

[43] Klingele KE, Kocher MS, Hresko MT, et al. Discoid lateral meniscus: Prevalence of peripheral rim instability. Journal of Pediatric Orthopedics. 2004;**24**(1):79-82

Section 4

Novel Techniques

Chapter 8

Novel Techniques in Histologic Research: Morphometry and Mass Spectrometry Imaging

Tatsuaki Tsuruyama and Takuya Hieatsuka

Additional information is available at the end of the chapter

http://dx.doi.org/10.5772/intechopen.81158

Abstract

Application of mass spectrometry (MS) has recently been developed for the identification of biomarkers using pathologic samples, whereas its application using formaldehyde-fixed paraffin-embedded (FFPE) tissues remains limited. In this review, we introduce MS imaging (MSI) using FFPE tissue. This method is still challenging for peptide ionization, and various pretreatment techniques have been conducted for enhancing the ionization signal of peptides. A simple chemical pretreatment method involving heating in acetonitrile-containing buffer under pressurized conditions is introduced. Further, two-dimensional MSI data are summarized in a DM for region of interest (ROI) and hierarchical cluster analyses. These techniques enable MALDI-MSI analysis of archived pathological FFPE samples to identify new biomarkers.

Keywords: mass spectrometry imaging, formalin-fixed paraffin-embedded (FFPE) tissues, acute myocardial infarction

1. Introduction

Over the past several decades, MS-based techniques are used in blood and urine analyses; however, their application to tissue analysis requires further development. Recently, matrix-assisted laser desorption/ionization (MALDI) has been applied for MS analysis for the identification of diagnostic markers [1–4]. As one of the applications of MALDI-MS (mass spectrometry), MALDI-MS imaging (MALDI-MSI) has been recently developed for the identification of phospholipids [5, 6] and peptides [7–10] and pharmacological monitoring for drug delivery system in various tissues using frozen samples [11–13]. Further, the MSI technique has been further developed in the use of formalin-fixed paraffin-embedded (FFPE) tissues and cells [7–10].

Thus, this new strategies and analytical methods are useful for the study of drug pharmacokinetics, metabolism, discovery of biomarkers, and treatment-specific effects on the proteome.

1.1. Tissue pretreatment of FFPE for MS imaging

Most of human tissues are preserved as FFPE samples in bioresource repositories. Formaldehyde reacts amino acid residues such as arginine containing amino group by methylene bridging for prevention of decomposition. There are a number of reports discussing procedures for pretreatment of FFPE sections for MALDI-MS [14, 15]. Researchers performed microdissection of pathologically diagnosed disease regions, followed by protein extraction and digestion of frozen samples for proteomic study using MS technique, but this technique is costly and time-consuming for storage of frozen samples. For broad application with the use of FFPE, there is a critical issue for study using MS technique, because the methylene bridge between amino acid residues makes it difficult to ionize peptides in samples. In fact, for immunohistochemical analysis of pathological samples, FFPE tissues are subjected to a retrieval protocol, including protein digestion by proteinase, microwave, or boiling treatment. Although the treatment using detergents is available for the retrieval of FFPE, this procedure may cause noise in the MS spectrum. There are some reports that surfactants improved MS sensitivity, but there is considerable limits regarding the subjects and the amounts to use for stable protocol [16]. In addition, enzymatic digestion is generally used to promote ionization by fragmentation; however, this enzymatic digestion is not sufficient to ionization for gaining intense MS signals. In general, collagens and elastin are commonly rich in most of all tissues, and these caused background noise of MS imaging and LC–MS. Angel et al. described availability of a matrix metalloproteinase (MMP) enzymes to access [17]. PAXgene, a type of alcohol-based non–cross-linking tissue fixative, can be used as an alternative fixative for multiomic tissue analysis [18].

A simple in situ histologic pretreatment technique for FFPE sections was developed for MALDI/TOF-MS imaging. Application of immunohistochemical method such as heating sample slides in a solution of ethylenediaminetetraacetic acid (EDTA) or citric acid may be available for enhancement of signal intensity [7]. Ronci et al. reported the imaging of human lens using this method. MALDI-MSI revealed a concentric distribution pattern of proteins of apolipoprotein E (ApoE) and collagen IV alpha-1 on the anterior surface of surgically removed lens capsule [19, 20].

1.2. MALDI-MSI of acute myocardial infarction (AMI)

Next, let us review a method for the identification of molecular markers to precisely identify mitochondrial and sarcomeric proteins in cardiac tissues. Ischemic heart failure remains a major cause of sudden cardiac death. MSI is a promising technique for understanding the pathogenesis of lethal acute myocardial infarction (AMI). MSI of cardiac tissue was recently reported by several groups including these authors [21, 22].

Histological analysis is certainly one of the key methods employed in cardiac muscle damage studies. Chronic cardiac infarcted lesions demonstrate gross fibrosis, and scarring; however, acute cardiac infarcted lesions rarely include such distinct histologic and macroscopic changes. However, the microscopic findings observed in AMI are not sufficiently informative of the phase immediately following the onset of the infarction episode [23]. Of course, wavy fibers

and contraction bands are histological hallmarks of myocardial injury [24], but these indicators are localized and not necessarily obvious. Depleted H-FABP staining could be seen in areas that normally show hematoxylin-eosin (H&E) staining [25].

Therefore, it is often difficult to diagnose AMI on autopsy for pathologist. In macroscopic findings in the autopsied heart, it is known that dark mottling is detectable within 4 h after the onset but variable by cases. A yellow tan may be detectable on damaged tissue within a few days. Transient thrombus in acute coronary syndrome (ACS) with coronary spasm is frequently lost. Thus, macroscopic findings are limited and not sufficiently informative at the phase immediately after the onset of the infarction episode. Therefore, evaluating the range of the infarction histologically remains difficult. Rather than these pathologic findings, a guideline for ECG has been recently developed for diagnosis of ACS [26, 27], such as ST-elevation and/or Q-wave, which is diagnostic data as well as chest pain or other pains on the onset of the infarction or other symptoms. Further, several studies have used ischemic models that facilitate a deeper understanding of cardiac muscular remodeling after hypoxic stress [28, 29]. Biochemical data of creatine kinase MB (CK-MB) is an alternative important diagnostic indicator. In clinical diagnosis, troponins [30] have been utilized for blood test. Serum markers are sensitive to time-dependent myocardial damage that is mainly caused by disruption of coronary artery blood flow. Heart-type fatty acid-binding protein (H-FABP) [31] is in clinical use, but their sustainability and sensitivity are insufficient (**Table 1**). Several studies have used ischemic models that facilitate a deeper understanding of cardiac muscular remodeling after hypoxic stress for identification of alternative markers [28, 29].

1.3. Laser-captured microdissection and proteomics

Liquid chromatography (LC)-MS techniques using laser microdissection technique were useful for identification of a promising biomarker for myocardial infraction [32].

In this process, contraction band and wavy fibers are hallmarks of AMI for dissection, which are localized in the infracted area. In collection of cardiac tissues, fibrotic area was excluded to prevent contaminating other types of injury. To extract proteins followed by liquid chromatography-mass spectrometry (LC–MS), each microdissected sample was suspended in NH_4HCO_3 containing CH_3CN. Tubes were heated at 95°C and cooling trypsin digestion was performed. Tubes were incubated at 37°C overnight and then heated at 95°C. After drying, samples were resuspended in trifluoroacetic acid CH_3CN. Following this process, 1.0×10^4 peptides and $10^{2–3}$ proteins are identified. The list of identified proteins is shown below (**Table 2**). An example of spectrum in LC-MS is shown in **Figure 1**.

	<2 h	2–4 h	4–6 h	6–12 h	12–24 h	24–72 h	72 h<
Myoglobin	○	○	○	○	○	Δ	×
H-FABP	○	○	○	○	○	Δ	×
Cardiac troponin	×	Δ	○	○	○	○	○
CK-MB	×	Δ	○	○	○	Δ	×
Myosin light chain	×	Δ	○	○	○	○	○

Table 1. Representative biomarkers of AMI. CK, creatine kinase.

1.4. MALDI-MSI and ROI analysis

The permeability of reaction buffer into FFPE tissues for hydrophilization has recently been improved such usability without tissue damage. The procedure enhances the crystallization of the peptide and matrix and organic low weight molecule, such as DHB, for MALDI/TOF-MS analysis. Here, let us review a method for the identification of molecular markers using MSI and tandem MS [6]. In detail, the tissue was incubated for 1 h at 37°C in the buffer containing NH_4HCO_3 and CH_3CN. After removal of the buffer, the tissue was incubated again with a

Collagen α-1 (I) chain
Collagen α-1 (III) chain
Filamin-C
Serum albumin
Hemoglobin subunit-β
Collagen α-2 (I) chain
Hemoglobin subunit-α
Keratin, type II cytoskeletal

Table 2. Nonspecific proteins in analysis of cardiac myocyte proteins in LC-MS using FFPE. These are commonly detected proteins of various organs that should be removed from protein filing.

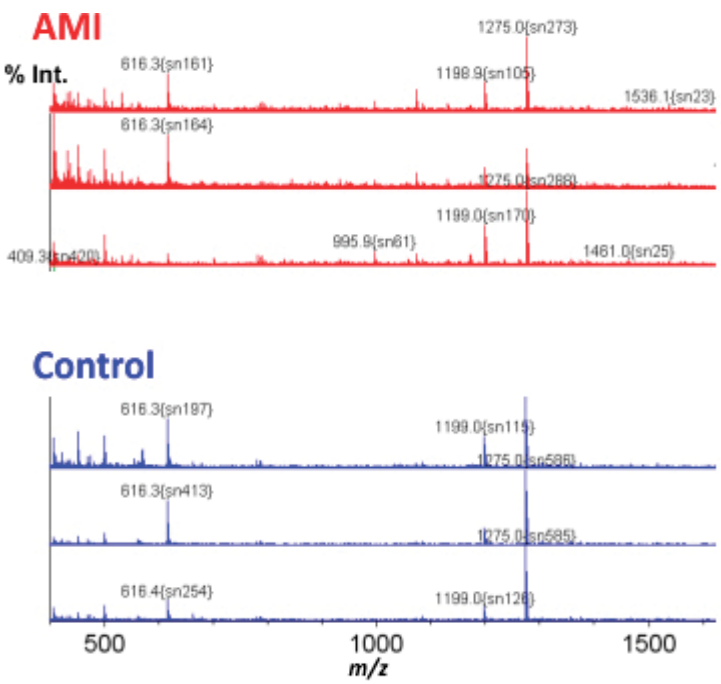

Figure 1. An example of LC-MS spectrum representing hemoglobin beta in AMI and control.

volume of buffer to cover the sample. The slide is subsequently covered with a cover glass and heated at 94°C on an aluminum hot plate. Next, trypsin solution is added on the tissue for protein digestion, and the slide is incubated at 37°C overnight (**Figure 1**). Long-term incubation in a buffer containing CH_3CN may increase in spaces between tissue fibers in cardiac tissue. The matrix (2,5-dihydroxybenzoic acid, DHB) solution (**Figure 2**), which is known to be suitable for analysis of peptides, is deposited in droplets at a spatial interval using several devices that were developed for matrix deposition (**Figure 2**). After drying, mass spectra were gained using a MALDI TOF/TOF mass spectrometer equipped with a nitrogen laser. Using this method, histone H2A was reported as a marker of colon cancer [6].

MALDI-MSI of hemoglobin beta demonstrates the two-dimensional distribution of blood flow in the cardiac tissue (**Figure 3**). Imaging MS Solution is a novel tool for ROI that was developed (Shimadzu Co. Ltd).

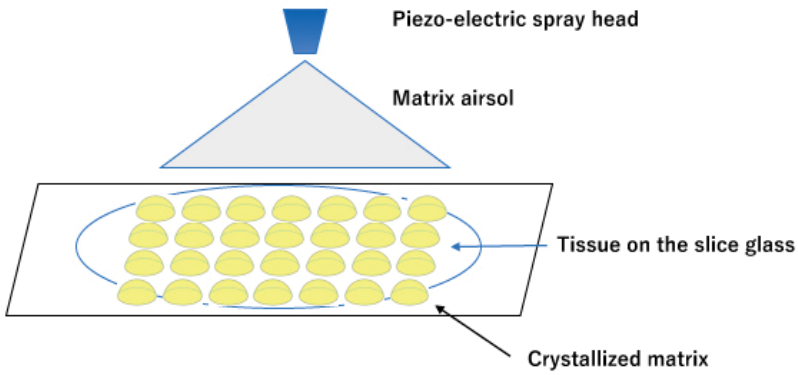

Figure 2. DHB in a solution of 50% methanol was deposited onto the sections using a piezoelectric head.

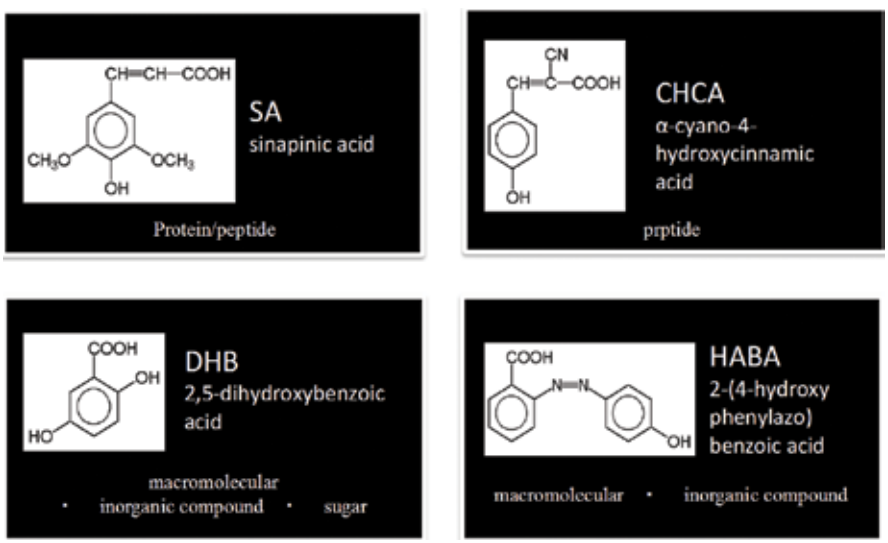

Figure 3. Available matrix for ionization of peptide.

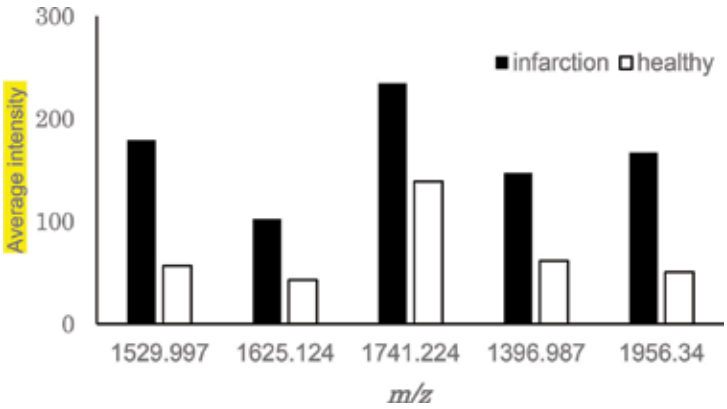

Figure 4. Examples of comparative ROI analysis. Black bar and white bar represent the average intensity of individual *m*/*z* values. The value 1530 corresponds to hemoglobin subunit alpha. HBA signals in the infarcted ROI of samples were measured for all pixels in the respective regions ($N = 4126$; healthy area, $N = 7554$).

Using this program, the intensity in individual measured point pixels is summarized in a DM that is used for computation (**Figure 4**). For this analysis, the observations are based upon PTAH and H&E staining; the endocardial area is selected as ROI, in which contraction bands, dilated arterioles, and endothelial damage are observed. In this way, ROI analysis is performed to test for intensity differences between infarcted ROI and healthy area in each batch of imaging data over all pixels. ROI analyses distinguished molecules that are specific to ROI (**Figures 5** and **6**).

Note: In analysis of big imaging data, *t*-test is not necessarily sufficient because *p*-value depends on a number of data. In particular, the pixel point in ROI analyses is greater than 1000. For ROI analysis, Cohen's *d*-value, which is independent of the numbers of data, supports *t*-test analytic data. The *d*-value is defined by

$$d = \frac{s_{\mathrm{i}} - s_{\mathrm{h}}}{\sqrt{\frac{(n_{\mathrm{i}}-1)\sigma_{\mathrm{i}}^2+(n_h-1)\sigma_h^2}{n_{\mathrm{i}}+n_h-2}}} \tag{1}$$

s_i and s_h represent the average signal intensity of the pixels in ROI and the control area, respectively. n_i and n_h represent the pixel numbers in ROI and the control, respectively. σ_i and σ_h represent the standard deviation of the intensity in the pixels ROI and the control, respectively [33]. Cohen's criteria are as follows: $d < 0.2$, not significant; $0.2 < d < 0.5$, small; $0.5 < d < 0.8$, medium; and $d > 0.8$, great (significant).

1.4.1. Hierarchical cluster analysis of MSI

Imaging MS solution® (Shimadzu, Kyoto, Japan) is applied for hierarchical clustering analysis (HCA) based on the IMS data. According to the algorithm, DM clustering is performed using intensity value information for each *m*/*z* peak. When performing hierarchical cluster analysis,

http://dx.doi.org/10.5772/intechopen.81158

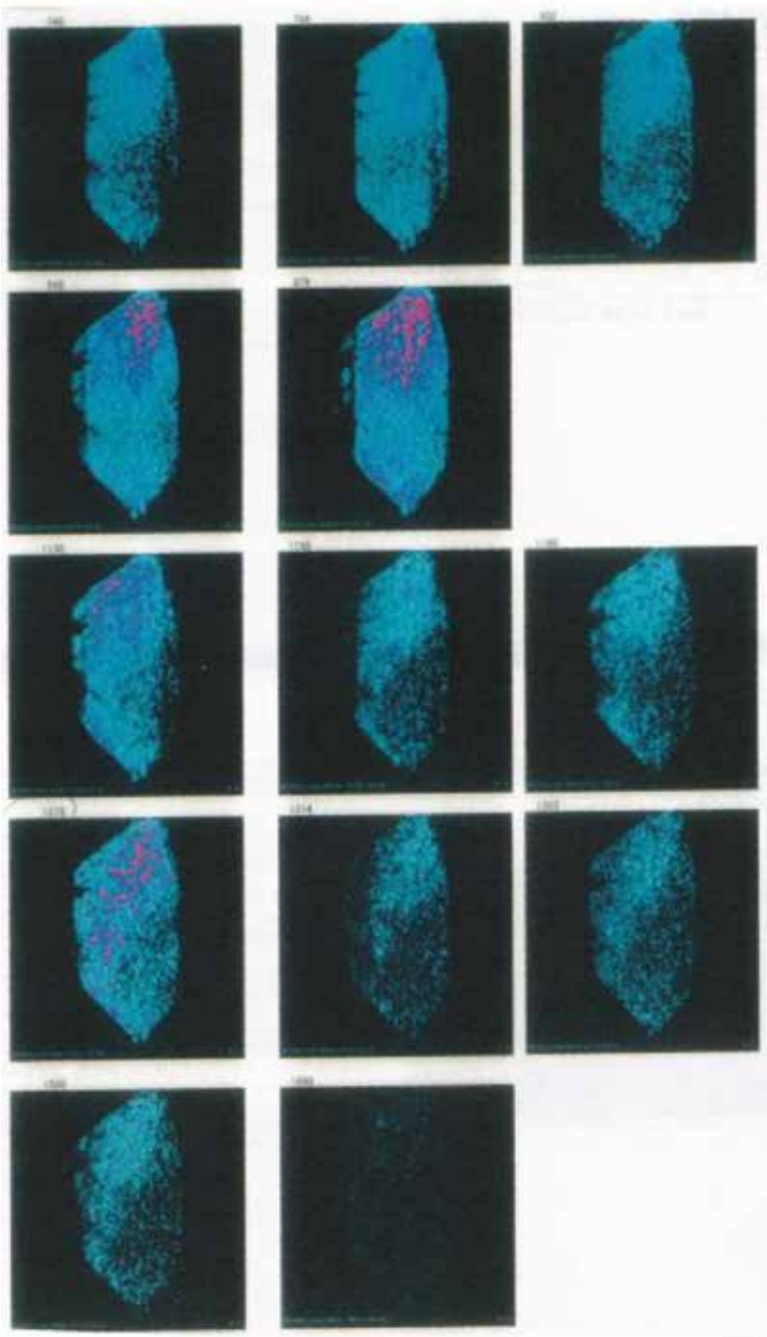

Figure 5. MALDI-MSI: *m*/*z* values are 748, 795, 932, 945, 976, 1130, 1165, 1194, 1275, 1314, 1337, 1530, and 1696, respectively. The intensity is illustrated on the cardiac tissue in a heat map manner. For visualization, raw MALDI-MS data were converted into the Imaging MS Solution ver. 1.20 (Shimadzu).

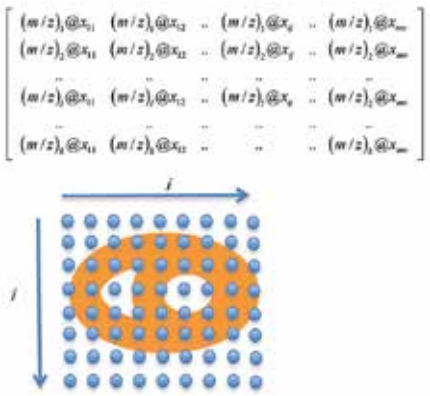

Figure 6. Examples of DM. The component $(m/z)_l@x_{ij}$ in the matrix signifies the lth m/z values ($1 \le l \le k$) for the pixels at the coordinate of x_{ij} ($1 \le i \le m$, $1 \le j \le n$) on the sample issue. This DM is the platform of the ROI analysis and other static analyses. The bottom illustration represents the coordinate on the cardiac tissue (indicated by orange circles). First, we measured the intensity values for $m/z = (m/z)_1$ of each pixel in the image and arranged the value as a column vector. Similarly, another value $m/z = (m/z)_2$ was measured, and the value was arranged as the next column vector. Further measurements of all detected intensity values *of* m/z (*1, 2,…l, …*) are arranged in the row direction. Row and column vectors yielded a DM for a single whole dataset of a tissue.

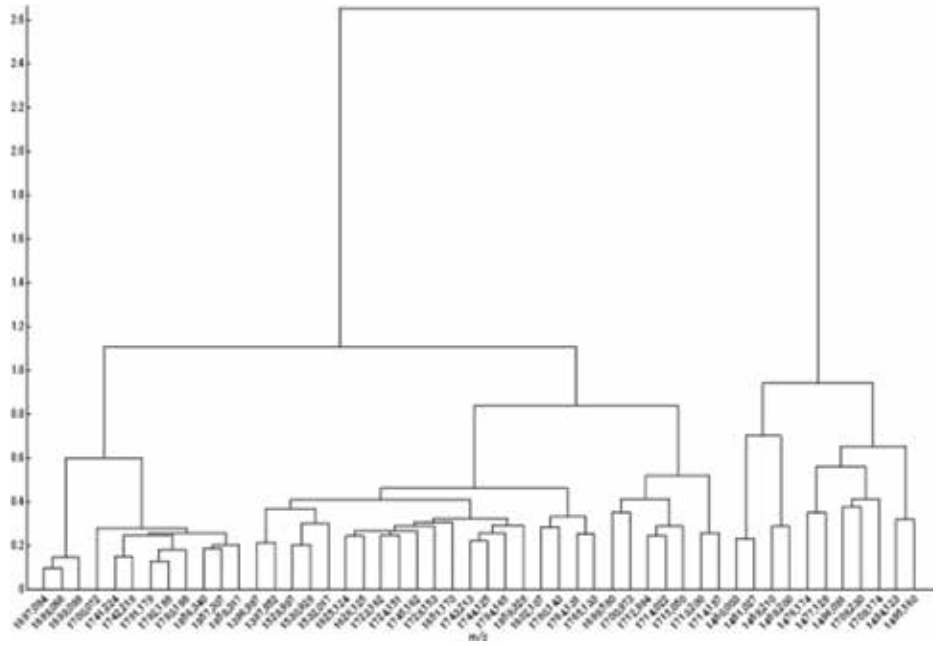

Figure 7. An example of HCA analysis. Distribution of hemoglobin subunit alpha peptide signal (m/z = 1529) is shown.

the Euclidean distance between data matrices was defined as performed (scalar values). We summarized the images close in distance as one larger cluster, and we then calculated the distance between the newly grouped individual clusters. By repeating this process, clustering

was carried out hierarchically in the dendrogram. For HCA, we analyzed data using Ward's method and the group average method. The vertical axis represents distance, and *m*/*z* values are represented on the horizontal axis. Comparing the distribution between hemoglobins is anticipated to provide an important data of relevance of blood flow carried by hemoglobin and mycotic injury due to infarction (**Figure 7**).

2. Conclusion

In this article, we reviewed analytical method in MSI analyses of FFPE tissues. This method for protein extraction from FFPE enabled proteomic analysis. With the combination of label-free LC-MS accompanied by precise laser microdissection enabled in situ proteomic analysis, new pathological findings are obtained.

Proteomic studies by MSI have recently been developed extensively for the identification of peptides in tissues [5, 34]. In this study, the application of MSI method leads to a significant improvement in the signal intensity FFPE tissues. The treatment improved the quality of signals obtained from FFPE specimens by swelling of the deparaffinized sample and increasing tissue permeability. For precise diagnosis, FFPE specimens provide more informatic histologic findings than frozen samples. Therefore, establishment of technique for proteomic study using FFPE contributes to the identification of novel diagnostic markers. To obtain specific markers, it is necessary to exclude nonspecific abundant proteins, including collagens, keratins, beta tubulin, and vimentin. Proteomic studies represent a promising approach to the discovery of novel diagnostic markers and understanding of the pathogenesis of cardiac remodeling. MSI may provide information about the histologic diagnosis of AMI, and several sarcomeric proteins may be a promising marker for the diagnosis of AMI. ROI and HCA analyses proved to be useful tools for the analysis of signal distribution patterns of infarcted tissues. When supplemented by these analyses, IMS may be a promising technique for the identification of biomarkers for pathological studies that involve the comparison of diseased and control areas.

Acknowledgements

This work was supported by a grant-in-aid from the Ministry of Education, Culture, Sports, Science, and Technology, Japan (Project No. 17013086; http://kaken.nii.ac.jp/ja/p/17013086). We thank Dr. Yu Kakimoto for providing MSI data (**Figures 1** and **5**).

Conflicts of interest

The authors have declared no conflicts of interest.

Appendices and nomenclature

MALDI	Matrix-assisted laser desorption ionization
MALDI-MS	MALDI mass spectrometry
MALDI-MSI	MALDI-MS imaging
FFPE	Formalin-fixed paraffin embedded
EDTA	Ethylenediaminetetraacetic acid
AMI	Acute myocardial infarction
DM	Dataset matrix
ROI	Region of interest
HCA	Hierarchical clustering analysis

Author details

Tatsuaki Tsuruyama* and Takuya Hieatsuka

*Address all correspondence to: tsuruyam@kuhp.kyoto-u.ac.jp

Department of Drug and Discovery Medicine, Pathology Division, Graduate School of Medicine, Kyoto University, Kyoto, Japan

References

[1] Karas M, Hillenkamp F. Laser desorption ionization of proteins with molecular masses exceeding 10,000 daltons. Analytical Chemistry. 1988;**60**:2299-2301

[2] Hillenkamp F, Karas M, Beavis RC, Chait BT. Matrix-assisted laser desorption/ionization mass spectrometry of biopolymers. Analytical Chemistry. 1991;**63**:1193A-1203A

[3] Brown RS, Lennon JJ. Mass resolution improvement by incorporation of pulsed ion extraction in a matrix-assisted laser desorption/ionization linear time-of-flight mass spectrometer. Analytical Chemistry. 1995;**67**:1998-2003

[4] Whittal RM, Li L. High-resolution matrix-assisted laser desorption/ionization in a linear time-of-flight mass spectrometer. Analytical Chemistry. 1995;**67**:1950-1954

[5] Casadonte R, Caprioli RM. Proteomic analysis of formalin-fixed paraffin-embedded tissue by MALDI imaging mass spectrometry. Nature Protocols. 2011;**6**:1695-1709. DOI: 10.1038/nprot.2011.388

[6] Kakimoto Y et al. Novel in situ pretreatment method for significantly enhancing the signal in MALDI-TOF MS of formalin-fixed paraffin-embedded tissue sections. PLoS One. 2012; **7**:e41607. DOI: 10.1371/journal.pone.0041607. PONE-D-12-07910 [pii]

[7] Ronci M et al. Protein unlocking procedures of formalin-fixed paraffin-embedded tissues: Application to MALDI-TOF imaging MS investigations. Proteomics. 2008;**8**:3702-3714. DOI: 10.1002/pmic.200701143

[8] Gustafsson JO, Oehler MK, McColl SR, Hoffmann P. Citric acid antigen retrieval (CAAR) for tryptic peptide imaging directly on archived formalin-fixed paraffin-embedded tissue. Journal of Proteome Research. 2010;**9**:4315-4328. DOI: 10.1021/pr9011766

[9] Bouschen W, Schulz O, Eikel D, Spengler B. Matrix vapor deposition/recrystallization and dedicated spray preparation for high-resolution scanning microprobe matrix-assisted laser desorption/ionization imaging mass spectrometry (SMALDI-MS) of tissue and single cells. Rapid Communications in Mass Spectrometry. 2010;**24**:355-364. DOI: 10.1002/rcm.4401

[10] Yang J, Caprioli RM. Matrix sublimation/recrystallization for imaging proteins by mass spectrometry at high spatial resolution. Analytical Chemistry. 2011;**83**:5728-5734. DOI: 10.1021/ac200998a

[11] Kenyon CN, Melera A, Erni F. Utilization of direct liquid inlet LC/MS in studies of pharmacological and toxicological importance. Journal of Analytical Toxicology. 1981;**5**:216-230

[12] Kim HY, Salem N Jr. A new technique for lipid analysis using liquid chromatography/mass spectrometry. Advances in Alcohol & Substance Abuse. 1988;**7**:241-247. DOI: 10.1300/J251v07n03_32

[13] Ramseier A, Siethoff C, Caslavska J, Thormann W. Confirmation testing of amphetamines and designer drugs in human urine by capillary electrophoresis-ion trap mass spectrometry. Electrophoresis. 2000;**21**:380-387

[14] Quanico J, Franck J, Wisztorski M, Salzet M, Fournier I. Combined MALDI mass spectrometry imaging and parafilm-assisted microdissection-based LC-MS/MS workflows in the study of the brain. Methods in Molecular Biology. 2017;**1598**:269-283. DOI: 10.1007/978-1-4939-6952-4_13

[15] Panderi I et al. Differentiating tumor heterogeneity in formalin-fixed paraffin-embedded (FFPE) prostate adenocarcinoma tissues using principal component analysis of matrix-assisted laser desorption/ionization imaging mass spectral data. Rapid Communications in Mass Spectrometry. 2017;**31**:160-170. DOI: 10.1002/rcm.7776

[16] Bornsen KO. Influence of salts, buffers, detergents, solvents, and matrices on MALDI-MS protein analysis in complex mixtures. Methods in Molecular Biology. 2000;**146**:387-404. DOI: 10.1385/1-59259-045-4:387

[17] Angel PM et al. Mapping extracellular matrix proteins in formalin-fixed, paraffin-embedded tissues by MALDI imaging mass spectrometry. Journal of Proteome Research. 2018;**17**:635-646. DOI: 10.1021/acs.jproteome.7b00713

[18] Urban C et al. PAXgene fixation enables comprehensive metabolomic and proteomic analyses of tissue specimens by MALDI MSI. Biochimica et Biophysica Acta. 2018;**1862**: 51-60. DOI: 10.1016/j.bbagen.2017.10.005

[19] Ronci M et al. MALDI-MS-imaging of whole human lens capsule. Journal of Proteome Research. 2011;**10**:3522-3529. DOI: 10.1021/pr200148k

[20] Ronci M, Sharma S, Martin S, Craig JE, Voelcker NH. MALDI MS imaging analysis of apolipoprotein E and lysyl oxidase-like 1 in human lens capsules affected by pseudoexfoliation syndrome. Journal of Proteomics. 2013;**82**:27-34. DOI: 10.1016/j.jprot.2013.01.008

[21] Angel PM et al. Advances in MALDI imaging mass spectrometry of proteins in cardiac tissue, including the heart valve. Biochimica et Biophysica Acta. 2017;**1865**:927-935. DOI: 10.1016/j.bbapap.2017.03.009

[22] Yajima Y et al. Region of interest analysis using mass spectrometry imaging of mitochondrial and sarcomeric proteins in acute cardiac infarction tissue. Scientific Reports. 2018;**8**: 7493. DOI: 10.1038/s41598-018-25817-7

[23] Carbone F, Nencioni A, Mach F, Vuilleumier N, Montecucco F. Pathophysiological role of neutrophils in acute myocardial infarction. Thrombosis and Haemostasis. 2013;**110**:501-514. DOI: 10.1160/TH13-03-0211

[24] Nakatani S et al. Left ventricular echocardiographic and histologic changes: Impact of chronic unloading by an implantable ventricular assist device. Journal of the American College of Cardiology. 1996;**27**:894-901

[25] Meng X, Ming M, Wang E. Heart fatty acid binding protein as a marker for postmortem detection of early myocardial damage. Forensic Science International. 2006;**160**:11-16. DOI: 10.1016/j.forsciint.2005.08.008

[26] Muller C. New ESC guidelines for the management of acute coronary syndromes in patients presenting without persistent ST-segment elevation. Swiss Medical Weekly. 2012;**142**:w13514. DOI: 10.4414/smw.2012.13514

[27] Hamm CW et al. ESC guidelines for the management of acute coronary syndromes in patients presenting without persistent ST-segment elevation: The task force for the management of acute coronary syndromes (ACS) in patients presenting without persistent ST-segment elevation of the European Society of Cardiology (ESC). European Heart Journal. 2011;**32**:2999-3054. DOI: 10.1093/eurheartj/ehr236

[28] Xia P. Letter by Xia regarding article, "High-density lipoproteins and their constituent, sphingosine-1-phosphate, directly protect the heart against ischemia/reperfusion injury in vivo via the S1P3 lysophospholipid receptor". Circulation. 2007;**115**:e393; author reply e394. DOI: 10.1161/CIRCULATIONAHA.106.667196

[29] Theilmeier G et al. High-density lipoproteins and their constituent, sphingosine-1-phosphate, directly protect the heart against ischemia/reperfusion injury in vivo via the S1P3 lysophospholipid receptor. Circulation. 2006;**114**:1403-1409. DOI: 10.1161/CIRCULATIONAHA.105.607135

[30] Tiwari RP et al. Cardiac troponins I and T: Molecular markers for early diagnosis, prognosis, and accurate triaging of patients with acute myocardial infarction. Molecular Diagnosis & Therapy. 2012;**16**:371-381. DOI: 10.1007/s40291-012-0011-6

[31] Haltern G et al. Comparison of usefulness of heart-type fatty acid binding protein versus cardiac troponin T for diagnosis of acute myocardial infarction. The American Journal of Cardiology. 2010;**105**:1-9. DOI: 10.1016/j.amjcard.2009.08.645

[32] Kakimoto Y et al. Sorbin and SH3 domain-containing protein 2 is released from infarcted heart in the very early phase: Proteomic analysis of cardiac tissues from patients. Journal of the American Heart Association. 2013;**2**:e000565. DOI: 10.1161/JAHA.113.000565

[33] Jacob C. Statistical Power Analysis for the Behavioral Sciences. 2nd ed. Hillsdale, NJ: Lawrence Erlbaum; 1988

[34] Chatterji B, Pich A. MALDI imaging mass spectrometry and analysis of endogenous peptides. Expert Review of Proteomics. 2013;**10**:381-388. DOI: 10.1586/14789450.2013.814939

Edited by Thomas Heinbockel and Vonnie D.C. Shields

Histology is the science of tissues and as such histology studies cells and tissues of organs using a variety of techniques. Histological techniques are used in different disciplines: research, teaching, and clinical applications. This book explores the research currently being carried out at the molecular, subcellular, and cellular levels, both in normal and pathological processes, from genetic mechanisms to intra- and intercellular signaling. This book includes cutting-edge research reviews and descriptions of technological advances to modify bodily cells and tissues. Targeted at students and researchers in biological, medical, and related disciplines, this book will provide an overview of the work being done in this field, and will highlight gaps and areas that would benefit from further exploration. The book contains eight chapters in four sections and presents reviews in different areas of histology written by experts in their respective fields. Basic histology, cell biology, histopathology, and histological techniques are featured prominently as a recurring theme throughout the chapters. This book will be a most valuable resource for histologists, cell biologists, pathologists, and other scientists alike and contribute to the training of current and future biomedical scientists.

Published in London, UK

IntechOpen

ISBN 978-1-83881-813-5